9
Turbomachinery

9.1 Introduction

In general, turbomachinery is classified as all those devices in which energy is transferred either to or from a continuously flowing fluid by the dynamic action of one or more moving blade rows.[37] The word *turbo or turbinis* is of Latin origin and implies that which spins or whirls around. Essentially, a rotating blade row or rotor changes the total enthalpy of the fluid moving through it by either doing work on the fluid or having work done on it by the fluid, depending on the effect required of the machine. These enthalpy changes are intimately linked with the pressure changes occurring simultaneously in the fluid.

This definition of turbomachinery embraces both open and enclosed turbomachines.[37] Open turbomachinery (such as propellers, windmills, and unshrouded fans) influence an indeterminate quantity of fluid. In enclosed turbomachinery (such as centrifugal compressors, axial-flow turbines, etc.), a finite quantity of fluid passes through a casing in unit time. In this chapter, we will focus on the enclosed turbomachinery used in gas turbine engines: fans, compressors, and turbines. There are many excellent references on enclosed turbomachinery, such as Refs. 4, 12, 22, 28, 29, and 37–47. Open turbomachines are covered in aeronautics textbooks such as Refs. 48, 49, and 50.

Turbomachines are further categorized according to the nature of the flow path through the passages of the rotor. When the path of the throughflow is wholly or mainly parallel to the axis of rotation, the device is termed an *axial-flow turbomachine*. When the path of the throughflow is wholly or mainly in a plane perpendicular to the rotation axis, the device is termed a *radial-flow turbomachine*. When the direction of the throughflow at the rotor outlet has both radial and axial velocity components present in significant amounts, the device is termed a *mixed-flow turbomachine*.

9.2 Euler's Turbomachinery Equations

In turbomachinery, power is added to or removed from the fluid by the rotating components. These rotating components exert forces on the fluid that change both the energy and the tangential momentum of the fluid. In this section, we will develop Euler's equations for turbomachinery that relate the change in energy to the change in tangential momentum.

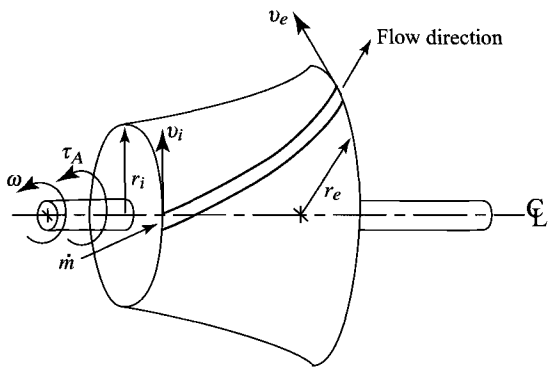

Fig. 9.1 Control volume for a general turbo-machine.

Consider the adiabatic flow of a fluid as shown in Fig. 9.1. The fluid in a stream tube enters a control volume at radius r_i with tangential velocity v_i and exits at r_e with tangential velocity v_e. For a compressor or pump with steady flow, the applied torque τ_A is equal to the change in angular momentum of the fluid, or

$$\tau_A = \frac{\dot{m}}{g_c}(r_e v_e - r_i v_i)$$

The input power is $\dot{W}_c = \omega \tau_A$, or

$$\dot{W}_c = \frac{\dot{m}\omega}{g_c}(r_e v_e - r_i v_i) \tag{9.1}$$

This equation is often referred to as the *Euler pump equation.* Application of the first law of thermodynamics to the flow through the control volume gives

$$\dot{W}_c = \dot{m}(h_{te} - h_{ti})$$

Combining this expression with Eq. (9.1) gives

$$h_{te} - h_{ti} = \frac{\omega}{g_c}(r_e v_e - r_i v_i) \tag{9.2}$$

Likewise, for a steady-flow turbine, the output torque τ_O is equal to the change in angular momentum of the fluid, or

$$\tau_O = \frac{\dot{m}}{g_c}(r_i v_i - r_e v_e)$$

The output power is

$$\dot{W}_t = \omega \tau_O$$

or

$$\dot{W}_t = \frac{\dot{m}\omega}{g_c}(r_i v_i - r_e v_e) \tag{9.3}$$

This equation is often referred to as the *Euler turbine equation*. Application of the first law of thermodynamics to the flow through the control volume gives

$$\dot{W}_t = \dot{m}(h_{ti} - h_{te})$$

Combining this expression with Eq. (9.3) gives

$$h_{ti} - h_{te} = \frac{\omega}{g_c}(r_i v_i - r_e v_e) \tag{9.4}$$

which is the same as Eq. (9.2).

In the design of turbomachinery for a compressible gas, the gas is often modeled as having constant specific heats. For this case, we can write Eq. (9.4) as

$$c_p(T_{ti} - T_{te}) = \frac{\omega}{g_c}(r_i v_i - r_e v_e) \tag{9.5}$$

This equation is also referred to as the *Euler turbine equation*. We will be using this equation throughout the analysis of turbomachinery for a compressible gas. Component efficiencies and the isentropic relationships will be used to relate total temperature changes to total pressure changes.

9.3 Axial-Flow Compressor Analysis

The axial-flow compressor is one of the most common compressor types in use today. It finds its major application in large gas turbine engines like those that power today's jet aircraft. A cutaway view of an axial-flow compressor is shown in Fig. 9.2. The compressor is made up of two major assemblies: the rotor with its blades, as shown in Fig. 9.2a, and the casing with its stationary blades (called *stators*), as shown in Fig. 9.2b.

This chapter investigates the relationships of the desired performance parameters to the related blade loading and resultant fluid flow angles. Because the flow is inherently three-dimensional, the problem of analysis seems almost

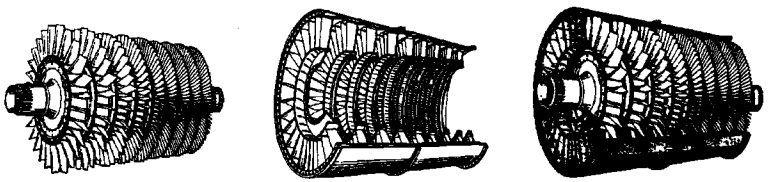

a) b) c)

Fig. 9.2 Axial-flow compressor: a) rotor with blades, b) case with stators, and c) compressor assembly. (Courtesy of Pratt & Whitney).

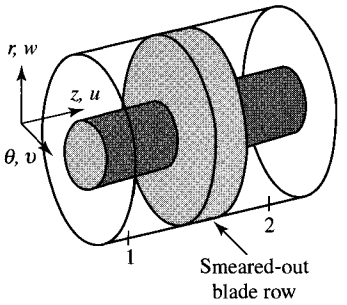

Fig. 9.3 Coordinate system and throughflow representation.

incomprehensible. *Do not fear*! This most complex flow can be understood by dividing the three-dimensional flowfield into three two-dimensional flowfields. The complete flowfield will be the "sum" of these less complex two-dimensional flows. The two-dimensional flowfields are normally called the *throughflow field*, the *cascade field* (or *blade-to-blade field*), and the *secondary flowfield*. Each of these fields is described in more detail next.

The *throughflow field* is concerned with the variation in fluid properties in only the radial r and axial z directions (see Fig. 9.3). No variations in the θ direction occur. A row of blades is modeled as a thin disk that affects the flowfield uniformly in the θ direction. If you imagine that the forces of the blades had been distributed among an infinite number of very thin blades, then you can begin to see the throughflow field model. As a result of throughflow field analysis, one will obtain the axial, tangential, and radial velocities as a function of r and z. Typical axial velocity profiles as a result of throughflow analysis are shown in Fig. 9.4a.

When the axial velocity changes, like that shown in Fig. 9.4a, conservation of mass requires that a downward flow of the fluid occur between stations 1 and 2. This downward flow could be shown by the stream surface as drawn in Fig. 9.4b.

The *cascade field* considers the flow behavior along stream surfaces (s coordinate) and tangentially through blade rows. Unwrapping the stream surface

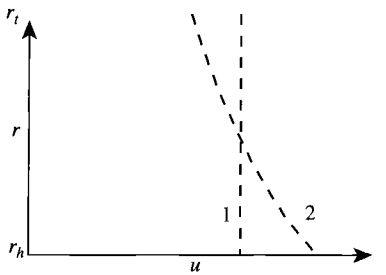

Fig. 9.4a Typical axial velocity profiles.

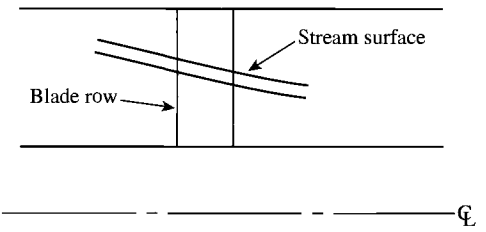

Fig. 9.4b Typical stream surface.

(like that shown in Fig. 9.5) gives the meridional projection of blade profiles, as shown in Fig. 9.6—a two-dimensional flowfield in the θ and the meridional (almost z) coordinates. If the curvature of the stream surfaces in the throughflow field is not too great, the flow at a radial location may be modeled as a meridional projection and a suitable blade profile determined for the flow conditions. By considering a number of such projections, the blade profiles for selected radial locations on the blade are determined. The complete blade shape necessary to describe the full three-dimensional blade can be obtained by blending in the desired blade profiles.

The most common method of obtaining performance data for different blade profiles is to run cascade tests. A set of airfoils of the desired blade shape is mounted in a conditioned flow stream, and the performance is experimentally measured. Figure 9.7 shows the complete flowfield about a typical cascade with the blades spaced a distance s apart.

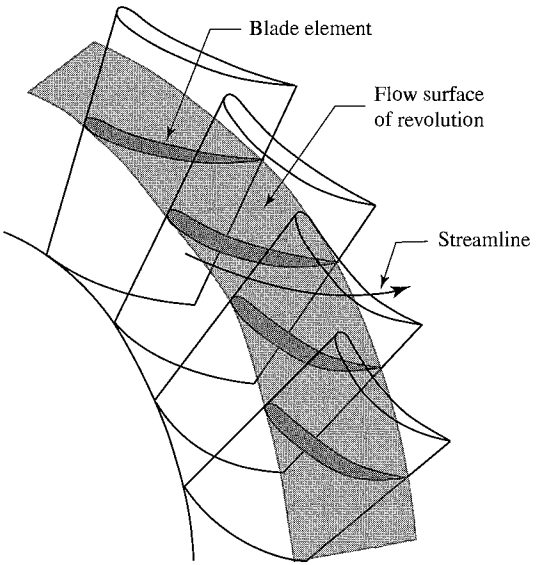

Fig. 9.5 Stream surface and streamlines.

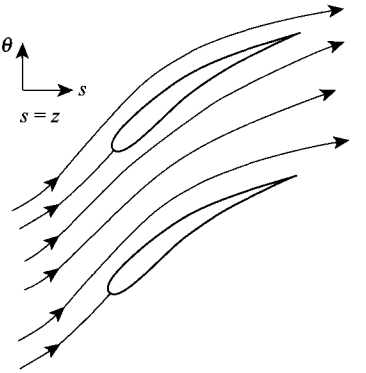

Fig. 9.6 Meridional projections of blade profiles.

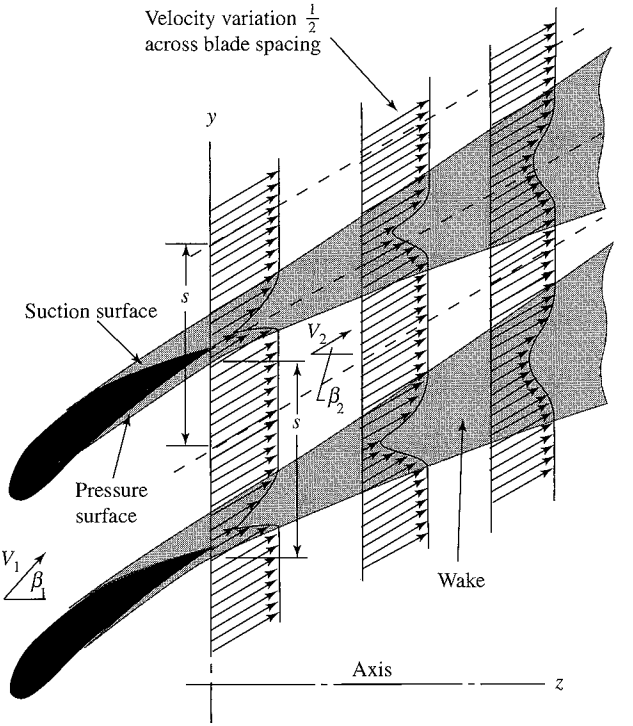

Fig. 9.7 Flowfield about cascade.

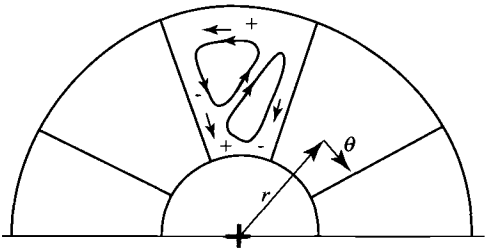

Fig. 9.8 Secondary flowfield within a stator row.

The *secondary flowfield* exists because the fluid near the solid surfaces (in the boundary layer) of the blades and passage walls has a lower velocity than that in the *freestream* (external to the boundary layer). The pressure gradients imposed by the freestream will cause the fluid in the boundary layers to flow from regions of higher pressure to regions of lower pressure. Figure 9.8 shows the possible secondary flowfield within a stator row.

9.3.1 Two-Dimensional Flow Through Blade Rows

A cross section and a top view of a typical axial-flow compressor are shown in Fig. 9.9. Depending on the design, an inlet guide vane (IGV) may be used to deflect the incoming airflow to a predetermined angle toward the direction of rotation of the rotor. The rotor increases the angular velocity of the fluid, resulting in increases in total temperature, total pressure, and static pressure. The following stator decreases the angular velocity of the fluid, resulting in an increase in the static pressure, and sets the flow up for the following rotor. A compressor stage is made up of a rotor and a stator.

The basic building block of the aerodynamic design of axial-flow compressors is the *cascade*, an endless repeating array of airfoils (Fig. 9.10) that results from the "unwrapping" of the stationary (stators) and rotating (rotor) airfoils. Each cascade passage acts as a small diffuser, and it is said to be well designed or

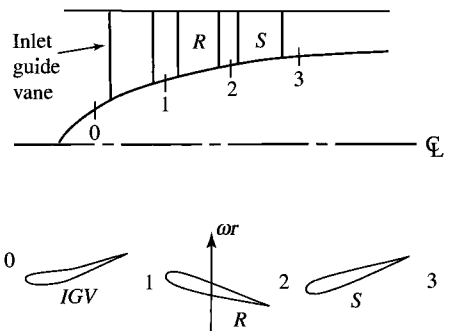

Fig. 9.9 Cross section and top view of a typical axial-flow compressor.

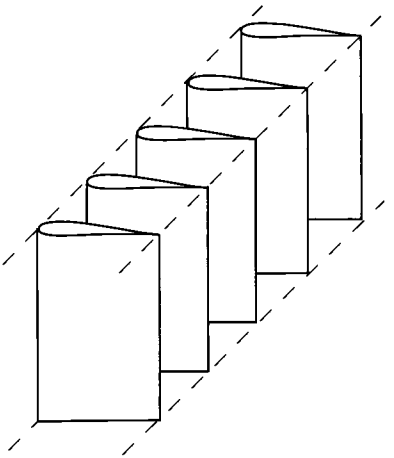

Fig. 9.10 Rectilinear cascade.

"behaved" when it provides a large static pressure rise without incurring unacceptable total pressure losses and/or flow instabilities due to shock waves and/or boundary-layer separation.

The changes in fluid velocity induced by the blade rows are related to changes in the fluid's thermodynamic properties in this section. The analysis is concerned with only the flow far upstream and far downstream of a cascade—the regions where the flowfields are uniform. In this manner, the details about the flowfield are not needed, and performance can be related to just the changes in fluid properties across a blade row.

In the analysis that follows, two different coordinate systems are used: one fixed to the compressor housing (absolute) and the other fixed to the rotating blades (relative). The static (thermodynamic) properties *do not* depend on the reference frame. However, the *total properties do depend on the reference frame*. The velocity of a fluid in one reference frame is easily converted to the other frame by the following equation:

$$\boldsymbol{V} = \boldsymbol{V}_R + \boldsymbol{U} \tag{9.6}$$

where

$\boldsymbol{V}$ = velocity in stationary coordinate system
$\boldsymbol{V}_R$ = velocity in moving coordinate system
$\boldsymbol{U}$ = velocity of moving coordinate system ($=\omega r$)

Consider the compressor stage made up of a rotor followed by a stator as shown in Fig. 9.11. The flow enters the rotor with velocity V_1 (relative velocity V_{1R}) and leaves with velocity V_2 (relative velocity V_{2R}). The rotor is moving upward at velocity ωr (the symbol $\boldsymbol{U}$ is also used). The flow enters the stator with velocity V_2 and leaves with velocity V_3. Rather than keep the axial velocity

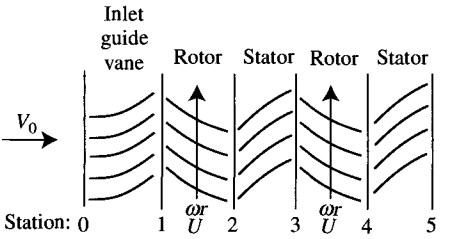

Fig. 9.11 Two repeating compressor stages with inlet guide vane.

constant, as is done in many textbooks, the following analysis permits variation in axial velocity from station to station.

Euler's equation:

$$c_p(T_{t2} - T_{t1}) = \frac{\omega}{g_c}(r_2 v_2 - r_1 v_1)$$

For $r_2 \cong r_1$,

$$c_p(T_{t2} - T_{t1}) = \frac{\omega r}{g_c}(v_2 - v_l) = \frac{U}{g_c}(v_2 - v_1)$$

Since

$$v_2 = \omega r - v_{2R} = \omega r - u_2 \tan \beta_2 = u_2 \tan \alpha_2$$

and

$$v_1 = \omega r - v_{1R} = \omega r - u_1 \tan \beta_1 = u_1 \tan \alpha_1$$

then

$$c_p(T_{t2} - T_{t1}) = \frac{(\omega r)^2}{g_c}\frac{u_1}{\omega r}\left(\tan \beta_1 - \frac{u_2}{u_1}\tan \beta_2\right)$$

$$= \frac{U^2}{g_c}\frac{u_1}{U}\left(\tan \beta_1 - \frac{u_2}{u_1}\tan \beta_2\right) \tag{9.7a}$$

or

$$c_p(T_{t2} - T_{t1}) = \frac{(\omega r)^2}{g_c}\frac{u_1}{\omega r}\left(\frac{u_2}{u_1}\tan \alpha_2 - \tan \alpha_1\right)$$

$$= \frac{U^2}{g_c}\frac{u_1}{U}\left(\frac{u_2}{u_1}\tan \alpha_2 - \tan \alpha_1\right) \tag{9.7b}$$

Hence the work done per unit mass flow can be determined from the rotor speed ($U = \omega r$), the velocity ratios (u_1/U and u_2/u_1), and either the rotor cascade flow angles (β_1 and β_2) or the absolute rotor flow angles (α_1 and α_2). Equations (9.7a) and (9.7b) are useful forms of the Euler equation for compressor stage design and show the dependence of the stage work on the rotor speed squared (U^2).

9.3.2 Velocity Diagrams

An axial-flow compressor stage consists of a rotor followed by a stator as shown in Fig. 9.12a. Two compressor stages (which are identical in geometry) are shown in Fig. 9.12b preceded by inlet guide vanes. The velocity diagrams depicted in Fig. 9.12b show the absolute velocities entering and leaving the guide vanes, rotor, and stator (solid vectors). In addition, for the rotors, the entering and leaving relative velocities (dashed vectors) and the rotor tangential velocity are shown. We have assumed, in the diagram, that the axial velocity component is constant.

Referring to Fig. 9.12b, we see that the guide vanes act as nozzles through which the static pressure decreases as the air velocity increases, and the fluid is given a tangential (swirl) component in the direction of the rotor velocity. The air leaves the inlet guide vanes with velocity V_1.

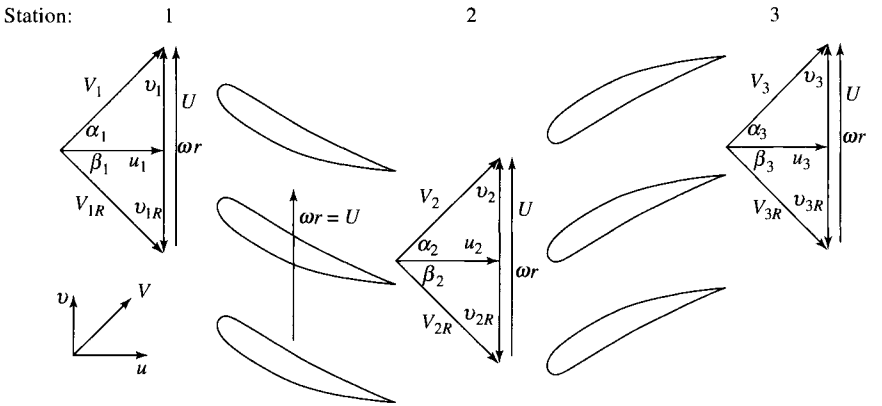

	Rotor	Stator
Velocities	$\mathbf{V}_1 = \mathbf{V}_{1R} + \mathbf{U}$	$\mathbf{V}_2 = \mathbf{V}_{2R} + \mathbf{U}$
	$u_1 = V_1 \cos \alpha_1$	$u_2 = V_2 \cos \alpha_2$
	$v_1 = V_1 \sin \alpha_1$	$v_2 = V_2 \sin \alpha_2$
	$u_1 = V_{1R} \cos \beta_1$	$u_2 = V_{2R} \cos \beta_2$
	$v_{1R} = V_{1R} \sin \beta_1 = u_1 \tan \beta_1$	$v_{2R} = V_{2R} \sin \beta_2 = u_2 \tan \beta_2$
	$v_1 + v_{1R} = \omega r = U$	$v_2 + v_{2R} = \omega r = U$

Fig. 9.12a Blade rows of a typical compressor.

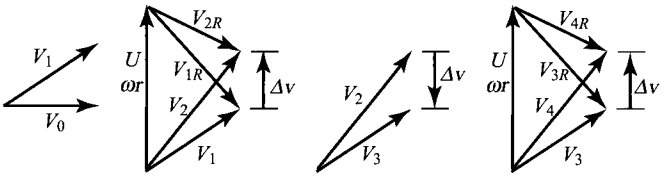

Fig. 9.12b Velocity diagrams for typical compressor.

The absolute velocity entering the rotor at station 1 is V_1. Subtracting the rotor speed ωr from V_1 vectorially, we obtain the relative velocity V_{1R} entering the rotor. In the rotor blade row, the blade passages act as diffusers, reducing the relative velocity from V_{1R} to V_{2R} as the static pressure is increased from P_1 to P_2. The relative velocity leaving the rotor is V_{2R}. Combining V_{2R} vectorially with ωr, we get their sum V_2—the absolute velocity leaving the rotor.

The velocity of the air leaving the rotor and entering the stator at station 2 is V_2. The stator diffuses the velocity to V_3 as the static pressure rises from P_2 to P_3. Because the velocity V_3 entering the rotor at station 3 is identical with V_1 entering the first-stage rotor, we find the velocity triangle for the second-stage rotor is a repeat of the triangle for the first stage.

The effects occurring in each compressor component are summarized in Table 9.1, where +, 0, and − mean increase, unchanged, and decrease, respectively. The table entries assume isentropic flow. In making entries in the table, it is important to distinguish between absolute and relative values. Because total pressure and total temperature depend on the speed of the gas, they have different values "traveling with the rotor" than for an observer not riding on the rotor. In particular, an observer on the rotor sees a force F (rotor on gas), but it is stationary; hence, in the rider's reference system, the force does no work on the gas. Consequently, the total temperature and total pressure do not change relative to an observer on the rotor as the gas passes through the rotor. An observer not on the rotor sees the force F (rotor on gas) moving at the rate ωr. Hence, to the stationary observer, work is done on the gas passing through the rotor, and the total temperature and total pressure increase.

Table 9.1 Property changes[a] in an isentropic compressor

Property	Inlet guide vanes	Rotor	Stator
Absolute velocity	+	+	−
Relative velocity	n/a	−	n/a
Static pressure	−	+	+
Absolute total pressure	0	+	0
Relative total pressure	n/a	0	n/a
Static temperature	−	+	0
Absolute total temperature	0	+	0
Relative total temperature	n/a	0	n/a

[a] + = increase, − = decrease, 0 = unchanged, n/a = not applicable.

9.3.3 Flow Annulus Area

For uniform total properties at a station i, the area of the flow annulus A_i can be obtained from the mass flow parameter (MFP) by using

$$A_t = \frac{\dot{m}\sqrt{T_{ti}}}{P_{ti}(\cos\alpha_i)\mathrm{MFP}(M_i)} \tag{9.8}$$

where α_i is the angle that the velocity V_i makes with the centerline of the annulus.

Example 9.1

Consider mean radius stage calculation—isentropic flow.

Given:

$$T_{t1} = 518.7°\mathrm{R}, \quad P_{t1} = 14.70\ \mathrm{psia}, \quad \omega = 1000\ \mathrm{rad/s}, \quad r = 12\ \mathrm{in.}$$
$$\alpha_1 = \alpha_3 = 40\ \mathrm{deg}, \quad \dot{m} = 50\ \mathrm{lbm/s}, \quad M_1 = M_3 = 0.7$$
$$u_2/u_1 = 1.1, \quad P_{t3}/P_{t1} = 1.3$$

Gas is air.

Note: For air, $\gamma = 1.4$, $c_p = 0.24\ \mathrm{Btu/(lbm \cdot °R)}$, $Rg_c = 1716\ \mathrm{ft^2/(s^2 \cdot °R)}$ $c_p g_c = 6006\ \mathrm{ft^2/(s^2 \cdot °R)}$

Solution:

$$T_1 = \frac{T_{t1}}{1 + [(\gamma - 1)/2]M_1^2} = -\frac{518.7°\mathrm{R}}{1 + 0.2 \times 0.7^2} = 472.4°\mathrm{R}$$

$$a_1 = \sqrt{\gamma R g_c T_1} = \sqrt{1.4 \times 1716 \times 472.4} = 1065.3\ \mathrm{ft/s}$$

$$V_1 = M_1 a_1 = 0.7 \times 1065.3\ \mathrm{ft/s} = 745.71\ \mathrm{ft/s}$$

$$u_1 = V_1 \cos\alpha_1 = 745.71\ \mathrm{ft/s} \times 0.766 = 571.21\ \mathrm{ft/s}$$

$$v_1 = V_1 \sin\alpha_1 = 745.71\ \mathrm{ft/s} \times 0.6428 = 479.34\ \mathrm{ft/s}$$

$$P_1 = \frac{P_{t1}}{\{1 + [(\gamma - 1)/2]M_1^2\}^{\gamma/(\gamma-1)}} = \frac{14.70\ \mathrm{psia}}{(1 + 0.2 + 0.7^2)^{3.5}} = 10.60\ \mathrm{psia}$$

$$\mathrm{MFP}(M_1) = 0.4859$$

$$A_1 = \frac{\dot{m}\sqrt{T_{t1}}}{P_{t1}(\cos\alpha_1)\mathrm{MFP}(M_1)} = \frac{50\sqrt{518.7}}{14.70 \times 0.7660 \times 0.4859} = 207.2\ \mathrm{in.}^2$$

$$\omega r = 1000 \times \frac{12}{12} = 1000\ \mathrm{ft/s}$$

$$v_{1R} = \omega r - v_1 = 1000 - 479.34 = 520.66\ \mathrm{ft/s}$$

$$\beta_1 = \tan^{-1}\frac{v_{1R}}{u_1} = \tan^{-1} 0.9114 = 42.35\ \mathrm{deg}$$

$$V_{1R} = \sqrt{u_1^2 + v_{1R}^2} = \sqrt{571.21^2 + 520.66^2} = 772.90 \text{ ft/s}$$

$$M_{1R} = \frac{V_{1R}}{a_1} = \frac{772.90}{1065.3} = 0.7255$$

$$T_{t1R} = T_1\left(1 + \frac{\gamma - 1}{2} M_{1R}^2\right) = 472.4(1 + 0.2 \times 0.7255^2) = 522.2^\circ\text{R}$$

$$P_{t1R} = P_1\left(\frac{T_{t1R}}{T_1}\right)^{\gamma/(\gamma-1)} = 10.60\left(\frac{522.1}{472.4}\right)^{3.5} = 15.04 \text{ psia}$$

$$P_{t2} = P_{t3} = 1.3 \times 14.70 = 19.11 \text{ psia}$$

$$T_{t3} = T_{t2} = T_{t1}\left(\frac{P_{t2}}{P_{t1}}\right)^{(\gamma-1)/\gamma} = 518.7(1.3)^{1/3.5} = 559.1^\circ\text{R}$$

$$\tan\beta_2 = \frac{u_1}{u_2}\left[\tan\beta_1 - \frac{g_c c_p}{\omega r\, u_1}(T_{t2} - T_{t1})\right]$$

$$= \frac{1}{1.1}\left[\tan 42.35 - \frac{6006}{1000 \times 571.21}(559.1 - 518.7)\right] = 0.4425$$

$$\beta_2 = 23.87 \text{ deg}$$

$$u_2 = \frac{u_2}{u_1} u_1 = 1.1 \times 571.21 = 628.33 \text{ ft/s}$$

$$v_{2R} = u_2 \tan\beta_2 = 628.33 \times 0.4425 = 278.04 \text{ ft/s}$$

$$V_{2R} = \sqrt{u_2^2 + v_{2R}^2} = \sqrt{628.33^2 + 278.04^2} = 687.10 \text{ ft/s}$$

$$v_2 = \omega r - v_{2R} = 1000 - 278.04 = 721.96 \text{ ft/s}$$

$$\alpha_2 = \tan^{-1}\frac{v_2}{u_2} = \tan^{-1}\frac{721.96}{628.33} = 48.97 \text{ deg}$$

$$V_2 = \sqrt{u_2^2 + v_2^2} = \sqrt{628.33^2 + 721.96^2} = 957.10 \text{ ft/s}$$

$$T_{t2R} = T_{t1R} = 552.5^\circ\text{R}$$

$$P_{t2R} = P_{t1R} = 15.04 \text{ psia}$$

$$T_2 = T_{t2} - \frac{V_2^2}{2 g_c c_p} = 559.1 - \frac{957.10^2}{2 \times 6006} = 482.8^\circ\text{R}$$

$$P_2 = P_{t2}\left(\frac{T_2}{T_{t2}}\right)^{\gamma/(\gamma-1)} = 19.11\left(\frac{482.8}{559.1}\right)^{3.5} = 11.43 \text{ psia}$$

$$a_2 = \sqrt{\gamma R g_c T_2} = \sqrt{1.4 \times 1746 \times 482.8} = 1077.0 \text{ ft/s}$$

$$M_2 = \frac{V_2}{a_2} = \frac{957.10}{1077.0} = 0.8887$$

$$M_{2R} = \frac{V_{2R}}{a_2} = \frac{687.10}{1077.0} = 0.6380$$

$$\text{MFP}(M_2) = 0.5260$$

$$A_2 = \frac{\dot{m}\sqrt{T_{t2}}}{P_{t2}(\cos\alpha_2)\text{MFP}(M_2)} = \frac{50\sqrt{559.1}}{19.11 \times 0.6566 \times 0.5260} = 179.1 \text{ in.}^2$$

$$T_3 = \frac{T_{t3}}{1 + [(\gamma - 1)/2]M_3^2} = \frac{559.1^\circ\text{R}}{1 + 0.2 \times 0.7^2} = 509.2^\circ\text{R}$$

$$P_3 = P_{t3}\left(\frac{T_3}{T_{t3}}\right)^{\gamma/(\gamma-1)} = 19.11\left(\frac{509.2}{559.1}\right)^{3.5} = 13.77 \text{ psia}$$

$$a_3 = \sqrt{\gamma R g_c T_3} = \sqrt{1.4 \times 1716 \times 509.2} = 1106.03 \text{ ft/s}$$

$$V_3 = M_3 a_3 = 0.7 \times 1106.03 = 774.22 \text{ ft/s}$$

$$u_3 = V_3 \cos\alpha_3 = 593.09 \text{ ft/s}$$

$$v_3 = V_3 \sin\alpha_3 = 497.66 \text{ ft/s}$$

$$A_3 = \frac{\dot{m}\sqrt{T_{t3}}}{P_{t3}(\cos\alpha_3)\text{MFP}(M_3)} = \frac{50\sqrt{559.1}}{19.11 \times 0.766 \times 0.4859} = 165.3 \text{ in.}^2$$

The results of this stage calculation for isentropic flow are summarized in Table 9.2, with the given data shown in bold type (SI results are shown within parentheses). Note that the flow through the rotor is adiabatic in the relative reference frame and, through the stator, is adiabatic in the absolute reference frame. Figure 9.13 is a representation of the flow properties for an isentropic stage on a *T-s* diagram.

9.3.4 Stage Parameters

9.3.4.1 Efficiencies. Several efficiencies are used to compare the performance of compressor stage designs. The two efficiencies most commonly used are stage efficiency and polytropic efficiency. The *stage efficiency* of an adiabatic compressor is defined as the ratio of the ideal work per unit mass to the actual work per unit mass between the same total pressures, or

$$\eta_s = \frac{h_{t3s} - h_{t1}}{h_{t3} - h_{t1}} \tag{9.9}$$

Table 9.2 Results for Example 9.1 axial-flow compressor stage calculation, insentropic flow

Property		Station 1	1*R*	2*R*	2	3
T_1	°R	**518.7**	522.1	522.1	559.1	559.1
	(K)	**(288.2)**	(290.1)	(290.1)	(310.6)	(310.6)
T	°R	472.4	472.4	482.8	482.8	509.2
	(K)	(262.4)	(262.4)	(268.2)	(268.2)	(282.9)
P_t	psia	**14.70**	15.04	15.04	19.11	**19.11**
	(kPa)	**(101.3)**	(103.7)	(103.7)	(131.7)	**(131.7)**
P	psia	10.60	10.60	11.43	11.43	13.77
	(kPa)	(73.05)	(73.05)	(78.85)	(78.85)	(94.96)
M		**0.700**	0.7255	0.6380	0.8887	0.700
V	ft/s	745.71	772.90	687.10	957.10	774.22
	(m/s)	(227.30)	(235.58)	(209.43)	(291.73)	(235.99)
u	ft/s	571.21	571.21	628.33	628.33	593.09
	(m/s)	(174.11)	(174.11)	(191.53)	(191.52)	(180.78)
v	ft/s	479.34	520.66	278.04	721.96	497.66
	(m/s)	(146.10)	(158.70)	(84.75)	(220.06)	(151.69)
α	deg	**40.00**	——	——	48.97	**40.00**
β	deg	——	42.35	23.87	——	——

For a calorically perfect gas, this simplifies to

$$\eta_s = \frac{T_{t3s} - T_{t1}}{T_{t3} - T_{t1}} = \frac{(P_{t3}/P_{t1})^{(\gamma-1)/\gamma} - 1}{T_{t3}/T_{t1} - 1} \tag{9.10}$$

where the states used in this equation for stage efficiency are plotted on the *T-s* diagram of Fig. 9.14a.

The *polytropic efficiency* of an adiabatic compressor is defined as the ratio of the ideal work per unit mass to the actual work per unit mass for a differential

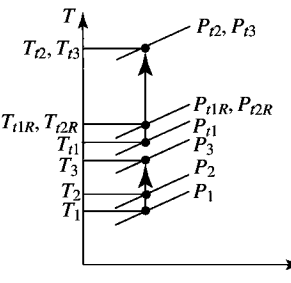

Fig. 9.13 Property changes of an isentropic compressor stage.

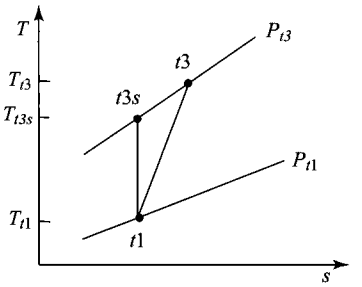

Fig. 9.14a Stages for definition of compressor stage efficiency.

pressure change, or

$$e_c = \frac{dh_{ti}}{dh_t} = \frac{dT_{ti}}{dT_t} = \frac{dT_{ti}/T_t}{dT_t/T_t} = \frac{\gamma - 1}{\gamma}\frac{dP_t/P_t}{dT_t/T_t}$$

For a constant polytropic efficiency e_c, integration between states $t1$ and $t3$ gives

$$e_c = \frac{\gamma - 1}{\gamma}\frac{\ell n\,(P_{t3}/P_{t1})}{\ell n\,(T_{t3}/T_{t1})} \tag{9.11}$$

A useful expression for stage efficiency, in terms of the pressure ratio and polytropic efficiency, can be easily obtained by using Eqs. (9.10) and (9.11). Solving Eq. (9.11) for the temperature ratio and substituting into Eq. (9.10) give

$$\eta_s = \frac{(P_{t3}/P_{t1})^{(\gamma-1)/\gamma} - 1}{(P_{t3}/P_{t1})^{(\gamma-1)/(\gamma e_c)} - 1} \tag{9.12}$$

In the limit, as the pressure ratio approaches 1, the stage efficiency approaches the polytropic efficiency. The variation in stage efficiency with stage pressure ratio is plotted in Fig. 9.14b for constant polytropic efficiency.

The compressor polytropic efficiency is useful in preliminary design of compressors for gas turbine engines to predict the compressor efficiency for a given level of technology. The value of the polytropic efficiency is mainly a

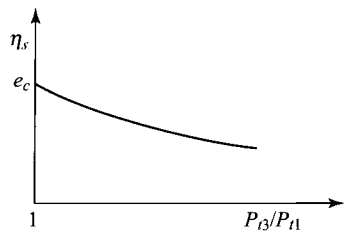

Fig. 9.14b Variation of stage efficiency with pressure ratio.

function of the technology level (see Table 6.2). Axial-flow compressors designed in the 1980s have a polytropic efficiency of about 0.88, whereas the compressors being designed today have a polytropic efficiency of about 0.9.

9.3.4.2 Degree of reaction. For compressible flow, the *degree of reaction* is defined as

$$^{\circ}R_c = \frac{\text{rotor static enthalpy rise}}{\text{stage static enthalpy rise}} = \frac{h_2 - h_l}{h_3 - h_1} \tag{9.13a}$$

For a calorically perfect gas, the static enthalpy rises in the equation become static temperature rises, and the degree of reaction is

$$^{\circ}R_c = \frac{T_2 - T_1}{T_3 - T_1} \tag{9.13b}$$

In the general case, it is desirable to have the degree of reaction in the vicinity of 0.5 because the rotor and stator rows then will "share the burden" of increasing the enthalpy of the flow. The degree of reaction for the stage data of Example 9.1 is approximately 0.28, which means the majority of the static temperature rise occurs in the stator.

9.3.4.3 Cascade airfoil nomenclature and loss coefficient. Figure 9.15 shows the cascade airfoil nomenclature and the airfoil and flow angles. Subscripts i and e are used for the inlet and exit states, respectively. The ratio of the airfoil chord c to the airfoil spacing s is called the *solidity* σ, which typically is near unity. At design, the incidence angle is nearly zero. The exit deviation can be determined by using Carter's rule:

$$\delta_c = \frac{\gamma_i - \gamma_e}{4\sqrt{\sigma}} \tag{9.14}$$

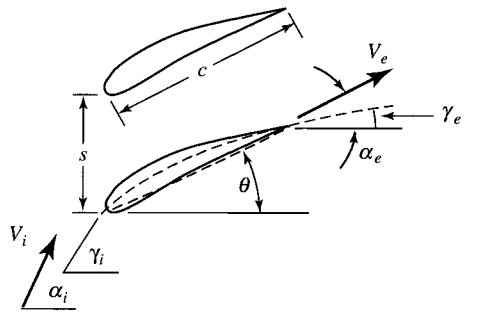

$\alpha_i - \alpha_e$ = turning angle
$\gamma_i - \gamma_e$ = airfoil camber angle
$\alpha_i - \gamma_i$ = incidence angle
$\alpha_e - \gamma_e = \delta_c$ = exit deviation
$\sigma = c/s$ = solidity
θ = stagger angle

Fig. 9.15 Cascade airfoil nomenclature.

The airfoil angles of both the rotor and the stator can be calculated from the flow angles, given the incidence angle and solidity for each. To obtain the exit airfoil angle, Eq. (9.14) is rearranged to give

$$\gamma_e = \frac{4\alpha_e\sqrt{\sigma} - \gamma_i}{4\sqrt{\sigma} - 1}$$

For the data of Example 9.1, we obtain the following airfoil angles, assuming a solidity of 1 and a zero incidence angle for both rotor and stator:

Rotor	$\gamma_i = 42.35\,\text{deg}$	$\gamma_e = 17.71\,\text{deg}$
Stator	$\gamma_i = 48.97\,\text{deg}$	$\gamma_e = 37.01\,\text{deg}$

Losses in cascade airfoils are normally quantified in terms of the drop in total pressure divided by the dynamic pressure of the incoming flow. This ratio is called the *total pressure loss coefficient* and is defined as

$$\phi_c \equiv \frac{P_{ti} - P_{te}}{\rho V_i^2/(2g_c)} \tag{9.15}$$

Figure 9.16 shows the typical total pressure loss behavior of compressor airfoils obtained from cascade tests. Note that these losses increase with Mach number and incidence angle. The loss coefficients shown in Fig. 9.16 include only the two-dimensional or "profile" losses and must be increased in compressor stage design to account for end losses (e.g., tip leakage, wall boundary layer, or cavity leakage).

9.3.4.4 Diffusion Factor. The total pressure loss of a cascade depends on many factors. The pressure and velocity distribution about a typical cascade airfoil is shown in Fig. 9.17. The upper (suction) side of the compressor blade has a large static pressure rise (due to the deceleration from $V_{\max}$ to V_e), which

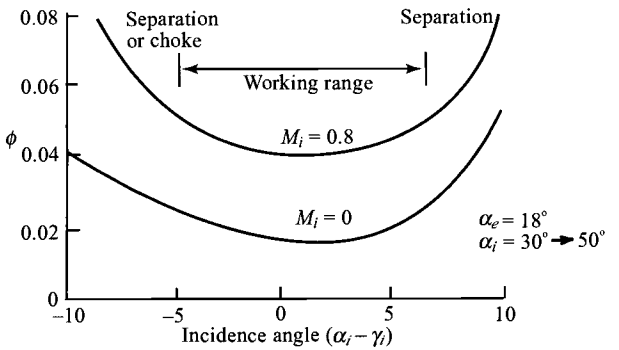

Fig. 9.16 Compressor cascade experimental behavior.

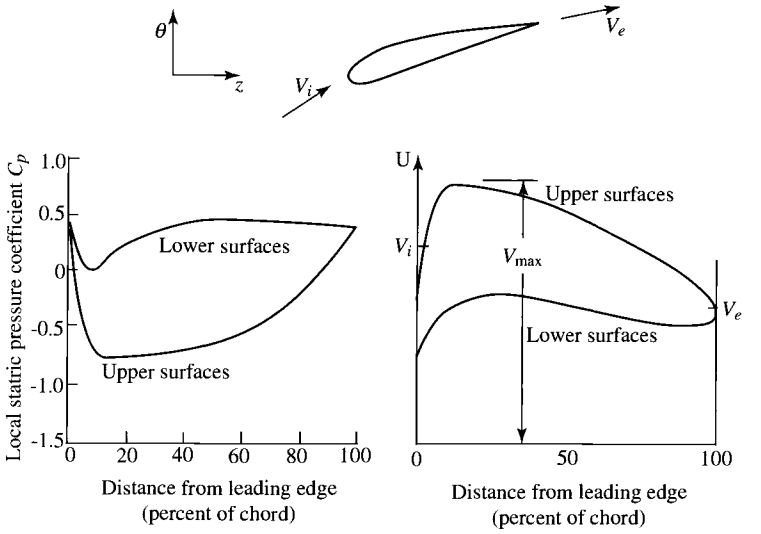

Fig. 9.17 Compressor airfoil pressure and velocity distribution (Ref. 41).

can cause the viscous boundary layer to separate. Boundary-layer separation is not desirable because of the associated higher losses in total pressure.

Cascade test results (see Fig. 9.18) show a direct correlation between total pressure loss and the deceleration (diffusion) on the upper (suction) side of blades. The amount of diffusion is measured by the diffusion factor D. The expression for the diffusion factor is based on the fact that the diffusion of the flow on the suction surface is approximated as

$$D \approx \frac{V_{\max} - V_e}{V_{\text{av}}} \approx \frac{V_{\max} - V_e}{V_i}$$

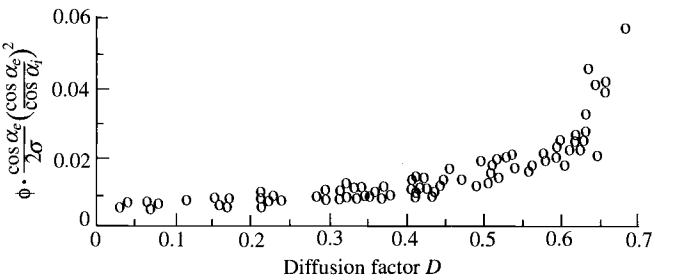

Fig. 9.18 Total pressure loss vs diffusion factor for typical compressor airfoil (Ref. 41).

where

$$V_{\max} \approx V_i + f\left(\frac{\Delta v}{\sigma}\right) \approx V_i + \frac{|\Delta v|}{2\sigma}$$

Thus the *diffusion factor D* is defined by

$$D \equiv 1 - \frac{V_e}{V_i} + \frac{|v_i - v_e|}{2\sigma V_i} \tag{9.16}$$

where the subscripts i and e refer to the inlet and exit, respectively. Note that for a compressor stage, there is a diffusion factor for the rotor and another for the stator.

The diffusion factor for the rotor D_r is in terms of the relative velocities at stations 1 and 2, or

$$D_r = 1 - \frac{V_{2R}}{V_{1R}} + \frac{|v_{1R} - v_{2R}|}{2\sigma V_{1R}} \tag{9.17}$$

The diffusion factor for the stator D_s is in terms of the absolute velocities at stations 2 and 3, or

$$D_s = 1 - \frac{V_3}{V_2} + \frac{|v_2 - v_3|}{2\sigma V_2} \tag{9.18}$$

Figure 9.18 shows a loss parameter vs diffusion factor for typical compressor cascade airfoils. This figure is useful for estimating total pressure losses during preliminary design. Because the total pressure loss increases dramatically for diffusion factors above 0.6, *designs of axial compressors are limited to diffusion factors less than or equal to 0.6*. The diffusion factors for the data of Example 9.1, with a solidity of 1, are

$$D_r = 1 - \frac{V_{2R}}{V_{1R}} + \frac{|v_{1R} - v_{2R}|}{2\sigma V_{1R}} = 1 - \frac{687.10}{772.90} + \frac{|520.66 - 278.04|}{2 \times 1 \times 772.90} = 0.2680$$

$$D_s = 1 - \frac{V_3}{V_2} + \frac{|v_2 - v_3|}{2\sigma V_2} = 1 - \frac{774.22}{957.10} + \frac{|721.96 - 497.66|}{2 \times 1 \times 957.10} = 0.3083$$

These values of diffusion factor show that both the rotor and stator of the example problem are lightly loaded.

9.3.4.5 Stage loading and flow coefficients. The ratio of the stage work to rotor speed squared is called the *stage loading coefficient* and is defined as

$$\psi \equiv \frac{g_c \Delta h_t}{(\omega r)^2} = \frac{g_c \Delta h_t}{U^2} \tag{9.19}$$

For a calorically perfect gas, the stage loading coefficient can be written as

$$\psi = \frac{g_c c_p \, \Delta T_t}{(\omega r)^2} = \frac{g_c c_p \, \Delta T_t}{U^2} \tag{9.20}$$

Modern axial-flow compressors used for aircraft gas turbine engines have stage loading coefficients in the range of 0.3–0.35 at the mean radius. For Example 9.1, the stage loading coefficient is 0.24, a low value.

The ratio of the axial velocity to the rotor speed is called the *flow coefficient* and is defined as

$$\Phi \equiv \frac{u_1}{\omega r} = \frac{u_1}{U} \tag{9.21}$$

The flow coefficients for modern axial-flow compressors of aircraft gas turbine engines are in the range of 0.45–0.55 at the mean radius. For Example 9.1, the flow coefficient is 0.57, a high value.

Equations (9.20) and (9.21) can be substituted into Eqs. (9.7a) and (9.7b), respectively, to give

$$\frac{\psi}{\Phi} = \tan\beta_1 - \frac{u_2}{u_1}\tan\beta_2 \quad \text{and} \quad \frac{\psi}{\Phi} = \frac{u_2}{u_1}\tan\alpha_2 - \tan\alpha_1 \tag{9.22}$$

Equation (9.22) is plotted in Fig. 9.19 for the case of constant axial velocity ($u_1 = u_2$). This figure can be used to determine the ratio of the stage loading

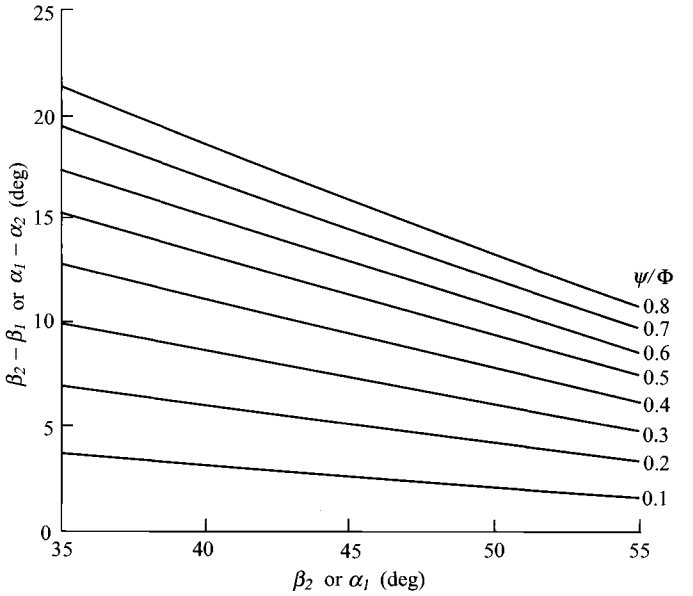

Fig. 9.19 Stage flow angles vs Ψ/Φ for constant axial velocity.

coefficient to the flow coefficient from stage flow angles. This figure also gives the combinations of flow angles that will give a desired value of ψ/Φ.

The flow coefficient can be expressed in terms of the flow angles (α_1 and β_1). From the velocity triangles, we have

$$U = u_1 \tan \alpha_1 + u_1 \tan \beta_1$$

Solving for the ratio u_1/U, we get

$$\Phi = \frac{1}{\tan \alpha_1 + \tan \beta_1} \tag{9.23}$$

This equation is plotted in Fig. 9.20. Given the flow angles (α_1 and, β_1), one can use Eq. (9.23) or Fig. 9.20 to determine the flow coefficient. On the other hand, Fig. 9.20 can be used to find the combination of the flow angles (α_1 and β_1) that gives a desired flow coefficient.

9.3.4.6 Stage pressure ratio. Equation (9.10) can be rewritten as

$$\frac{P_{t3}}{P_{t1}} = \left(1 + \eta_s \frac{\Delta T_t}{T_{t1}}\right)^{\gamma/(\gamma-1)} \tag{9.24}$$

Likewise, Eq. (9.11) can be rewritten as

$$\frac{P_{t3}}{P_{t1}} = \left(\frac{T_{t2}}{T_{t1}}\right)^{\gamma e_c/(\gamma-1)} = \left(1 + \frac{\Delta T_t}{T_{t1}}\right)^{\gamma e_c/(\gamma-1)} \tag{9.25}$$

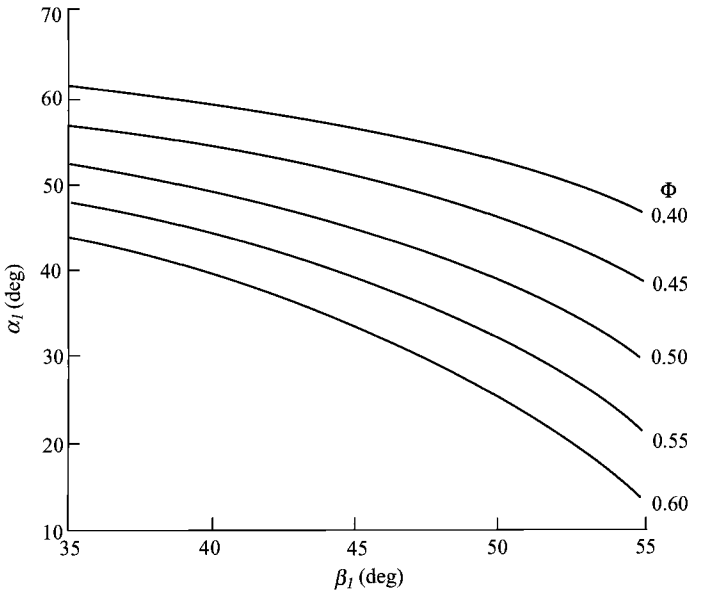

Fig. 9.20 Flow coefficient Φ vs flow angles α_1 and β_1.

The stage pressure ratio can be calculated given the stage total temperature rise and the stage efficiency or polytropic efficiency from Eq. (9.24) or (9.25), respectively. We can see from these equations and Eq. (9.20) that a high stage pressure ratio requires high work loading (change in T_t).

When the stage efficiency and polytropic efficiency are unknown, the stage pressure ratio can be determined by using loss coefficients based on cascade data and other losses. The total pressure for a compressor stage can be written in terms of loss coefficients of the rotor ϕ_{cr} and stator ϕ_{cs}. Noting that the total pressure loss of the rotor is based on the relative velocity, we write

$$\phi_{cr} \equiv \frac{P_{t1R} - P_{t2R}}{\rho_1 V_{1R}^2/(2g_c)} \tag{9.26}$$

Then

$$\frac{P_{t2R}}{P_{t1R}} = 1 - \phi_{cr}\frac{\rho_1 V_{1R}^2}{2g_c P_{t1R}} = 1 - \phi_{cr}\frac{\gamma P_1 M_{1R}^2}{2P_{t1R}}$$

or

$$\frac{P_{t2R}}{P_{t1R}} = 1 - \phi_{cr}\frac{\gamma M_{1R}^2/2}{\{1 + [(\gamma - 1)/2]M_{1R}^2\}^{\gamma/(\gamma-1)}} \tag{9.27}$$

Likewise,

$$\phi_{cs} \equiv \frac{P_{t2} - P_{t3}}{\rho_2 V_2^2/(2g_c)} \tag{9.28}$$

then

$$\frac{P_{t3}}{P_{t2}} = 1 - \phi_{cs}\frac{\gamma M_2^2/2}{\{1 + [(\gamma - 1)/2]M_2^2\}^{\gamma/(\gamma-1)}} \tag{9.29}$$

The total pressure ratio of a stage can be written in the following form:

$$\frac{P_{t3}}{P_{t1}} = \left(\frac{P_{t3}}{P_{t2}}\right)_{\phi_{cs},\, M_2}\left(\frac{P_{t2}}{P_2}\right)_{M_2}\left(\frac{P_2}{P_{t2R}}\right)_{M_{2R}}\left(\frac{P_{t2R}}{P_{t1R}}\right)_{\phi_{cr},\, M_{1R}} \times \left(\frac{P_{t1R}}{P_1}\right)_{M_1 R}\left(\frac{\rho_1}{P_{t1}}\right)_{M_1} \tag{9.30}$$

where the subscripts for the ratio inside the parentheses indicate the variables of the ratio. The loss coefficient of the rotor ϕ_{cr} required in Eq. (9.27) is obtained from cascade data with allowance for other losses (tip leakage, side wall boundary layer, etc.) and can range in value from 0.05 to 0.12. Likewise, the stator's loss coefficient ϕ_{cs} required in Eq. (9.28) is also obtained from cascade data with allowance for other losses and can range in value from 0.03 to 0.06.

Figure 9.21 is a *T-s* diagram of a compressor stage with losses. It shows the losses in total pressure in the rotor and the stator. Comparison with the *T-s* diagram for an ideal compressor stage (Fig. 9.13) can help one see the effects of losses on the process through a compressor stage.

9.3.4.7 Blade Mach number M_b. Equation (9.7) can be written in terms of the flow angles (α_1 and β_2) and rearranged to give

$$\frac{\Delta T_t}{T_{t1}} = \frac{(\omega r)^2}{g_c c_p T_{t1}} \left[1 - \frac{u_2}{\omega r} \left(\tan \beta_2 + \frac{u_1}{u_2} \tan \alpha_1 \right) \right]$$

or

$$\frac{\Delta T_t}{T_{t1}} = \frac{(\omega r)^2}{g_c c_p T_1} \frac{T_1}{T_{t1}} \left[1 - \frac{u_2}{\omega r} \left(\tan \beta_2 + \frac{u_1}{u_2} \tan \alpha_1 \right) \right]$$

Note that

$$\frac{(\omega r)^2}{g_c c_p T_1} = \frac{\gamma R}{c_p} \frac{(\omega r)^2}{\gamma R g_c T_1} = (\gamma - 1) \frac{(\omega r)^2}{a_1^2} = (\gamma - 1) M_b^2$$

where M_b is the blade tangential Mach number based on the upstream speed of sound a_1,

$$\frac{T_1}{T_{t1}} = \frac{1}{1 + [(\gamma - 1)/2] M_1^2} \quad \text{and} \quad \frac{u_2}{\omega r} = (\cos \alpha_1) \frac{M_1}{M_b} \frac{u_2}{u_1}$$

Then

$$\frac{\Delta T_t}{T_{t1}} = \frac{(\gamma - 1) M_b^2}{1 + [(\gamma - 1)/2] M_1^2} \left[1 - (\cos \alpha_1) \frac{M_1}{M_b} \left(\frac{u_2}{u_1} \tan \beta_2 + \tan \alpha_1 \right) \right] \tag{9.31}$$

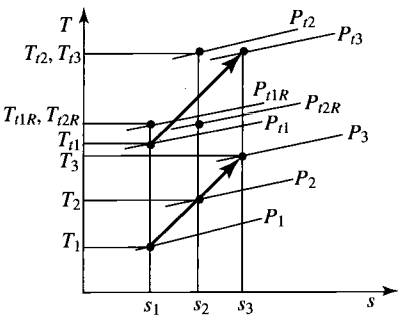

Fig. 9.21 The *T-s* diagram of a typical compressor stage with losses.

If we consider that the flow angles and the velocity ratio u_2/u_1 are functions of the geometry, then the stage temperature rise is mainly a function of M_b and the ratio M_1/M_b. From Eq. (9.31), we can see that high M_b is desirable to give higher stage temperature rise. The blade Mach number for Example 9.1 is about 0.94.

Example 9.2

Consider mean radius stage calculation—flow with losses.

Given:

$$T_{t1} = 288.16\ \text{K}, \quad P_{t1} = 101.3\ \text{kPa}, \quad \omega = 1000\ \text{rad/s}$$
$$r = 0.3048\ \text{m}, \quad \alpha_1 = \alpha_3 = 40\ \text{deg}, \quad \sigma = 1$$
$$\dot{m} = 22.68\ \text{kg/s}, \quad M_1 = M_3 = 0.7, \quad u_2/u_1 = 1.1$$
$$\Delta T_t = 22.43\ \text{K}, \quad \phi_{cr} = 0.09, \quad \phi_{cs} = 0.03$$

Gas is air. The input data are the same as in Example 9.1 with the same ΔT_t specified.

Note: For air, $\gamma = 1.4$, $c_p = 1.004\ \text{kJ/(kg} \cdot \text{K)}$, and $R = 0.287\ \text{kJ/(kg} \cdot {}^\circ\text{R)}$.

Solution:

$$T_1 = \frac{T_{t1}}{1 + [(\gamma - 1)/2]M_1^2} = \frac{288.16\ \text{K}}{1 + 0.2 \times 0.7^2} = 262.44\ \text{K}$$

$$a_1 = \sqrt{\gamma R g_c T_1} = \sqrt{1.4 \times 287 \times 1 \times 262.44} = 324.73\ \text{m/s}$$

$$V_1 = M_1 a_1 = 0.7 \times 324.73 = 227.31\ \text{m/s}$$

$$u_1 = V_1 \cos\alpha_1 = 227.31 \times 0.7660 = 174.13\ \text{m/s}$$

$$v_1 = V_1 \sin\alpha_1 = 227.31 \times 0.6428 = 146.11\ \text{m/s}$$

$$P_1 = \frac{P_{t1}}{\{1 + [(\gamma - 1)/2]M_1^2\}^{\gamma/(\gamma-1)}}$$

$$= \frac{101.3\ \text{kPa}}{(1 + 0.2 \times 0.7^2)^{3.5}} = 73.03\ \text{kPa}$$

$$\text{MFP}(M_1) = 0.03700$$

$$A_1 = \frac{\dot{m}\sqrt{T_{t1}}}{P_{t1}(\cos\alpha_1)\text{MFP}(M_1)} = \frac{22.68\sqrt{288.16}}{101,300 \times 0.7660 \times 0.0370}$$

$$= 0.134\ \text{m}^2$$

$$\omega r = 1000 \times 0.3048 = 304.8\ \text{m/s}$$

$$v_{1R} = \omega r - v_1 = 304.80 - 146.11 = 158.69\ \text{m/s}$$

$$\beta_1 = \tan^{-1}\frac{v_{1R}}{u_1} = \tan^{-1} 0.9113 = 42.34 \text{ deg}$$

$$V_{1R} = \sqrt{u_1^2 + v_{1R}^2} = \sqrt{174.13^2 + 158.69^2} = 235.59 \text{ m/s}$$

$$M_{1R} = \frac{V_{1R}}{a_1} = \frac{235.59}{324.73} = 0.7255$$

$$T_{t1R} = T_1\left(1 + \frac{\gamma - 1}{2}M_{1R}^2\right) = 262.44(1 + 0.2 \times 0.7255^2) = 290.07 \text{ K}$$

$$P_{t1R} = P_1\left(\frac{T_{t1R}}{T_1}\right)^{\gamma/(\gamma-1)} = 73.03\left(\frac{290.07}{262.44}\right)^{3.5} = 103.67 \text{ kPa}$$

$$P_{t2R} = P_{t1R}\left(\frac{P_{t2R}}{P_{t1R}}\right)_{\phi_{cr}, M_{1R}}$$

$$= P_{t1R}\left(1 - \phi_{cr}\frac{\gamma M_{1R}^2/2}{\{1 + [(\gamma - 1)/2]M_{1R}^2\}^{\gamma/(\gamma-1)}}\right)$$

$$P_{t2R} = 103.67\left[1 - \frac{0.09 \times 0.7 \times 0.7255^2}{(1 + 0.2 \times 0.7255^2)^{3.5}}\right]$$

$$= 103.67 \times 0.9766 = 101.24 \text{ kPa}$$

$$T_{t2R} = T_{t1R} = 290.07 \text{ K}$$

$$T_{t2} = T_{t1} + \Delta T_t = 288.16 + 22.43 = 310.59 \text{ K}$$

$$\tan\beta_2 = \frac{u_1}{u_2}\left[\tan\beta_1 - \frac{g_c c_p}{\omega r u_1}(T_{t2} - T_{t1})\right]$$

$$\tan\beta_2 = \frac{1}{1.1}\left[\tan 42.34 - \frac{1004}{304.8 \times 174.13}(310.59 - 288.16)\right]$$

$$= 0.4426$$

$$\beta_2 = 23.87 \text{ deg}$$

$$u_2 = \frac{u_2}{u_1}u_1 = 1.1 \times 174.13 = 191.54 \text{ m/s}$$

$$v_{2R} = u_2 \tan\beta_2 = 191.54 \times 0.4426 = 84.78 \text{ m/s}$$

$$V_{2R} = \sqrt{u_2^2 + v_{2R}^2} = \sqrt{191.54^2 + 84.78^2} = 209.46 \text{ m/s}$$

$$v_2 = \omega r - v_{2R} = 304.80 - 84.78 = 220.02 \text{ m/s}$$

$$\alpha_2 = \tan^{-1}\frac{v_2}{u_2} = \tan^{-1}\frac{220.02}{191.54} = 48.96 \text{ deg}$$

$$V_2 = \sqrt{u_2^2 + v_2^2} = \sqrt{191.54^2 + 220.02^2} = 291.71\,\text{m/s}$$

$$T_2 = T_{t2} - \frac{V_2^2}{2g_c c_p} = 310.59 - \frac{291.71^2}{2 \times 1 \times 1004} = 268.21\,\text{K}$$

$$P_2 = P_{t2R}\left(\frac{T_2}{T_{t2R}}\right)^{\gamma/(\gamma-1)} = 101.24\left(\frac{268.21}{290.07}\right)^{3.5} = 76.96\,\text{kPa}$$

$$a_2 = \sqrt{\gamma R g_c T_2} = \sqrt{1.4 \times 287 \times 268.21} = 328.28\,\text{m/s}$$

$$M_2 = \frac{V_2}{a_2} = \frac{291.71}{328.28} = 0.8886$$

$$M_{2R} = \frac{V_{2R}}{a_2} = \frac{209.46}{328.28} = 0.6381$$

$$P_{t2} = P_2\left(\frac{T_{t2}}{T_2}\right)^{\gamma/(\gamma-1)} = 76.96\left(\frac{310.59}{268.21}\right)^{3.5} = 128.61\,\text{kPa}$$

$$\text{MFP}(M_2) = 0.04004$$

$$A_2 = \frac{\dot{m}\sqrt{T_{t2}}}{P_{t2}(\cos\alpha_2)\text{MFP}(M_2)} = \frac{22.68\sqrt{310.59}}{128{,}610 \times 0.65659 \times 0.04004}$$
$$= 0.118\,\text{m}^2$$

$$T_{t3} = T_{t2} = T_{t1} + \Delta T_t = 310.59\,\text{K}$$

$$T_3 = \frac{T_{t3}}{1 + [(\gamma-1)/2]M_3^2} = \frac{310.59\,\text{K}}{1 + 0.2 \times 0.7^2} = 282.87\,\text{K}$$

$$P_{t3} = P_{t2}\left(\frac{P_{t3}}{P_{t2}}\right)_{\phi_{cs}, M_2}$$
$$= P_{t2}\left(1 - \phi_{cs}\frac{\gamma M_2^2/2}{\{1 + [(\gamma-1)/2]M_2^2\}^{\gamma/(\gamma-1)}}\right)$$
$$= 128.61\left[1 - \frac{0.03 \times 0.7 \times 0.8887^2}{(1 + 0.2 \times 0.8887^2)^{3.5}}\right]$$
$$= 128.61 \times 0.09900 = 127.32\,\text{kPa}$$

$$P_3 = P_{t3}\left(\frac{T_3}{T_{t3}}\right)^{\gamma/(\gamma-1)} = 127.32\left(\frac{282.87}{310.59}\right)^{3.5} = 91.79\,\text{kPa}$$

$$a_3 = \sqrt{\gamma R g_c T_3} = \sqrt{1.4 \times 287 \times 282.87} = 337.13\,\text{m/s}$$

$$V_3 = M_3 a_3 = 0.7 \times 337.13 = 235.99\,\text{m/s}$$

$$u_3 = V_3 \cos \alpha_3 = 180.78 \text{ m/s}$$

$$v_3 = V_3 \sin \alpha_3 = 151.69 \text{ m/s}$$

$$A_3 = \frac{\dot{m}\sqrt{T_{t3}}}{P_{t3}(\cos \alpha_3)\text{MFP}(M_3)} = \frac{22.68\sqrt{310.59}}{127{,}320 \times 0.7660 \times 0.0370} = 0.111 \text{ m}^2$$

$$^{\circ}R_c = \frac{T_2 - T_1}{T_3 - T_1} = \frac{268.21 - 262.44}{282.87 - 262.44} = 0.2824$$

$$D_r = 1 - \frac{V_{2R}}{V_{1R}} + \frac{|v_{1R} - v_{2R}|}{2\sigma V_{1R}} = 1 - \frac{209.46}{235.59} + \frac{|158.69 - 84.78|}{2 \times 1 \times 235.59} = 0.2678$$

$$D_s = 1 - \frac{V_3}{V_2} + \frac{|v_2 - v_3|}{2\sigma V_2} = 1 - \frac{235.99}{291.71} + \frac{|220.02 - 151.69|}{2 \times 1 \times 291.71} = 0.3081$$

$$\eta_s = \frac{(P_{t3}/P_{t1})^{(\gamma-1)/\gamma} - 1}{T_{t3}/T_{t1} - 1} = \frac{(127.32/101.30)^{1/3.5} - 1}{310.59/288.16} = 0.8672$$

$$e_c = \frac{\gamma - 1}{\gamma} \frac{\ell n(P_{t3}/P_{t1})}{\ell n(T_{t3}/T_{t1})} = \frac{1}{3.5} \frac{\ell n(127.32/101.30)}{\ell n(310.59/288.16)} = 0.8714$$

$$\psi = \frac{g_c c_p \Delta T_t}{(\omega r)^2} = \frac{1 \times 1004 \times 22.43}{304.8^2} = 0.2424$$

$$\Phi = \frac{u_1}{\omega r} = \frac{174.13}{304.8} = 0.5713$$

The results of this example stage calculation with losses are summarized in Table 9.3, with the given data listed in boldface type (results in English units are shown within parentheses). One sees, by comparison with the isentropic flow results of Example 9.1 (see Table 9.2), that all the properties are the same except the total and static pressures at stations $2R$, 2, and 3. One might also want to compare the change in flow properties listed in Table 9.3 with those sketched in Fig. 9.21.

With losses, the resulting stage pressure ratio of Example 9.2 is 1.257. Without losses, the same amount of work per unit mass gives a pressure ratio of 1.300 for Example 9.1. Also note that the flow areas at stations 2 and 3 are larger in Example 9.2 than in Example 9.1 because of the lower total pressures resulting from losses.

9.3.5 Repeating-Stage, Repeating-Row, Mean-Line Design

The analysis and design of an axial-flow compressor is complex with many design choices. To simplify the design, we will consider a stage (Fig. 9.22) whose exit velocity and flow angle equal those at its inlet (repeating stage), made up of "repeating" (i.e., mirror-image) rows of airfoils. The analysis will

Table 9.3 Results for Example 9.2 axial-flow compressor stage calculation, flow with loss

Property		Station 1	1*R*	2*R*	2	3
T_t	K	**288.2**	290.1	290.1	310.6	**310.6**
	(°R)	(518.7)	(522.1)	(522.1)	(559.1)	(559.1)
T	K	262.4	262.4	268.2	268.2	282.9
	(°R)	(472.4)	(472.4)	(482.8)	(482.8)	(509.2)
P_t	kPa	**101.3**	103.7	101.2	128.6	127.3
	(psia)	(14.69)	(15.04)	(14.68)	(18.65)	(18.46)
P	kPa	73.03	73.03	76.96	76.96	91.79
	(psia)	(10.59)	(10.59)	(11.16)	(11.16)	(13.31)
M		**0.700**	0.7255	0.6381	0.8886	**0.700**
V	m/s	227.31	235.59	209.46	291.71	235.99
	(ft/s)	(745.76)	(772.92)	(687.20)	(957.04)	(774.24)
u	m/s	174.13	174.13	191.54	191.54	180.78
	(ft/s)	(571.29)	(571.29)	(628.40)	(628.40)	(593.10)
v	m/s	146.11	158.69	84.78	220.02	151.69
	(ft/s)	(479.36)	(520.63)	(278.15)	(721.84)	(497.66)
α	deg	**40.00**	——	——	48.96	**40.00**
β	deg	——	42.34	23.87	——	——

be based on the behavior of the flow at the *average radius* (halfway between the hub radius and the tip radius), known henceforth as the *mean radius*. With this introduction in mind, the development of design tools for compressors follows.

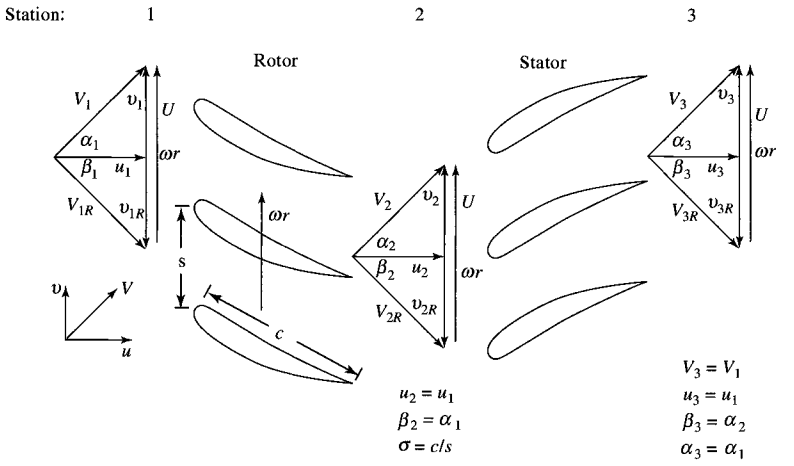

Fig. 9.22 Repeating-row compressor stage nomenclature.

9.3.5.1 Assumptions. We make the following assumptions for this analysis:

1) Repeating-row, repeating-airfoil cascade geometry ($\alpha_1 = \beta_2 = \alpha_3$, $\beta_1 = \alpha_2 = \beta_3$, $u_1 = u_2 = u_3$)
2) Two-dimensional flow (i.e., no variation or component of velocity normal to the page)
3) Polytropic efficiency e_c representing stage losses
4) Constant mean radius

9.3.5.2 Analysis. We assume that the following data are given: $D, M_1, \gamma, \sigma, e_c$. The analysis of the repeating-row, repeating-stage, mean-line design follows.

Conservation of mass: Application of this law for steady one-dimensional flow gives

$$\rho_1 u_1 A_1 = \rho_2 u_2 A_2 = \rho_3 u_3 A_3$$

or

$$\rho_1 A_1 = \rho_2 A_2 = \rho_3 A_3 \tag{9.32}$$

Repeating-row constraint: Since $\beta_2 = \alpha_1$, then

$$v_{2R} = v_1 = \omega r - v_2$$

or

$$v_1 + v_2 = \omega r \tag{9.33}$$

Also, since $\beta_3 = \alpha_2$, then $v_{3R} = v_2$ and $v_3 = v_1$; thus, the stage exit conditions are indeed identical to those at the stage entrance.

Diffusion factor: Since both

$$D = 1 - \frac{V_{2R}}{V_{1R}} + \frac{v_{1R} - v_{2R}}{2\sigma V_{1R}} = 1 - \frac{V_3}{V_2} + \frac{v_2 - v_3}{2\sigma V_2}$$

and

$$D = 1 - \frac{\cos \alpha_2}{\cos \alpha_1} + \frac{\tan \alpha_2 - \tan \alpha_1}{2\sigma} \cos \alpha_2 \tag{9.34}$$

are the same for both the rotor and stator, D is evaluated only once for the stage. Rearranging Eq. (9.34) to solve for α_2, we find that

$$\cos \alpha_2 = \frac{2\sigma(1 - D)\Gamma + \sqrt{\Gamma^2 + 1 - 4\sigma^2(1 - D)^2}}{\Gamma^2 + 1} \tag{9.35}$$

where

$$\Gamma \equiv \frac{2\sigma + \sin \alpha_1}{\cos \alpha_1} \tag{9.36}$$

In other words, Eq. (9.35) shows that there is *only* one value of α_2 that corresponds to the chosen values of D and σ for each α_1. Thus the entire flowfield geometry is indicated by those choices.

Stage total temperature ratio: From the Euler equation, we have for constant radius

$$c_p(T_{t3} - T_{t1}) = \frac{\omega r}{g_c}(v_2 - v_1)$$

From Eq. (9.33)

$$\omega r = v_1 + v_2$$

then

$$c_p(T_{t3} - T_{t1}) = \frac{1}{g_c}(v_2 + v_1)(v_2 - v_1)$$
$$= \frac{v_2^2 - v_1^2}{g_c} = \frac{V_2^2 - V_1^2}{g_c}$$

Thus

$$\frac{T_{t3}}{T_{t1}} - 1 = \frac{V_2^2 - V_1^2}{c_p g_c T_{t1}}$$

or

$$\tau_s \equiv \frac{T_{t3}}{T_{t1}} = \frac{(\gamma - 1)M_1^2}{1 + [(\gamma - 1)/2]M_1^2}\left(\frac{\cos^2 \alpha_1}{\cos^2 \alpha_2} - 1\right) + 1 \tag{9.37}$$

Stage pressure ratio: From Eq. (9.11), we can write

$$\pi_s \equiv \frac{P_{t3}}{P_{t1}} = \left(\frac{T_{t3}}{T_{r1}}\right)^{\gamma e_c/(\gamma - 1)}$$

or

$$\pi_s = (\tau_s)^{\gamma e_c/(\gamma - 1)} \tag{9.38}$$

Degree of reaction: A special characteristic of repeating-stage, repeating-row compressor stages is that the degree of reaction must be exactly 0.5, as shown in the following:

$$^{\circ}R_c = \frac{T_2 - T_1}{T_3 - T_1} = 1 - \frac{T_3 - T_2}{T_3 - T_1} = 1 - \frac{(V_2^2 - V_3^2)/(2g_c c_p)}{T_{t3} - T_{t1}}$$
$$= 1 - \frac{(V_2^2 - V_1^2)/(2g_c c_p)}{(V_2^2 - V_1^2)/(g_c c_p)} = \frac{1}{2}$$

Stage efficiency: From Eq. (9.10), we have

$$\eta_s = \frac{\pi_s^{(\gamma-1)/\gamma} - 1}{\tau_s - 1} \tag{9.39}$$

Stage exit Mach number: Since

$$V_3 = V_1 \quad \text{and} \quad V^2 = M^2 \gamma R g_c T$$

then

$$\frac{M_3}{M_1} = \sqrt{\frac{T_1}{T_3}}$$

$$= \sqrt{\frac{1}{\tau_s\{1 + [(\gamma-1)/2]M_1^2\} - [(\gamma-1)/2]M_1^2}} \leq 1 \tag{9.40}$$

Inlet velocity/wheel speed ratio $V_1/(\omega r)$: One of the most important trigonometric relationships for the stage is that between the total cascade inlet velocity V_1 and the mean wheel speed ωr. Since

$$V_1 = \frac{u_1}{\cos \alpha_1}$$

and

$$\omega r = v_1 + v_2 = u_1(\tan \alpha_1 + \tan \alpha_2)$$

then u_1 can be eliminated to yield

$$\frac{\omega r}{V_1} = (\cos \alpha_1)(\tan \alpha_1 + \tan \alpha_2) \tag{9.41}$$

Stage loading and flow coefficients: The stage loading coefficient ψ for the repeating-stage, repeating-row, mean-line design can be expressed in terms of the flow angles α_1 and α_2 as

$$\psi = \frac{g_c c_p \Delta T_t}{(\omega r)^2} = \frac{\tan \alpha_2 - \tan \alpha_1}{\tan \alpha_1 + \tan \alpha_2} \tag{9.42a}$$

Likewise, the flow coefficient can be expressed in terms of the flow angles α_1 and α_2 as

$$\Phi = \frac{u_1}{\omega r} = \frac{1}{\tan \alpha_1 + \tan \alpha_2} \tag{9.42b}$$

9.3.5.3 General solution. The behavior of all possible repeating-row compressor stages with given values of D, M_1, γ, σ, and e_c can now be computed. This is done by selecting any α_1 and using the following sequence of equations, expressed as functional relationships:

$$\alpha_2 = f(D, \sigma, \alpha_1) \tag{9.35}$$

$$\Delta\alpha = \alpha_2 - \alpha_1$$

$$\tau_s = f(M_1, \gamma, \alpha_1, \alpha_2) \tag{9.37}$$

$$\pi_s = f(\tau_s, \gamma, e_c) \tag{9.38}$$

$$\eta_s = f(\tau_s, \pi_s, \gamma, e_c) \tag{9.39}$$

$$\frac{\omega r}{V_1} = f(\alpha_1, \alpha_2) \tag{9.41}$$

In most cases, T_{t1} is also known, so that selecting M_1 fixes V_1 and ωr is known.

We can now generate plots of α_2, $\Delta\alpha$, π_s, η_s, and $V_1/(\omega r)$ vs α_1. Note that only π_s depends on M_1 and that the process may be repeated to cover the entire range of reasonable values of α_1.

These calculations have been carried out for $D = 0.6$; $M_1 = 0.45$, 0.5, 0.55, 0.6, 0.65, and 0.7; $\gamma = 1.4$; $e_c = 0.9$; and $0\,\text{deg} < \alpha_1 < 70$ deg. The results are presented on Fig. 9.23. The most notable characteristics of these data are that the most direct way to increase π_s is to increase M_1 and that to operate at higher values of α_1, a large wheel speed is required.

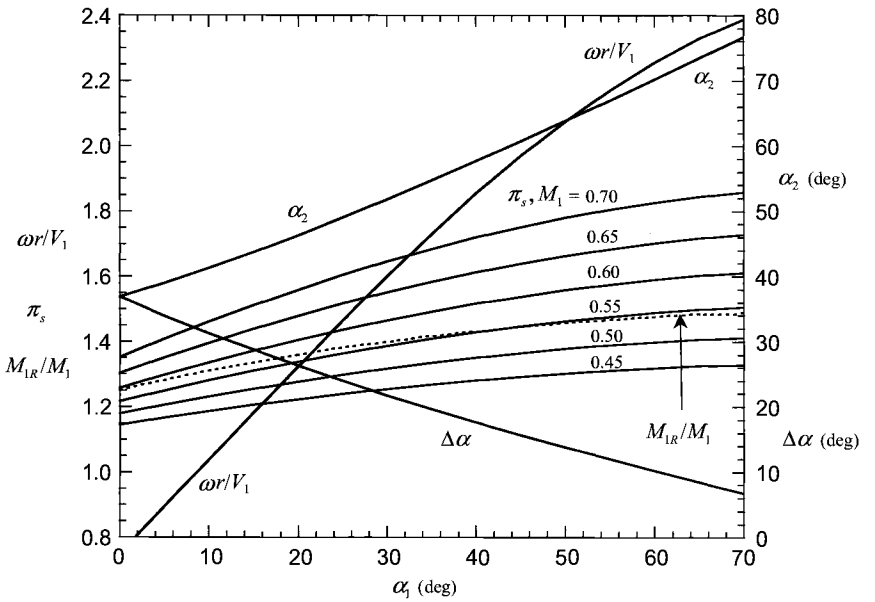

Fig. 9.23 Repeating compressor stage ($D = 0.5$, $\sigma = 1$, and $e_c = 0.9$).

The following two simple examples illustrate the use of this method and are based on the parameters of Fig. 9.23.

Example 9.3

Given:

$$M_1 = 0.6,\ a_1 = 360\,\text{m/s},\ \text{and}\ \omega r = 300\,\text{m/s}$$

Then

$$\frac{\omega r}{V_1} = \frac{\omega r}{a_1 M_1} = 1.39$$

$$\alpha_1 = 22\,\text{deg} \quad \Delta\alpha = 25\,\text{deg}$$

$$\alpha_2 = 47\,\text{deg} \quad \pi_s = 1.42$$

Example 9.4

Given:

$$a_1 = 320\,\text{m/s and } M_1/\alpha_1 = 0.5/20\,\text{deg and } 0.6/30\,\text{deg}$$

Then

M_1	α_1	$\frac{\omega r}{V_1}$	$\frac{\omega r}{a_1}$	π_s
0.5	40 deg	1.852	0.926	1.351
0.6	50 deg	2.075	1.245	1.558

Since a_1 is unaffected by the cascade and affected only slightly by M_1, the price of higher π_s is a greatly increased ωr (that is, $1.245/0.926 = 1.344$).

Figures 9.24 and 9.25 show how the performance of repeating compressor stages changes with diffusion factor and solidity, respectively. For a given inlet flow angle α_1 and inlet velocity V_1, we can see from Fig. 9.24 that increasing the diffusion factor D will increase the exit flow angle α_2, stage pressure ratio π_s, and wheel speed ωr. Likewise, for a given inlet flow angle α_1 and inlet velocity V_1, Fig. 9.25 shows that increasing the solidity σ will increase the exit flow angle α_2, stage pressure ratio π_s, and wheel speed ωr.

For a multistage compressor composed of numerous stages designed by using the repeating-stage, repeating-row, mean-line design, the total temperature change across each of these stages will be the same. Also the mean-line radius for each of these stages is the same. Because the ratio of M_3/M_1 is less than 1, the pressure ratio of any downstream repeating stages will be lower.

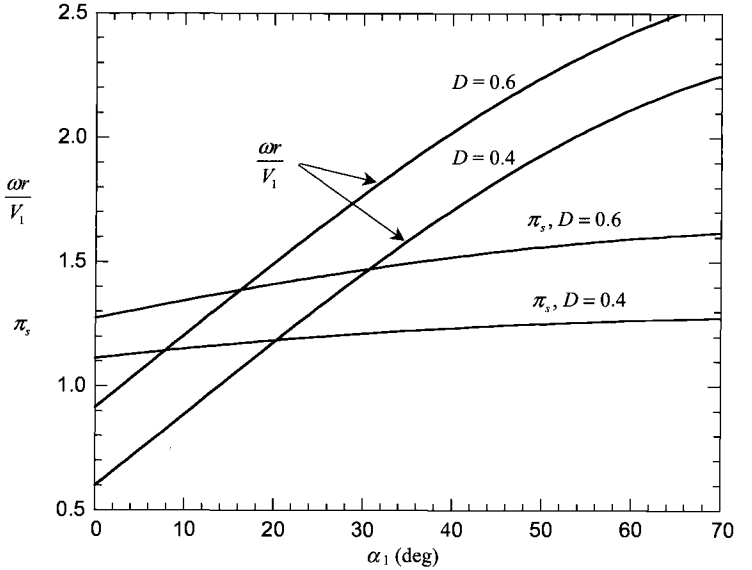

Fig. 9.24 Repeating compressor stage—variation with D ($M_1 = 0.5$, $\sigma = 1$, and $e_c = 0.9$).

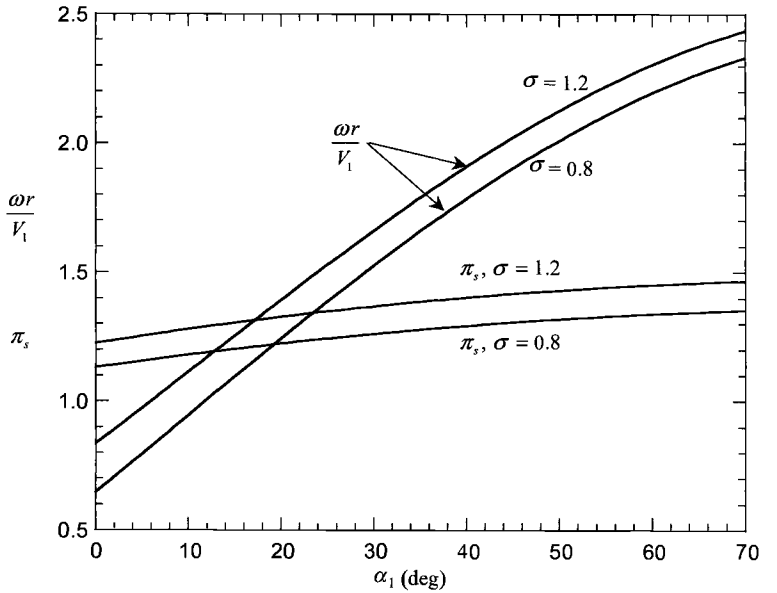

Fig. 9.25 Repeating compressor stage—variation with σ ($M_1 = 0.5$, $D = 0.5$, and $e_c = 0.9$).

Example 9.5

Given:

$$\alpha_1 = 40\,\text{deg}, \quad D = 0.6, \quad \sigma = 1, \quad \gamma = 14, \quad M_1 = 0.5, \quad e_c = 0.9$$

Solution:

$$\Gamma = \frac{2\sigma + \sin\alpha_1}{\cos\alpha_1} = \frac{2 + \sin 40\,\text{deg}}{\cos 40\,\text{deg}} = 3.4499$$

$$\cos\alpha_2 = \frac{2 \times 0.4 \times 3.4499 + \sqrt{3.4499^2 + 1 - 4 \times 1^2 \times 0.4^2}}{3.4499^2 + 1} = 0.4853$$

$$\alpha_2 = 60.966\,\text{deg}$$

$$\tau_s = \frac{0.4 \times 0.5^2}{1 + 0.2 \times 0.5^2}\left(\frac{\cos^2 40\,\text{deg}}{\cos^2 60.966\,\text{deg}} - 1\right) + 1 = 1.142$$

$$\pi_s = 1.142^{3.5 \times 0.9} = 1.519$$

$$\eta_s = \frac{1.519^{1/3.5} - 1}{1.142 - 1} = 0.893$$

$$\frac{M_3}{M_1} = \sqrt{\frac{1}{1.142(1 + 0.2 \times 0.5^2) - 0.4 \times 0.5^2}} = 0.954$$

$$\frac{M_{1R}}{M_1} = \frac{\cos 40\,\text{deg}}{\cos 60.966\,\text{deg}} = 1.578$$

$$M_{1R} = 0.789$$

$$\frac{\omega r}{V_1} = (\cos 40\,\text{deg})(\tan 40\,\text{deg} + \tan 60.966\,\text{deg}) = 2.023$$

$$\psi = \frac{\tan 60.966\,\text{deg} - \tan 40\,\text{deg}}{\tan 40\,\text{deg} + \tan 60.966\,\text{deg}} = 0.364$$

$$\Phi = \frac{1}{\tan 40\,\text{deg} + \tan 60.966\,\text{deg}} = 0.379$$

The flow angles and Mach numbers of a repeating-stage, repeating-row, mean-line design are defined by the preceding calculations. The velocities and temperatures throughout this stage can now be determined by knowing either a velocity or a temperature at any station in the stage. For example, if $T_{t1} = 288.16$ K, then simple calculations give

$$a_1 = 332\,\text{m/s}, \quad V_1 = V_{2R} = V_3 = 166\,\text{m/s}, \quad \omega r = 336\,\text{m/s}$$
$$V_{1R} = V_2 = 261.9\,\text{m/s}, \quad \text{and} \quad \Delta T_t = 40.9\,\text{K}$$

9.3.6 Flow Path Dimensions

9.3.6.1 Annulus area. The preliminary design of multistage axial-flow compressors is typically based on determining each stage's flow properties along the compressor mean line (line along compressor axis that corresponds to the mean radius). The annulus area at any station is based on the flow properties (T_t, P_t, Mach number, and flow angle) at the mean radius and the total mass flow rate. Equation (9.8) is the easiest equation to calculate the flow area at any station i:

$$A_i = \frac{\dot{m}\sqrt{T_{ti}}}{P_{ti}(\cos \alpha_i)\text{MFP}(M_i)}$$

The *mean radius* of a flow annulus is defined as the average of the tip radius and hub radius. Consider Fig. 9.26, which shows a typical annulus area.

In many calculations, the flow area can be calculated and the mean radius is tied to the required rotor speed at the mean radius ωr_m. The designer can select ω and calculate the required mean radius. Then the root radius and tip radius are calculated directly from the mean radius and flow area. In some calculations, the designer may want to select the ratio of the hub radius to the tip radius r_h/r_t. The hub/tip ratio at the inlet to a multistage compressor normally is between 0.6 and 0.75, whereas that at the compressor exit is in the range of 0.9 to 0.92. Then the tip, hub, and mean radii directly follow from the geometry:

$$A = (r_t^2 - r_h^2) = \pi r_t^2 \left[1 - \left(\frac{r_h}{r_t}\right)^2\right]$$

$$r_t = \sqrt{\frac{A}{\pi[1 - (r_h/r_t)^2]}} \qquad r_h = r_t\left(\frac{r_h}{r_t}\right) \qquad r_m = \frac{r_t + r_h}{2}$$

The variation of the flow area and the associated dimensions of the flow path from one station to the next can be calculated easily by using the preceding relationships and the results sketched. Figure 9.27 is a sketch of typical results. The calculation of the axial dimensions requires additional data.

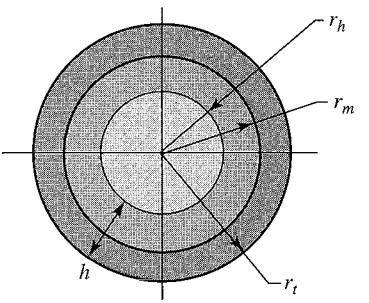

$$r_m = \frac{r_t + r_h}{2}$$

$$A = \pi(r_t^2 - r_h^2)$$

$$A = \pi(r_t + r_h) \times (r_t - r_h)$$

$$A = 2\pi\left(\frac{r_t + r_h}{2}\right) \times (r_t - r_h)$$

$$A = 2\pi r_m \times h, \text{ where } h = r_t - r_h$$

Fig. 9.26 Flow annulus dimensions.

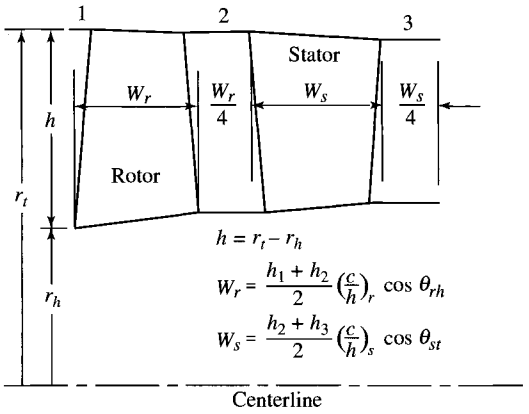

Fig. 9.27 Typical axial dimensions of a compressor stage.

9.3.6.2 Axial dimensions. The axial dimensions of a typical stage are also shown in Fig. 9.27, and these can be used to estimate the axial length of a stage. Blade axial widths (W_r and W_s) of a stage are calculated in the program COMPR along with the blade spacings ($W_r/4$ and $W_s/4$) based on user-input chord-to-height ratios c/h for the rotor and stator blades and assuming a constant chord length for each blade. A minimum width of $\frac{1}{4}$ in. (0.006 m) and a minimum spacing of $\frac{1}{8}$ in. (0.003 m) are used in the plot of compressor cross section and calculation of axial length.

The value of the chord/height ratio c/h selected for a blade depends on such factors as the stage loading coefficient, diffusion factor, etc. Typical values of c/h range from 0.2 to 0.8. Higher values of c/h lead to longer stages and fewer blades.

The chord of a blade c is obtained by multiplying its height h by the user-input chord/height ratio c/h. The blade width (W_r or W_s) is the maximum value of the axial chord c_x for that blade, which depends on the stagger angle θ as shown in Fig. 9.15. The maximum axial chord c_x normally occurs at the hub for a rotor blade and at the tip for a stator blade.

9.3.6.3 Number of blades. The COMPR program calculates the number of blades n_b for the rotor and stator of a stage based on the user-input values of the solidity σ along the mean line. For a rotor or stator, the blade spacing s along the mean line is equal to the blade chord c divided by its solidity ($\sigma = c/s$). The number of blades is simply the circumference of the mean line divided by the blade spacing, rounded up to the next integer.

9.3.6.4 Blade profile. The shapes of compressor rotor and stator blades are based on airfoil shapes developed specifically for compressor applications. One such airfoil shape is the symmetric NACA 65A010 compressor airfoil whose profile shape is shown in Fig. 9.28 and specified in Table 9.4. This airfoil has a thickness that is 10% of its chord c.

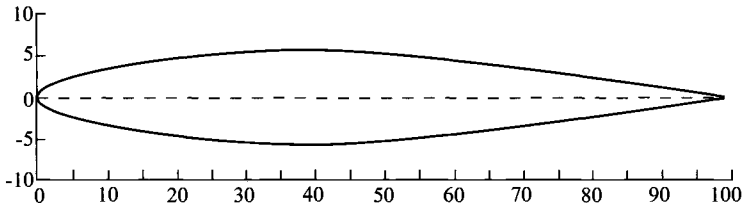

Fig. 9.28 NACA 65A010 blade shape.

To obtain the desired change in fluid flow direction, the airfoil's chamber line is curved and the symmetric shape of the airfoil profile is distributed about the chamber line. The curved chamber line of the airfoil and nomenclature used for flow through a compressor cascade are shown in Fig. 9.15. Normally, the curved chamber line is that of a circular arc or a parabola. If a circular arc is used, then the stagger angle of the airfoil θ is the average of the chamber line's inlet angle γ_i and exit angle γ_e. From Fig. 9.29 and basic trigonometry, the radius of the chamber line is given by

$$r = \frac{c \sin \theta}{\cos \gamma_e - \cos \gamma_i} \tag{9.43}$$

The COMPR computer program uses the NACA 65A010 compressor profile with circular arc chamber line to sketch the blade shapes for a stage. The user can change the blade thickness for the rotor or stator blades, select the desired stage, specify the number of blades to be sketched, and specify the percentage of chord

Table 9.4 NACA 65A010 compressor airfoil[a,b]

x/c, %	y/c, %	x/c, %	y/c, %
0.0	0.0	40	4.995
0.5	0.765	45	4.983
0.75	0.928	50	4.863
1.25	1.183	55	4.632
2.5	1.623	60	4.304
5	2.182	65	3.809
7.5	2.65	70	3.432
10	3.04	75	2.912
15	3.658	80	2.352
20	4.127	85	1.771
25	4.483	90	1.188
30	4.742	95	0.604
35	4.912	100	0.0

[a]Leading-edge radius = 0.00636c. Trailing-edge radius = 0.00023c.
[b]Source: Ref. 51.

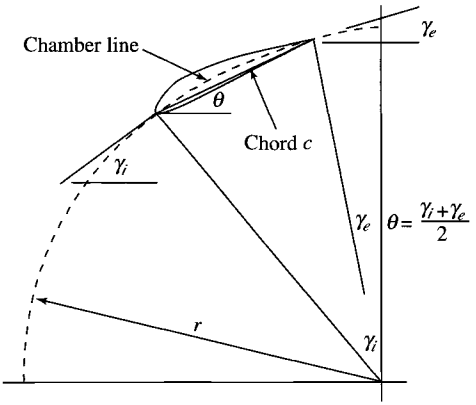

Fig. 9.29 Circular arc chamber line.

for stacking blade profiles. The user can view one or more blades in the rotor and stator at a time.

If the user selects to view just one blade, the program initially sketches the blade shape at the mean radius as a solid, and the shapes at the hub and tip are drawn in dashed outline stacked over the other profile at the user-selected stacking location. Figure 9.30 is a copy of the blade profile plot screen for one blade. The user can move the slider for percentage of blade height by using the up and down arrows and replot the blade shape at a new height (radial location).

If the user selects to view more than one blade, the program initially sketches the blade shapes at the mean radius. Figure 9.31 is a copy of the blade profile plot screen for three blades. The user can move the slider for percentage of blade height by using the up and down arrows and replot the blade shape at a new height (radial location).

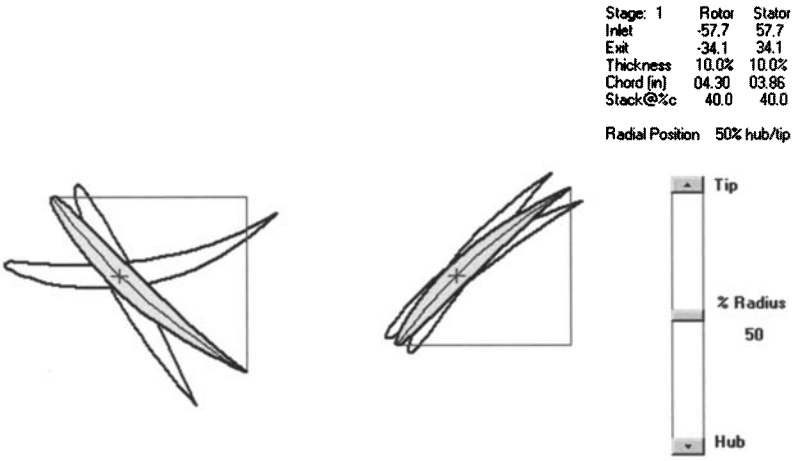

Fig. 9.30 Single-blade profile sketch from COMPR.

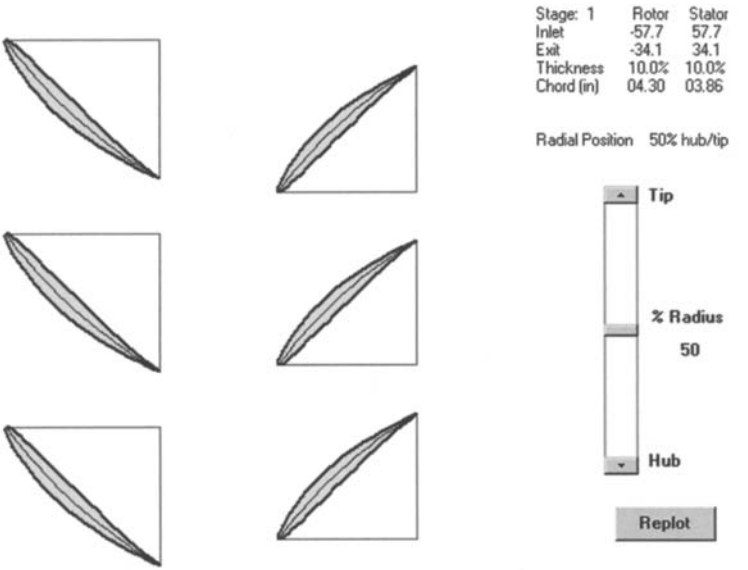

Fig. 9.31 Three-blade profile sketch from COMPR.

9.3.7 Radial Variation

A practical goal of a design is to do a constant amount of work on the fluid passing through a stage that is independent of radius. For this to occur, the Euler pump equation [Eq. (9.1)] reveals that less "turning" of the fluid will be required as the radius increases. In addition, the static pressure must increase with the radius to maintain the radial equilibrium of the swirling flow. All airfoil and flow properties must, therefore, vary with radius.

In the following analysis, the relationships are developed for the radial variation of flow between the rows of airfoils (stage stations 1, 2, and 3). Initially, a general equation for radial equilibrium is developed, assuming no radial velocity. Then specific radial variations of the velocity are analyzed for the case of constant work on the fluid.

9.3.7.1 Radial equilibrium equation. The main features of the radial variation of flow *between* the rows of airfoils are accounted for in the following analysis. These equations are valid at stations 1, 2, and 3 at any radius. We assume the following:

1) Constant losses (entropy s = constant with respect to radius)
2) No circumferential variations
3) No radial velocity

The definition of total (stagnation) enthalpy with no radial velocity gives

$$dh_t = dh + \frac{d(u^2 + v^2)}{2g_c} \tag{i}$$

Gibbs' equation can be written as

$$T\,\mathrm{d}s = \mathrm{d}h - \frac{\mathrm{d}P}{\rho}$$

With s = constant, Gibbs' equation becomes

$$\mathrm{d}h = \frac{\mathrm{d}P}{\rho} \tag{ii}$$

Equations (i) and (ii) can be combined to give

$$\mathrm{d}h_t = \frac{\mathrm{d}P}{\rho} + \frac{u\,\mathrm{d}u}{g_c} + \frac{v\,\mathrm{d}v}{g_c}$$

When h_t is a constant, this equation becomes the well-known Bernoulli equation. We rewrite the preceding equation as

$$\frac{\mathrm{d}h_t}{\mathrm{d}r} = \frac{1}{\rho}\frac{\mathrm{d}P}{\mathrm{d}r} + \frac{1}{g_c}\left(u\frac{\mathrm{d}u}{\mathrm{d}r} + v\frac{\mathrm{d}v}{\mathrm{d}r}\right) \tag{iii}$$

For radial equilibrium, the pressure gradient in the radial direction must balance the centrifugal acceleration, or

$$\frac{\mathrm{d}P}{\mathrm{d}r} = \frac{\rho v^2}{r g_c} \tag{iv}$$

Equations (iii) and (iv) may be combined to yield

$$\frac{\mathrm{d}h_t}{\mathrm{d}r} = \frac{1}{g_c}\left(u\frac{\mathrm{d}u}{\mathrm{d}r} + v\frac{\mathrm{d}v}{\mathrm{d}r} + \frac{v^2}{r}\right) \tag{9.44}$$

This general form of the radial equilibrium equation prescribes the relationship between the radial variations of the three variables: h_t, u, and v. The designer can specify the radial variation of any two variables, and Eq. (9.44) specifies the radial variation of the third variable.

9.3.7.2 Free-vortex variation of swirl. We consider the case where the axial velocity u and total enthalpy h_t do not vary with radius. For this case, Eq. (9.44) becomes

$$v\frac{\mathrm{d}v}{\mathrm{d}r} + \frac{v^2}{r} = 0 \quad \text{or} \quad \frac{\mathrm{d}v}{v} + \frac{\mathrm{d}r}{r} = 0$$

for which the integrated solution is

$$rv = \text{const}$$

or

$$v = v_m \frac{r_m}{r} \tag{9.45}$$

where the subscript m refers to values at the mean radius. Because v varies inversely with radius, this is known as *free-vortex* flow. Thus, if the flow at station 1 has $v_1 r = v_{m1} r_m$ and the rotor airfoils modify the flow to $v_2 r = v_{m2} r_m$, then the Euler equation confirms that this is a constant-work machine because

$$\begin{aligned} \omega r(v_2 - v_1) &= \omega r\left(\frac{v_{m2} r_m}{r} - \frac{v_{m1} r_m}{r}\right) \\ &= \omega r_m (v_{m2} - v_{m1}) \\ &= \text{const} \end{aligned}$$

Equation (9.45) also shows that as long as r does not vary substantially from r_m (say, $\pm 10\%$), the airfoil and flow properties will not vary much from those of the original mean-line design.

If the compressor has constant axial velocity and repeating stages (not rows) for which $v_1 = v_3$, then the degree of reaction can be shown to be

$$^{\circ}R_c = 1 - \frac{v_1 + v_2}{2\omega r} \tag{9.46}$$

which, for a free-vortex machine, becomes

$$^{\circ}R_c = 1 - \frac{v_{m1} r_m + v_{m2} r_m}{2\omega r^2} = 1 - \frac{\text{const}}{(r/r_m)^2} \tag{9.47}$$

For a stage whose degree of reaction is 50% at the mean radius (where $(\omega r = v_1 + v_2)$, it becomes more difficult to design rotor airfoils at $r > r_m$ and stator airfoils at $r < r_m$. In fact, since $^{\circ}R_c = 0$ at $r = r_m/\sqrt{2}$, the rotor will actually experience accelerating flow for smaller radii, whereas this is never the case for the stator. Because of these problems, compressor designers have looked at other swirl distributions.

9.3.7.3 Swirl distributions. We now consider the case where the total enthalpy does not vary with the radius and where the swirl velocity at the inlet and exit to the rotor has the following general variation with radius:

$$v_1 = a\left(\frac{r}{r_m}\right)^n - b\frac{r_m}{r} \quad \text{and} \quad v_2 = a\left(\frac{r}{r_m}\right)^n + b\frac{r_m}{r} \tag{9.48}$$

where a, b, and r_m are constants. From the Euler equation, the work per unit mass flow is

$$\Delta h_t = \frac{\omega r(v_2 - v_1)}{g_c} = \frac{2b\omega r_m}{g_c} \tag{9.49}$$

which is independent of the radius. Note from the preceding relationship that the constant b in Eq. (9.48) is determined by the total enthalpy rise across the rotor and the mean rotor speed. As will be shown next, constant a in Eq. (9.48) is related to the degree of reaction at the mean radius. Three cases of the swirl distribution of Eq. (9.48) are considered: $n = -1$, $n = 0$, and $n = 1$.

1) For $n = -1$:

$$v_1 = a\frac{r_m}{r} - b\frac{r_m}{r} \quad \text{and} \quad v_2 = a\frac{r_m}{r} + b\frac{r_m}{r} \tag{9.50}$$

which is the *free-vortex* swirl distribution. For this case and constant h_t, Eq. (9.44) required that the axial velocity u not vary with the radius. Using Eq. (9.46) for a repeating stage ($v_3 = v_1$), we see that the degree of reaction is

$$^{\circ}R_c = 1 - \frac{a}{\omega r_m}\left(\frac{r_m}{r}\right)^2 \tag{9.51}$$

An equation for the constant a in Eq. (9.48) is obtained by evaluating the preceding equation at the mean radius. Thus

$$a = \omega r_m(1 - {}^{\circ}R_{cm}) \tag{9.52}$$

2) For $n = 0$:

$$v_1 = a - b\frac{r_m}{r} \quad \text{and} \quad v_2 = a + b\frac{r_m}{r} \tag{9.53}$$

This is called the *exponential* swirl distribution. Before solving for the axial velocity distribution, we rewrite Eq. (9.44) for constant total enthalpy h_t in terms of the dimensionless radius r/r_m as

$$u\,\mathrm{d}u + v\,\mathrm{d}V + v^2\frac{\mathrm{d}(r/r_m)}{r/r_m} = 0$$

Integration of the preceding equation from the mean radius to any radius r gives

$$\frac{1}{2}(u^2 - u_m^2) = -\frac{1}{2}(v^2 - v_m^2) - \int_1^{r/r_m} v^2\frac{\mathrm{d}(r/r_m)}{r/r_m} \tag{9.54}$$

At the entrance to the rotor (station 1), substitution of the equation for v_1 into Eq. (9.54) and integration give the axial velocity profile

$$u_1^2 = u_{1m}^2 - 2\left(a^2\ell n\frac{r}{r_m} + \frac{ab}{r/r_m} - ab\right) \tag{9.55}$$

Likewise, at the exit from the rotor (station 2), we obtain

$$u_2^2 = u_{2m}^2 - 2\left(a^2 \ell n \frac{r}{r_m} - \frac{ab}{r/r_m} + ab\right) \tag{9.56}$$

Because the axial velocity is not constant, we must start with Eq. (9.13b) to obtain an expression for the degree of reaction for the velocity distribution given by Eqs. (9.53), (9.55), and (9.56). We start by noting for repeating stages ($V_3 = V_1$) that

$$\begin{aligned} {}^{\circ}R_c &= \frac{T_2 - T_1}{T_3 - T_1} = \frac{T_{t2} - T_{t1}}{T_{t3} - T_{t1}} - \frac{V_2^2 - V_1^2}{2g_c c_p (T_{t3} - T_{t1})} \\ &= 1 - \frac{V_2^2 - V_1^2}{2g_c c_p (T_{t3} - T_{t1})} = 1 - \frac{u_2^2 - u_1^2}{2g_c c_p (T_{t3} - T_{t1})} - \frac{v_2^2 - v_1^2}{2g_c c_p (T_{t3} - T_{t1})} \end{aligned}$$

From the Euler equation, we write $g_c c_p (T_{t3} - T_{t1}) = \omega r (v_2 - v_1)$, and the preceding becomes

$$\begin{aligned} {}^{\circ}R_c &= 1 - \frac{u_2^2 - u_1^2}{2\omega r (v_2 - v_1)} - \frac{v_2^2 - v_1^2}{2\omega r (v_2 - v_1)} \\ {}^{\circ}R_c &= 1 + \frac{u_1^2 - u_2^2}{2\omega r (v_2 - v_1)} - \frac{v_2 + v_1}{2\omega r} \end{aligned} \tag{9.57}$$

For the case where $u_{1m} = u_{2m}$, Eqs. (9.55) and (9.56) give

$$u_1^2 - u_2^2 = 4ab\left(1 - \frac{r_m}{r}\right)$$

and from the swirl distribution of Eq. (9.53), we have

$$v_2 + v_1 = 2a \quad \text{and} \quad v_2 - v_1 = 2b\frac{r_m}{r}$$

Thus the degree of reaction for the exponential swirl distribution is given by

$${}^{\circ}R_c = 1 + \frac{a}{\omega r_m} - \frac{2a}{\omega r} \tag{9.58}$$

3) For $n = 1$:

$$v_1 = a\frac{r}{r_m} - b\frac{r_m}{r} \quad \text{and} \quad v_2 = a\frac{r}{r_m} + b\frac{r_m}{r} \tag{9.59}$$

This is called *first-power* swirl distribution. At the entrance to the rotor (station 1), substitution of the equation for v_1 into Eq. (9.54) and integration give the

axial velocity profile

$$u_1^2 = u_{1m}^2 - 2\left[a^2\left(\frac{r}{r_m}\right)^2 + 2ab\,\ell n\frac{r}{r_m} - a^2\right] \tag{9.60a}$$

Likewise, at the exit from the rotor (station 2), we obtain

$$u_2^2 = u_{2m}^2 - 2\left[a^2\left(\frac{r}{r_m}\right)^2 - 2ab\,\ell n\frac{r}{r_m} - a^2\right] \tag{9.60b}$$

An equation for the degree of reaction for the case of $u_{1m} = u_{2m}$ is obtained in the same manner. The resulting relationship is

$$^{\circ}R_c = 1 + \frac{2a\,\ell n(r/r_m)}{\omega r_m} - \frac{a}{\omega r_m} \tag{9.61}$$

9.3.7.4 Comparison. Equations (9.51), (9.58), and (9.61) give the radial variation of the degree of reaction for the free-vortex, exponential, and first-power swirl distributions, respectively. The value of the constant a is evaluated at the mean radius and is given by Eq. (9.52) for all three cases. Consider the case where the degree of reaction at the mean radius is 0.5. Results from Eqs. (9.51), (9.58), and (9.61) are plotted in Fig. 9.32 for the range $0.5 < r/r_m < 1.5$. Note that at any radius other than the mean, the free-vortex swirl distribution results in the lowest value for the degree of reaction, and the first-power swirl distribution gives the highest value.

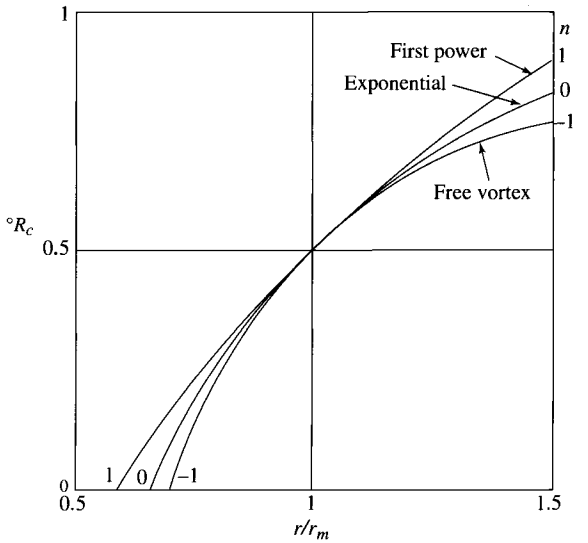

Fig. 9.32 Radial variation of degree of reaction (from Ref. 29).

The low (nonzero) values for the degree of reaction can occur at the hub for stages having small hub/tip ratios r_h/r_t. The variation with the radius ratio r/r_t for the degree of reaction can be obtained from Eqs. (9.51), (9.58), and (9.61) and the following relationship between r/r_t and r/r_m:

$$\frac{r}{r_m} = \frac{r}{r_m}\frac{1 + r_h/r_t}{2} \tag{9.62}$$

For the free-vortex swirl distribution with 0.5 degree of reaction at the mean radius, the degree of reaction is 0 at $r/r_m = 0.707$, which corresponds to the hub radius for a stage having a hub/tip ratio of 0.547. It is not uncommon for the initial stages of a compressor to have a hub/tip ratio of 0.4. The degree of reaction at the hub can be increased by increasing the degree of reaction at the mean radius for stages with low hub/tip ratios. Another way to increase the degree of reaction at the hub is to change the swirl distribution.

For the first-power swirl distribution with 0.5 degree of reaction at the mean radius, the degree of reaction is 0 at $r/r_m = 0.6065$, which corresponds to the hub radius for a stage having a hub/tip ratio of 0.435. Even with this improvement over the free-vortex distribution, the degree of reaction at the mean radius will have to be greater than 0.5 to have a positive degree of reaction at the hub of a stage with a hub/tip ratio of 0.4.

Because of the problems encountered with the preceding swirl distribution, modern compressor designers have looked to nonconstant work machines. However, these are absolutely dependent on large computers for their definition.

Example 9.6

Consider the results using program COMPR. The program COMPR can perform the calculations for repeating-row, repeating-stage, mean-line stage design. To have values for the total pressure and static pressures at stations 2 and 2*R*, the program requires a value of the stator loss coefficient ϕ_{cs} in addition to the polytropic efficiency for repeating-row, repeating-stage calculations. The program assumes that the solidity σ varies inversely with radius (constant chord length) for calculation of the radial variation in the diffusion factor. The free-vortex swirl distribution is used for the radial variation of the tangential velocity v in this example.

Given:

$$\dot{m} = 22.68\,\text{kg/s}\ (50\,\text{lbm/s}), \qquad P_t = 101.3\,\text{kPa}\ (14.70\,\text{psia})$$
$$T_t = 288.16\,\text{K}\ (518.7^\circ\text{R}), \quad \omega = 900\,\text{rad/s}, \quad e_c = 0.9, \quad \phi_{cs} = 0.03$$
$$\text{on mean line: } \sigma = 1, \quad \alpha_1 = 45\,\text{deg}, \quad D = 0.5, \quad M_1 = 0.5$$

Solution: Tables 9.5a and 9.5b summarize the results obtained from COMPR. Note that the Mach numbers at the hub of stations 1, 2, and 3 are higher than on

Table 9.5a Flow property results for Example 9.6

Property		Station										
		$1/h$	$1m$	$1t$	$1Rm$	$2Rm$	$2h$	$2m$	$2t$	$3h$	$3m$	$3t$
T_t	K	288.2	288.2	288.2	303.1	303.1	318.1	318.1	318.1	318.1	318.1	318.1
	(°R)	(518.7)	(518.7)	(518.7)	(545.6)	(545.6)	(572.6)	(572.6)	(572.6)	(572.6)	(572.6)	(572.6)
T	K	272.7	274.4	275.7	274.4	289.4	284.5	289.4	293.1	303.0	304.4	305.4
	(°R)	(490.8)	(494.0)	(496.3)	(494.0)	(520.9)	(512.1)	(520.9)	(527.6)	(545.4)	(547.9)	(549.8)
P_t	kPa	101.3	101.3	101.3	120.9	117.7	139.3	139.3	139.3	138.3	138.3	138.3
	(psia)	(14.70)	(14.70)	(14.70)	(17.55)	(17.08)	(20.21)	(20.21)	(20.21)	(20.06)	(20.06)	(20.06)
P	kPa	83.5	85.4	86.8	85.4	100.1	94.3	100.1	104.6	116.7	118.5	119.9
	(psia)	(12.11)	(12.39)	(12.59)	(12.39)	(14.52)	(13.67)	(14.52)	(15.18)	(16.93)	(17.19)	(17.40)
M		0.533	0.500	0.475	0.723	0.487	0.769	0.704	0.653	0.499	0.475	0.456
V	m/s	176	166	158	240	166	260	240	224	174	166	160
	(ft/s)	(578)	(545)	(519)	(788)	(545)	(853)	(788)	(735)	(571)	(545)	(524)
u	m/s	117	117	117	117	117	117	117	117	117	117	117
	(ft/s)	(385)	(385)	(385)	(385)	(385)	(385)	(385)	(385)	(385)	(385)	(385)
v	m/s	132	117	106	209	117	232	209	191	128	117	108
	(ft/s)	(432)	(385)	(348)	(687)	(385)	(761)	(687)	(626)	(421)	(385)	(355)
α	deg	48.25	45.00	42.08	——	——	63.14	60.72	58.41	47.57	45.00	42.64
β	deg	——	——	——	60.72	45.00	——	——	——	——	——	——
radii	m	0.324	0.363	0.402	0.363	0.363	0.328	0.363	0.398	0.332	0.363	0.394
	(in.)	(12.76)	(14.30)	(15.83)	(14.30)	(14.30)	(12.91)	(14.30)	(15.68)	(13.07)	(14.30)	(15.52)

Table 9.5b Stage results for Example 9.6

Hub	$^{\circ}R_c = 0.3888$	$D_r = 0.5455$	$D_s = 0.5101$
Mean	$^{\circ}R_c = 0.5000$	$D_r = 0.5000$	$D_s = 0.5000$
Tip	$^{\circ}R_c = 0.5850$	$D_r = 0.4476$	$D_s = 0.4906$

$\Delta T_t = 29.93\,\text{K}$ $\eta_s = 89.55\%$ $AN^2 = 1.184 \times 10^7\,\text{m}^2 \cdot \text{rpm}^2$

$$\psi = \frac{g_c c_p \Delta T_t}{(\omega r)^2} = 0.281 \qquad \Phi = \frac{u_1}{\omega r} = 0.359$$

the mean radius due to the swirl distribution. This affects both the static temperatures and the static pressures at the hub.

The cross section of this stage, as created by COMPR, is shown in Fig. 9.33. The stage length of 0.099 m is based on a chord/height ratio of 0.75 for both the rotor and stator blades.

The variation in tangential and axial velocities with radius across the rotor is shown in Fig. 9.34 for the free-vortex swirl distribution. To obtain the 30.5°C (54.9°F) temperature rise across the rotor, the tangential velocity is increased 92 m/s (302 ft/s).

9.3.8 Design Process

The theory and design tools presented in previous sections can now be applied to the design of a multistage axial-flow compressor. The design process requires

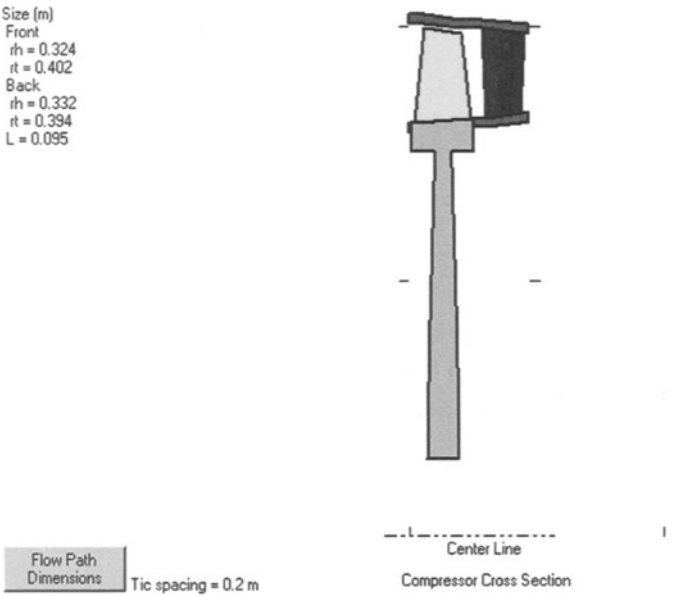

Fig. 9.33 Cross section of a single stage from COMPR.

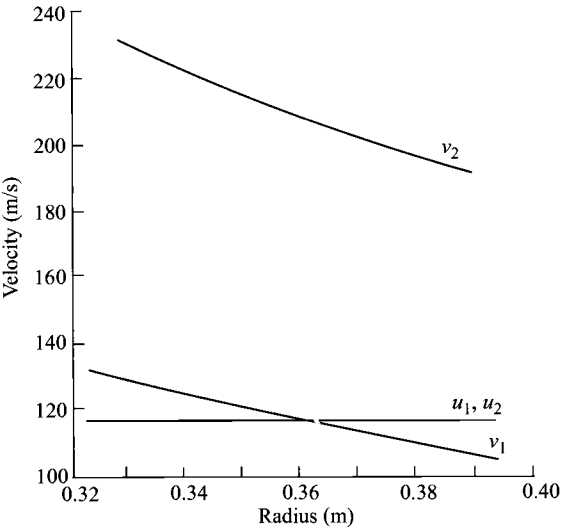

Fig. 9.34 Axial and swirl velocity profiles at stations 1 and 2.

both engineering judgment and knowledge of typical design values. We will consider the design of a compressor suitable for a simple turbojet gas turbine engine. It is assumed that such a compressor will require inlet guide vanes.

From engine cycle calculations, a suitable design point for the compressor of such an engine at sea-level, standard-day conditions [$P/T = 14.70$ psia/518.7°R ($P/T = 101.3$ kPa/288.2 K)] may emerge as

Compressor pressure ratio	10.2
Air mass flow rate	150 lbm/s (68.04 kg/s)
Temperature entering turbine	3200°R (1778 K)

From these specified data, we will now investigate the aerodynamic design of an axial-flow compressor.

The complete design process for the compressor will include the following items:

1) Selection of rotational speed and annulus dimensions
2) Selection of the number of stages
3) Calculation of airflow angles for each stage at the mean radius
4) Calculation of airflow angle variations from the hub to tip for each stage
5) Selection of blading using experimental cascade data
6) Verification of compressor efficiency based on cascade loss data
7) Prediction of off-design performance
8) Rig testing of design

Items 1–4 will be covered in this section. Many of the remaining steps will be discussed in following sections. The design process is inherently iterative, often requiring return to an earlier step when prior assumptions are found to be

Table 9.6 Range of axial-flow compressor design parameters

Parameter	Design range
Fan or low-pressure compressor	
Pressure ratio for one stage	1.5–2.0
Pressure ratio for two stages	2.0–3.5
Pressure ratio for three stages	3.5–4.5
Inlet corrected mass flow rate	40–42 lbm/(s · ft^2) [195–205 kg/(s · m^2)]
Tip speed	1400–1500 ft/s (427–457 m/s)
Diffusion factor	0.50–0.55
High-pressure compressor	
Inlet corrected mass flow rate	36–38 lbm/(s · ft^2) [175–185 kg/(s · m^2)]
Hub/tip ratio at inlet	0.60–0.75
Hub/tip ratio at exit	0.90–0.92
Maximum rim speed at exit	1300–1500 ft/s (396–457 m/s)
Flow coefficient	0.45–0.55
Stage loading coefficient	0.30–0.35
Diffusion factor	0.50–0.55

invalid. Table 9.6 lists ranges for some design parameters of axial-flow compressors and can be used as a guide.

Many technical specialities are interwoven in a design, e.g., an axial-flow air compressor involves at least thermodynamics, aerodynamics, structures, materials, manufacturing processes, and controls. Design requires the active participation and disciplined communication by many technical specialists.

9.3.8.1 Selection of rotational speed and annulus dimensions. Selection of the rotational speed is not a simple matter. For a simple turbojet engine, it depends on a balance of the requirements of both components on the common shaft—the compressor and the turbine. Typically, the rotational speed can be found by assuming values for the rotor blade-tip speed, the hub/tip ratio, and axial velocity of the first stage. A check of the magnitude of AN^2 (related to blade stress) is also made. For the first stage of typical compressors, the hub/tip ratio is between 0.6 and 0.75, the axial Mach number is between 0.48 and 0.6, and the rotor blade-tip speed is between 1150 and 1500 ft/s (350 to 460 m/s) (higher values for first-stage fans without inlet guide vanes).

Initially, we select a modest value for the axial Mach number M_0 of 0.5 entering the inlet guide vanes. Because the inlet guide vanes will accelerate and turn the flow to an angle of 30–45 deg, we will start with a compressor inlet Mach number M_1 of 0.6 and a high tip speed U_t of 1400 ft/s (426.7 m/s). From the

definition of mass flow parameter, we can write

$$A = \frac{\dot{m}\sqrt{T_t}}{(\cos\alpha)(P_t)\text{MFP}(M)}$$

For the given mass flow rate and the inlet total pressure, total temperature, and Mach number, we can determine the flow annulus area at the entrance to the inlet guide vanes:

$$\text{MFP}(M_0) = 0.3969$$

$$A_0 = \frac{\dot{m}\sqrt{T_{t0}}}{P_{t0}\text{MFP}(M_0)} = \frac{150\sqrt{518.7}}{14.70 \times 0.3969}$$

$$= 585.7\,\text{in.}^2\ (0.3780\,\text{m}^2)$$

Likewise, the area at the face of the first-stage rotor, assuming a flow angle of 40 deg, is

$$\text{MFP}(M_1) = 0.4476$$

$$A_1 = \frac{\dot{m}\sqrt{T_t}}{(\cos\alpha_1)(P_t)\text{MFP}(M)} = \frac{150\sqrt{518.7}}{0.7660 \times 14.70 \times 0.4476}$$

$$= 677.8\ \text{in.}^2\ (0.4375\,\text{m}^2)$$

The tip radius r_t and mean radius r_m are directly related to the flow area A and hub/tip ratio r_h/r_t by

$$r_t = \sqrt{\frac{A}{\pi[1 - (r_h/r_t)^2]}}$$

$$r_m = r_t \frac{1 + r_h/r_t}{2}$$

The rotational speeds ω and N are related to the rotor tip speed by

$$\omega = \frac{U_t}{r_t} \quad \text{and} \quad N = \frac{30}{\pi}\omega$$

From the preceding relationships, we can calculate r_t, ω, N, and AN^2 over the hub/tip ratio range and obtain the data in Table 9.7a for a tip speed of 1400 ft/s (426.7 m/s).

With the information in Table 9.7a, it is most appropriate for the compressor designer to get together with the turbine designer to select a rotational speed. The first stages of turbines typically have tip speeds of about 1400 ft/s (426.7 m/s),

Table 9.7a Variation of first-stage size and speed for a tip speed of 1400 ft/s

$\frac{r_h}{r_t}$	r_t, in.	r_m, in.	ω, rad/s	N, rpm	AN^2, in.^{2} · rpm^2
0.60	18.36	14.69	914.8	8735.7	5.17×10^{10}
0.65	19.33	15.95	869.0	8298.2	4.67×10^{10}
0.70	20.57	17.49	816.6	7798.2	4.12×10^{10}
0.75	22.21	19.44	756.4	7222.7	3.54×10^{10}

a hub/tip ratio of 0.85 to 0.9, and Mach number entering the rotor of 1.2 at 60 deg to the centerline of the turbine. Assuming a fuel/air ratio of 0.04, the turbine mass flow rate is 156 lbm/s. For $\gamma = 1.3$ and a 5% total pressure loss through the combustor, the annulus area at the turbine rotor is

$$\text{MFP}(M) = 0.5021$$

$$A = \frac{\dot{m}\sqrt{T_t}}{(\cos\alpha)(P_t)\text{MFP}(M)} = \frac{156\sqrt{3200}}{\cos 60\,\text{deg} \times 142.40 \times 0.5021}$$

$$= 246.8\,\text{in.}^2\,(0.1593\,\text{m}^2)$$

For a hub/tip ratio of 0.9, the tip radius is 20.3 in. (0.516 m). The rotor speed of 1400 ft/s (426.7 m/s) requires a rotational speed of 826 rad/s. For a hub/tip ratio of 0.85, the tip radius is 16.8 in. (0.427 m), and the corresponding rotational speed is 998 rad/s. At this time, *we select a rotor speed of 800 rad/s for the compressor* to keep the AN^2 of the compressor and turbine low. This value will be used in the preliminary design of the compressor stages. The corresponding hub, mean, and tip radii of the compressor's first stage will be 15, 18, and 21 in., respectively.

9.3.8.2 Inlet guide vanes. We will now consider the inlet guide vanes. The inlet guide vanes change both the direction of flow and its Mach number. For isentropic flow through the inlet guide vanes, the following relationship can be written with stations 0 and 1 corresponding to the inlet and exit, respectively:

$$(\cos\alpha_1)(A_1)\text{MFP}(M_1) = A_0\text{MFP}(M_0) \tag{9.63}$$

For our case, where the entrance Mach number is 0.5, the preceding relationship can be used to calculate α_1 vs M_1 for different values of A_1/A_0. Results for $A_1/A_0 = 1.15$, 1.10, 1.05, and 1.0 are plotted in Fig. 9.35. Because the inlet guide vane sets up the flow for the first stage of the compressor, we will use this plot in conjunction with the repeating-stage design curves to help select the area ratio A_1/A_0 for the desired inlet Mach number M_1 and flow angle α_1.

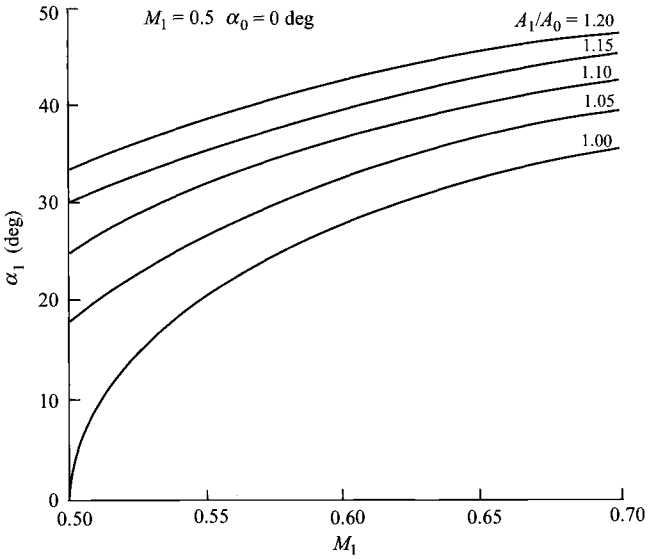

Fig. 9.35 Mean exit conditions from inlet guide vanes.

9.3.8.3 Selection of the number of stages. The number of compressor stages depends on the overall pressure ratio and the change in total temperature of each stage. Normally the changes in total temperature of the first and last stages are less than those of the other stages. In the absence of inlet guide vanes, the inlet flow to the first stage is axial, and less work can be done than in a stage whose inlet flow has swirl. The exit flow from the last stage is normally axial, which reduces the work of this stage.

The preliminary compressor design is based on repeating-row, repeating stage design. Thus the repeating-row, repeating-stage design equations and Figs. 9.23, 9.24, and 9.25 can be used to estimate the number of compressor stages. We will base the design on a mean-line diffusion factor D of 0.5, a mean-line solidity σ of 1, and a polytropic efficiency e_c of 0.9.

Because the stage inlet Mach number decreases through the compressor, the stage pressure ratio of a repeating-row, repeating-stage design will decrease. However, *the change in total temperature across each stage will remain constant* for this type of design.

For $M_1 = 0.6$ and α_1 between 30 and 40 deg, the data in Table 9.7b for the first stage can be obtained from the equations for repeating-row, repeating-stage design. Thus, for the assumed value of M_1 and range of α_1, we see from Table 9.7b that the total temperature change for a stage will be between 66.9 and 73.3°R. The total temperature rise for the whole compressor will be approximately

$$\Delta T_t = T_{ti}[(\pi_c)^{(\gamma-1)/(\gamma e_c} - 1] = 518.7[(10.2)^{1/(3.5\times0.9)} - 1] = 565.5°\text{R}$$

Table 9.7b Variation in repeating-row, repeating-stage designs with inlet flow angle

α_1, deg	α_2, deg	τ_s	π_s	ΔT_t, °R	$V_1/(\omega r)$	M_{1R}	ψ	Φ
30.0	51.79	1.1290	1.465	66.9	0.6250	0.840	0.375	0.541
32.0	52.94	1.1316	1.476	68.3	0.6051	0.844	0.359	0.513
34.0	54.10	1.1342	1.487	69.6	0.5867	0.848	0.344	0.486
36.0	55.28	1.1367	1.497	70.9	0.5697	0.852	0.330	0.461
38.0	56.47	1.1390	1.507	72.1	0.5541	0.856	0.318	0.437
40.0	57.67	1.1413	1.516	73.3	0.5396	0.859	0.306	0.413

The number of stages will then be either 9 (565.5/66.9 = 8.45) or 8 (565.5/73.3 = 7.71). *We select eight stages for this design.* Because the first stage has inlet guide vanes, we will use the same change in total temperature for this stage as for the other compressor stages. In addition, we will allow the last stage to have exit swirl (this can be removed by an additional set of stators) and will use the same change in total temperature for the last stage as for the other compressor stages. Thus each stage will have an equal temperature rise of 70.7°R (565.5/8). For the first stage, this corresponds to a temperature ratio of 1.136, which requires α_1 of about 36 deg and $V_1/(\omega r)$ of 0.57.

We select an inlet flow angle of 36 deg. The inlet air at $T_t = 518.7$°R and $M = 0.6$ has a velocity of 647 ft/s. The resulting stage loading coefficient is 0.3302 and flow coefficient is 0.4609, both within the range of these coefficients for modern axial-flow compressors. For a rotor speed of 800 rad/s, the mean radius is about 17 in. The inlet annulus area of the first stage will be

$$\text{MFP}(M_1) = 0.44757$$

$$A_1 = \frac{\dot{m}\sqrt{T_{t1}}}{(\cos\alpha_1)(P_{t1})\text{MFP}(M_1)} = \frac{150\sqrt{518.7}}{\cos 36\,\text{deg} \times 14.70 \times 0.4475}$$

$$= 641.8\,\text{in.}^2\ (0.4142\,\text{m}^2)$$

This area is 1.1 times the inlet area of the guide vanes. The corresponding tip radius and hub radius at the inlet to the first stage are about 20 and 14 in., respectively, giving a first-stage hub/tip ratio of 0.7.

Example 9.7

Consider the preliminary design of mean line. The COMPR program was used to perform the following analysis of a repeating-row, repeating-stage, mean-line design with a free-vortex swirl distribution. The following input data were entered:

Number of stages: 8
Rotor angular speed ω: 800 rad/s
Inlet total temperature T_t: 518.7°R
Mass flow rate: 150 lbm/s
Inlet total pressure P_t: 14.70 psia
Inlet flow angle α_1: 36 deg

Table 9.8a Summary of eight-stage compressor design

Stage	1	2	3	4	5	6	7	8
M_1	0.600	0.560	0.528	0.500	0.476	0.456	0.438	0.422
π_s	1.497	1.430	1.379	1.338	1.306	1.279	1.256	1.237
P_{t1}, psia	14.70	22.01	31.47	43.39	58.07	75.81	96.9	121.8
T_{r1}, °R	518.7	589.6	660.5	731.4	802.3	873.1	944.0	1014.9
r_h, in.	14.03	14.80	15.32	15.67	15.93	16.12	16.27	16.38
r_t, in.	20.03	19.26	18.75	18.39	18.14	17.94	17.80	17.68
A_1, in.^{2}	641.8	476.9	367.4	291.1	236.0	194.9	163.5	139.0

Inlet Mach number M_1: 0.6
Solidity σ: 1.0
Rotor c/h: 0.6
Gas constant: 53.34 ft . lbf/(lbm · °R)
Diffusion factor D: 0.5
Polytropic efficiency e_c: 0.9
Stator c/h: 0.6
Ratio of specific heats γ: 1.4

The results from COMPR are summarized in Table 9.8a for the mean-line design. The mean radius is 17.032 in. and the flow angle at the entrance to the stator α_2 is 55.28 deg. A cross-sectional sketch of the eight stages as plotted by COMPR and captured on a laser printer is shown in Fig. 9.36a. The estimated length of the compressor is 25.53 in. The resulting number of blades and blade chord lengths are given in Table 9.8b based on the input chord/height ratio of 0.6 for both the rotor and stator of all stages.

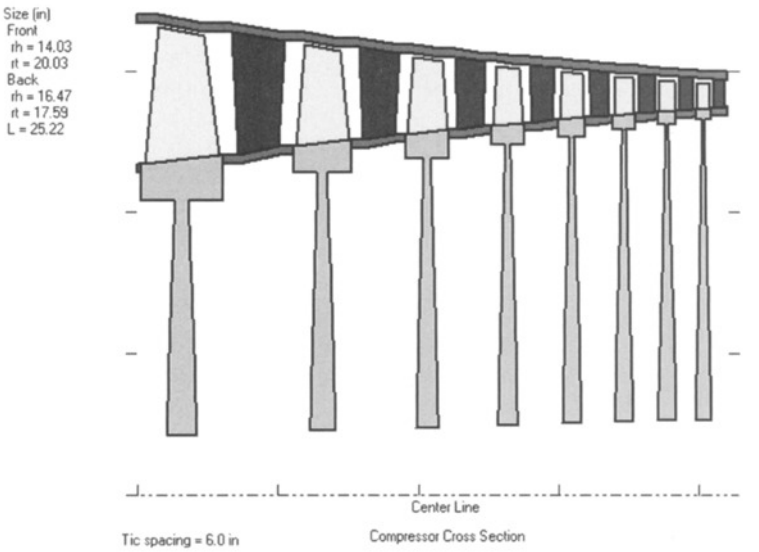

Fig. 9.36a Sketch of compressor cross section from COMPR with constant c/h.

Table 9.8b Number of blades with same c/h value for each row

Stage	1	2	3	4	5	6	7	8
Rotor								
c/h	0.60	0.60	0.60	0.60	0.60	0.60	0.60	0.60
Blades	33	43	56	70	86	103	122	143
Chord, in.	3.362	2.518	1.953	1.555	1.266	1.050	0.883	0.753
Stator								
c/h	0.60	0.60	0.60	0.60	0.60	0.60	0.60	0.60
Blades	38	49	63	77	94	112	132	154
Chord, in.	2.899	2.211	1.739	1.401	1.151	0.962	0.814	0.698

The number of blades in a rotor or stator now can be reduced by increasing its chord/height ratio. Because COMPR uses the same chord/height ratio for each blade row, for repeating-row, repeating-stage design, the user must select and run the program with the constant-mean-radius design. To obtain the same stage loss coefficients, the program is first run with the repeating-row, repeating-stage design. Then the user selects the constant mean-line design, inputs the desired chord/height ratios in the stage data screen for the rotor and stator of each stage, and performs the new calculations with a mean radius of 17.032 in. This procedure was used to reduce the number of blades in a row of stages 3 through 8, and the results are shown in Table 9.8c and Fig. 9.36b. For these stages, note that the number of blades is reduced and that the chord lengths are increased (see Table 9.8c). In addition, the estimated length of the compressor has increased to 30.36 in. (see Fig. 9.36b).

The AN^2 and estimated rim speed (assuming a rim height equal to the blade chord) at the inlet to each rotor are listed in Table 9.8d along with the relative total temperature on the mean line. These data values are related to the stresses in the turbomachinery (see Appendix J), and they can be used as a guide in blade and rim material selection and determining disk requirements. Based on

Table 9.8c Number of blades with different c/h values for each row

Stage	1	2	3	4	5	6	7	8
Rotor								
c/h	0.60	0.60	0.63	0.73	0.83	0.93	1.03	1.13
Blades	33	43	53	58	62	67	72	76
Chord, in.	3.362	2.518	2.050	1.892	1.752	1.627	1.516	1.418
Stator								
c/h	0.60	0.60	0.60	0.70	0.80	0.90	1.00	1.10
Blades	38	49	63	66	71	75	80	85
Chord, in.	2.899	2.211	1.739	1.634	1.535	1.442	1.357	1.280

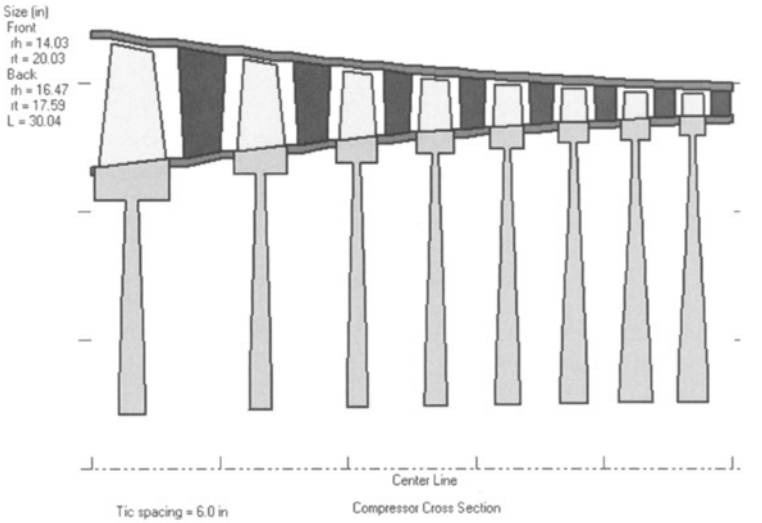

Fig. 9.36b Sketch of compressor cross section from COMPR with variable c/h.

the analytical tools and material properties of Appendix J, the rotor blades of stages 1–8 will require material 2 (a titanium alloy). The rim stress requirements can be met for these eight stages by using the same type of material as the blade. Since W_d/W_{dr} is greater than zero for each stage, each stage requires a disk.

The resulting total pressure and total temperature leaving the eight-stage compressor are 150.6 psia and 1086°R, respectively. The compressor efficiency is 86.32%. For axial flow at the exit with $M = 0.4$, an exit area of 98.15 in.^{2} (0.0633 m^2) is required for this compressor.

COMPR program calculates the variation in flow angle, diffusion factor, degree of reaction, Mach number, etc., of each stage for the selected swirl distribution. The minimum and maximum results and their location are listed in Table 9.9 for the free-vortex swirl distribution.

For this design, the inlet guide vanes have an inlet Mach number of 0.5, an exit Mach number of 0.6, and a flow angle of 36 deg. From Eq. (9.63), the flow area must increase from 585.7 to 639.4 in.^{2} For the same means radius as in the compressor stages, the entrance to the guide vanes will have a tip radius of 19.59 in. and a hub radius of 14.05 in.

The swirl velocity distributions v and flow angles β at the inlet and exit of the rotor are plotted in Fig. 9.37. Note the significant variation with radius of the swirl velocity and flow angles for the first stage ($14 < r < 20$) and very little for the last stage ($16.4 < r < 17.7$). In the first-stage rotor, the relative flow turns about 30 deg at the hub and only about 10 deg at the tip. The large radial variation in the rotor inlet flow angle for the first stage requires that its rotor blades have a lot of twist in them, whereas most of the relative flow in the last-stage rotor is turned about 20 deg and its rotor blades do not require a lot of twist.

Table 9.8d Material selection calculations for rotor blades, rims, and disks

Stage	1	2	3	4	5	6	7	8
AN^2 ($\times 10^{10}$ in.$^2 \cdot$ rpm^2)	3.2530	2.4598	1.9209	1.5389	1.2587	1.0474	0.88422	0.75579
σ_c/ρ, ksi/(slug/ft^3)[a]	2.7377	1.0702	1.6166	1.2951	1.0593	0.8815	0.7442	0.6361
T_{t1R}, °R	554	625	696	767	838	909	979	1050
T_{t1R}, °F	94	165	236	307	378	449	519	590
Blade material	← Material 2 →							
r_h, in.	14.03	14.80	15.32	15.67	15.93	16.12	16.27	16.38
ωr_h ft/s	953.33	986.67	1021.3	1044.7	1062.0	1074.7	1084.7	1092.0
h_r[b] in.	3.362	2.518	2.050	1.892	1.752	1.627	1.516	1.418
r_r, in.	10.668	12.282	13.270	13.778	14.178	14.493	14.754	14.962
Rim material	← Material 2 →							
σ_r/ρ, ksi/(slug/ft^3)	4	4	4	4	4	4	4	4
$\rho\,(\omega r)^2/\sigma_r$	1.5188	1.6901	1.8110	1.8947	1.9581	2.0050	2.0425	2.0702
W_{dr}/W_r[c]	0.4578	0.3367	0.2856	0.2735	0.2616	0.2500	0.2395	0.2299
ωr, ft/s	711.20	818.80	884.67	918.53	945.20	966.20	983.60	997.47
σ_d/ρ, ksi/(slug/ft^3)[d]	0.8781	1.1639	1.3587	1.4648	1.5510	1.6207	1.6796	1.7273
Disk material	← Material 2 →							

[a]Based on Eq. (E.6) and a blade taper ratio of 1.0.
[b]Based on h_r equal to blade chord.
[c]Based on Eq. (E.10) and $\bar{\sigma}_{\text{blades}}/\sigma_r = 0.1$.
[d]Based on Eq. (E.12).

Table 9.9 Extreme values in eight-stage compressor design

Item	Value	Location
Maximum α_1, deg	41.41	Hub at entrance to first-stage rotor
Minimum α_1, deg	31.71	Tip at entrance to first-stage rotor
Maximum β_1, deg	62.68	Tip at entrance to first-stage rotor
Minimum β_1, deg	42.15	Hub at entrance to first-stage rotor
Maximum M	0.943	Hub at exit of first-stage rotor
Maximum M_R	1.053	Tip at entrance to first-stage rotor
Maximum D	0.526	Hub of first-stage stator
Minimum D	0.450	Tip of first-stage rotor
Maximum reaction	0.625	Tip of first stage
Minimum reaction	0.309	Hub of first stage

9.3.9 Compressor Performance

The pumping characteristics of axial-flow compressors are best represented by a plot (based on experimental data) called the *compressor map*. The data are presented in terms of *corrected quantities* that are related to the performance of the compressor. A compressor is tested in a rig similar to the sketch of Fig. 9.38. The rotational speed is controlled by the electric motor and the mass flow rate by the valve. The inlet and exit conditions are measured along with the rotational speed and input power. These data are reduced to give the resulting compressor map.

9.3.9.1 Corrected quantities. For a compressor, the four corrected quantities shown in Table 9.10 are normally used to map its performance. The corrected rotational speed is directly proportional to the ratio of the axial to rotational velocity. The corrected mass flow rate is directly proportional to the Mach number of the entering flow. We note that

$$\dot{m}_i = \frac{P_{ti}}{\sqrt{T_{t_i}}} A_i \, \mathrm{MFP}(M_i)$$

Table 9.10 Compressor corrected quantities

Item	Symbol	Corrected
Pressure	P_{t_i}	$\delta_t = \dfrac{P_{ti}}{P_{\text{ref}}}$ where $P_{\text{ref}} = 14.696$ psia
Temperature	T_{t_i}	$\theta_t = \dfrac{T_{t_i}}{T_{\text{ref}}}$ where $T_{\text{ref}} = 518.7°\text{R}$
Rotational speed	$N = \text{RPM}$	$\dfrac{N}{\sqrt{\theta_t}}$
Mass flow rate	$\dot{m}_t$	$\dot{m}_{ct} = \dfrac{\dot{m}_t \sqrt{\theta_t}}{\delta_t}$

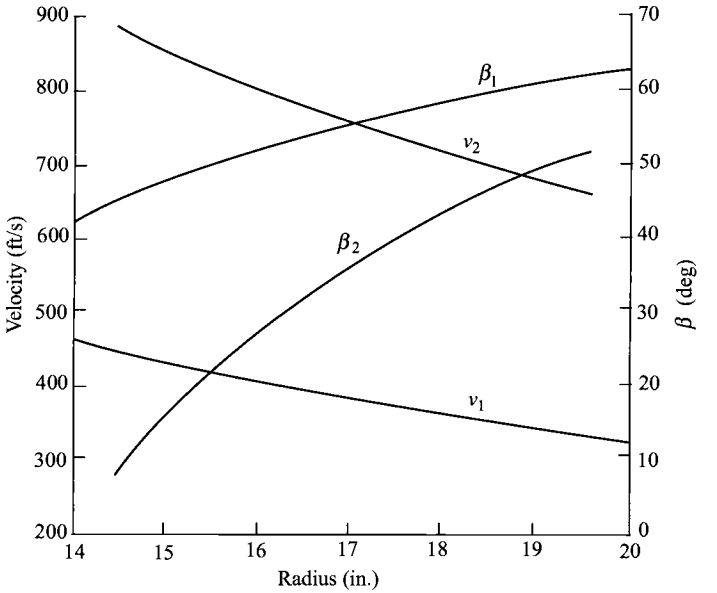

Fig. 9.37 Swirl velocity distribution and variation of rotor flow angles.

Then

$$\dot{m}_{ci} = \frac{\dot{m}_i\sqrt{T_{ti}}}{P_{ti}}\frac{P_{\text{ref}}}{\sqrt{T_{\text{ref}}}} = \frac{P_{\text{ref}}}{\sqrt{T_{\text{ref}}}}A_i\,\text{MFP}(M_i)$$

Therefore,

$$\dot{m}_{ci} = f(M_i)$$

At engine station 2 (entrance to compressor or fan)

$$\dot{m}_{c2} = \frac{P_{\text{ref}}}{\sqrt{T_{\text{ref}}}}A_2\,\text{MFP}(M_2) \tag{9.64}$$

Thus the corrected mass flow rate is directly proportional to a the Mach number at the entrance to the compressor.

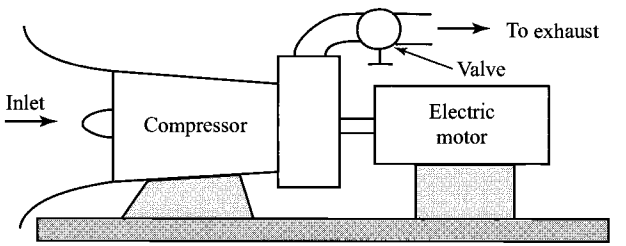

Fig. 9.38 Sketch of compressor test rig.

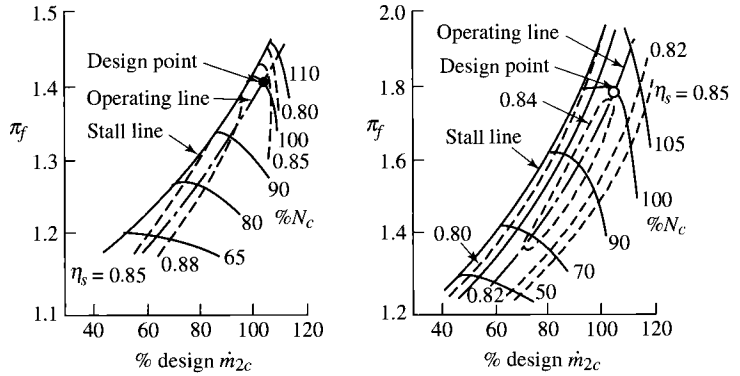

a) Subsonic tangential Mach **b) Supersonic tangential Mach**

Fig. 9.39 Typical fan stage maps (Ref. 52).

9.3.9.2 Compressor map. The performance of two modern high-performance fan stages is shown in Fig. 9.39. They have no inlet guide vanes. One has a low tangential Mach number (0.96) to minimize noise. The other has supersonic tip speed and a considerably larger pressure ratio. Both have high axial Mach numbers.

Variations in the axial-flow velocity in response to changes in pressure cause the multistage compressor to have quite different mass flow vs pressure ratio characteristics from those of one of its stages. The performance map of a typical high-pressure-ratio compressor is shown in Fig. 9.40.

A limitation on fan and compressor performance of special concern is the stall or surge line. Steady operation above the line is impossible, and entering the region even momentarily is dangerous to the compressor and its application.

9.3.9.3 Compressor starting problems. The cross section of a multistage compressor is shown in Fig. 9.41. Also shown (in solid lines) at three locations in the machine are mean-line rotor inlet velocity diagrams for on-design operation. The design shown here has a constant mean radius, a constant axial velocity, and zero swirl at the rotor-inlet stations.

Let us apply the continuity equation, which states that the mass flow rate is the same at all stations in the compressor. Then, at the inlets to the first and last stages,

$$\dot{m} = \rho_1 A_1 u_1 = \rho_3 A_3 u_3$$

or

$$\frac{u_1}{u_3} = \frac{\rho_3 A_3}{\rho_1 A_1} \tag{9.65}$$

At the design point, since $u_3 = u_1$, then $\rho_3/\rho_1 = A_1/A_3$. When the compressor is operating at a lower speed, however, it is not able to produce as high a density

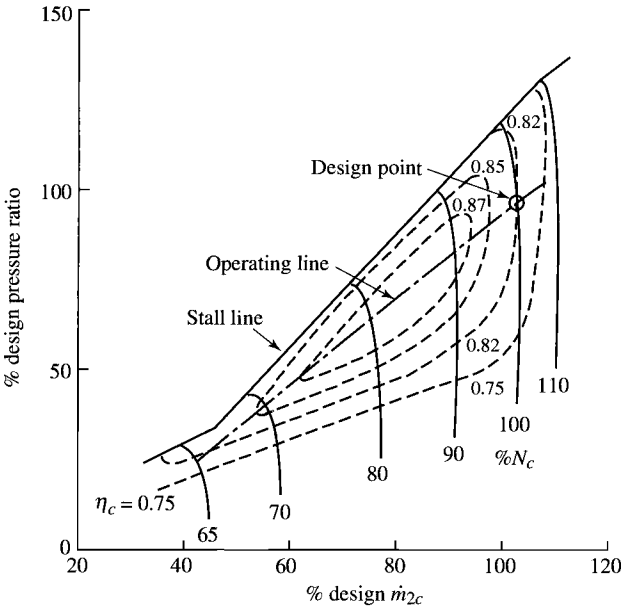

Fig. 9.40 Typical compressor map.

ratio (or pressure ratio) as at design speed, and because the area ratio remains fixed, it follows from Eq. (9.65) that the inlet/outlet axial velocity ratio must have a value less than that at design. In Fig. 9.41, the velocity diagrams shown (in dashed lines) indicate the rotor inlet conditions at partial speed. For each of the three stages represented, the blade speed is the same, but the inlet stage axial velocity is shown less than that for the outlet stage in accordance with

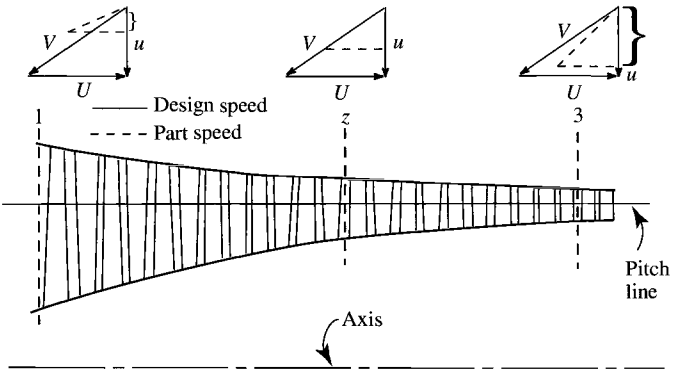

Fig. 9.41 Cross section of a multistage compressor. Rotor-inlet velocity diagrams are shown for inlet, middle, and exit stages.

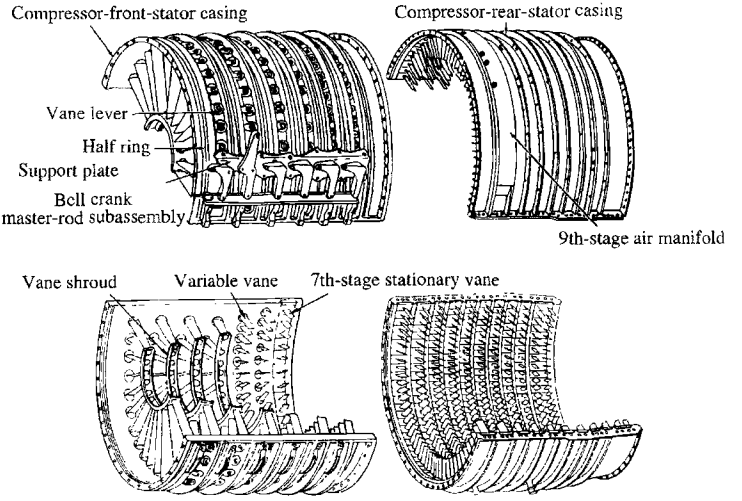

Fig. 9.42 Compressor case for the General Electric J-79 turbojet engine. (Courtesy of General Electric.)

Eq. (9.65). Because of the varying axial velocity, it is possible for only one stage near the middle of the machine (called the *pivot stage*) to operate with the same angle of attack at all speeds. At lower speeds, the blading forward of the pivot stage is pushed toward stall, and the blading aft of the pivot stage is windmilling with a tendency toward choking. At speeds higher than the design value, these trends are reversed.

Several techniques have been utilized to reduce the low-speed and starting effects:

1) Use bleed valves. Release air from the middle stages, reducing the tendency to windmill in later stages.

2) Use multispool compressors. Run different spools at their own suitable speeds.

3) Use variable stators in the early rows.

4) Use combinations of the preceding techniques.

An example of an early high-performance compressor is that used in the General Electric J-79 turbojet engine. This compressor has 17 stages on a single spool that results in a pressure ratio of 13.5. Figure 9.42 shows the compressor case of this engine with the variable stators used on the first six stages and the manifold for the bleed valves on the ninth stage. Most modern engines have compressors with multiple spools and bleed valves. The need for variable stators in the early rows is less for the multispool compressors.

9.4 Centrifugal-Flow Compressor Analysis

The centrifugal compressor has been around for many years. It was used in turbochargers before being used in the first turbojet engines of Whittle and von

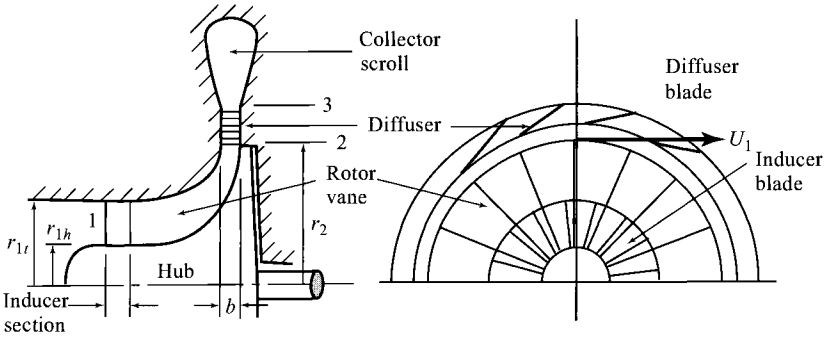

a) Cross-sectional view **b) View of rotor and diffuser**

Fig. 9.43 Centrifugal-flow compressor.

Ohain. Figure 9.43 shows a sketch of a centrifugal-flow compressor with radial rotor (or impeller) vanes. Flow passes through the annulus between r_{1h} and r_{1t} at station 1 and enters the inducer section of the rotor (also called *rotating guide vanes*). Flow leaves the rotor at station 2 through the cylindrical area of radius r_2 and width b. The flow then passes through the diffuser, where it is slowed and then enters the collector scroll at station 3.

The velocity diagrams at the entrance and exit of the rotor (impeller) are shown in Fig. 9.44. The inlet flow is assumed to be axial of uniform velocity u_1. The relative flow angle of the flow entering the rotor increases from hub to tip and thus the twist of the inlet to the inducer section of the rotor. The flow leaves the rotor with a radial component of velocity w_2 that is approximately equal to the inlet axial velocity u_1 and a swirl (tangential) component of velocity v_2 that is about 90% of the rotor velocity U_t. The diffuser (which may be vaneless) slows the velocity of the flow v_3 to about 90 m/s (300 ft/s).

Application of the Euler equation to flow of a calorically perfect gas through a centrifugal-flow compressor with axial flow entering gives

$$T_{t3} - T_{t1} = \frac{v_2 U_t}{g_c c_p} \tag{9.66}$$

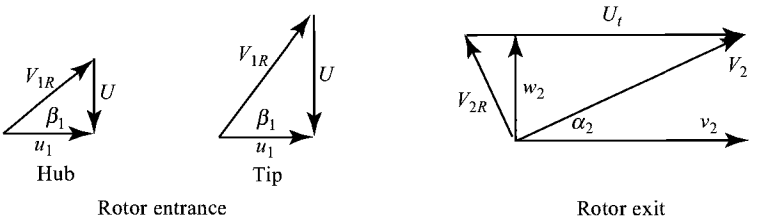

Fig. 9.44 Velocity diagrams for radial vaned centrifugal compressor.

Ideally, the fluid leaving the rotor wheel has a swirl velocity v_2 equal to the rotor speed U_t. Because of slip between the rotor and fluid, the fluid leaving the rotor wheel attains only a fraction of the rotor speed. The ratio of the exit swirl velocity to the rotor speed is called the *slip factor* ε:

$$\varepsilon = \frac{v_2}{U_t} \tag{9.67}$$

The slip factor is related to the number of vanes on the rotor. As the number of vanes n is increased, the slip factor approaches 1 and the frictional losses of the rotor increase. Selection of the number of vanes is a balance between high slip factor and reasonable losses, which usually results in a slip factor of 0.9. A useful correlation between the slip factor ε and number of vanes n *is*

$$\varepsilon = 1 - \frac{2}{n} \tag{9.68}$$

Substitution of Eq. (9.67) into Eq. (9.66) gives a relationship for the compressor temperature rise in terms of the rotor speed U_t and slip factor ε:

$$T_{t3} - T_{t1} = \frac{\varepsilon U_t^2}{g_c c_p} \tag{9.69}$$

By using the polytropic compressor efficiency e_c and Eq. (9.69), the compressor pressure ratio can be expressed as

$$\pi_c = \frac{P_{t3}}{P_{t1}} = \left(1 + \frac{\varepsilon U_t^2}{g_c c_p T_{t1}}\right)^{\gamma e_c/(\gamma-1)} \tag{9.70}$$

From Eq. (9.70), compressor pressure ratio π_c is plotted vs rotor speed U_t in Fig. 9.45 for air [$\gamma = 1.4$, $c_p = 1.004$ kJ/(kg · K)] at standard conditions ($T_{t1} = 288.16$ K) with a slip factor ε of 0.9. For rotors with light alloys, U_t is limited to about 450 m/s (1500 ft/s) by the maximum centrifugal stresses of the rotor, which corresponds to compressor pressure ratios of about 4. More extensive materials permit higher speeds and pressure ratios up to about 8.

Equation (9.70) can also be written in terms of the compressor adiabatic efficiency η_c as

$$\pi_c = \frac{P_{t3}}{P_{t1}} = \left(1 + \frac{\eta_c \varepsilon U_t^2}{g_c c_p T_{t1}}\right)^{\gamma/(\gamma-1)} \tag{9.71}$$

The *T-s* diagram for the centrifugal compressor is shown in Fig. 9.46. This diagram is very useful during the analysis of centrifugal-flow compressors. Even though the rotor exit velocity v_2 may be supersonic, the flow leaving the rotor will choke only when the radial exit velocity w_2 is sonic. For determining the total pressure at station 2, an estimate must be made of the split in total

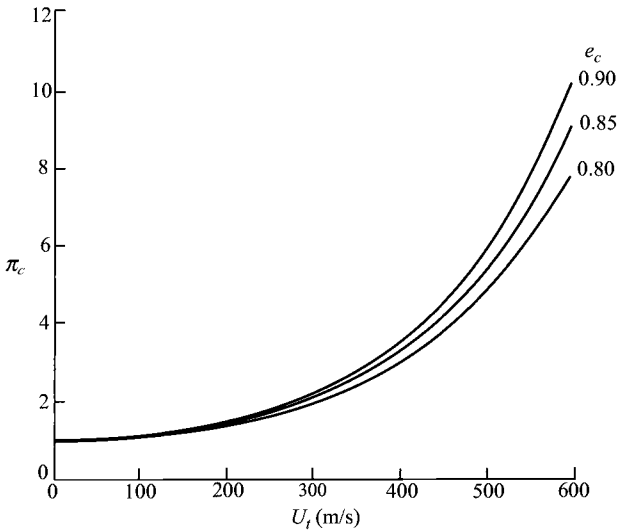

Fig. 9.45 Compressor pressure ratio vs rotor speed.

pressure loss between the rotor and diffuser. As an estimate, we equate the total pressure ratio of the diffuser P_{t3}/P_{t2} to the actual/ideal total pressure ratio leaving the rotor P_{t2}/P_{t3s}, or

$$\frac{P_{t2}}{P_{t3s}} = \frac{P_{t3}}{P_{t2}} = \sqrt{P_{t3}/P_{t3s}} \tag{9.72}$$

The radial component of velocity leaving the rotor w decreases with radius due to the increase in radial flow area. If frictional losses are neglected, the tangential

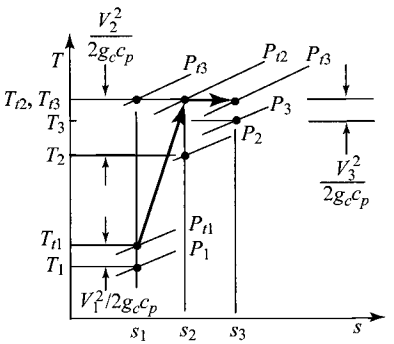

Fig. 9.46 The *T-s* diagram for centrifugal compressor.

momentum rv will remain constant, or

$$rv = \text{const} = r_2 v_2$$

As a result of the decreases in both the radial and tangential velocities, the velocity entering the diffuser is less than that leaving the rotor.

The diffuser further decreases the velocity and may turn the flow with blades. The flow leaving the diffuser is collected in the scroll (see Fig. 9.43). The flow area of the scroll A_θ must increase in proportion to the mass flow being added to keep the flow properties constant. We can write

$$\frac{dA_\theta}{d\theta} = \frac{1}{\rho_3 V_3} \frac{d\dot{m}}{d\theta} = r_3 b_3 \tag{9.73}$$

Centrifugal-flow compressors are used in gas turbine engines when the corrected mass flow rate is small (less than about 10 kg/s). For small corrected mass flow rates, the rotor blades of axial-flow compressors are very short, and the losses are high. The performance of a centrifugal compressor for low flow rates can be as good as or better than that of the axial-flow compressor.

The performance of a centrifugal-flow compressor is presented as a compressor map (similar to the map of an axial-flow compressor). The map of a typical centrifugal compressor is shown in Fig. 9.47. Note that the overall pressure ratio is limited to about 4. Gas turbine engine cycles normally require a pressure ratio greater than 4 and additional stages of compression are needed. For engines with entering corrected mass flow rates greater than 10 kg/s, additional compression is obtained from axial-flow stages in front of the centrifugal compressor. When the corrected mass flow is less than 10 kg/s, higher cycle pressure ratios are obtained by using two or more centrifugal compressors in series.

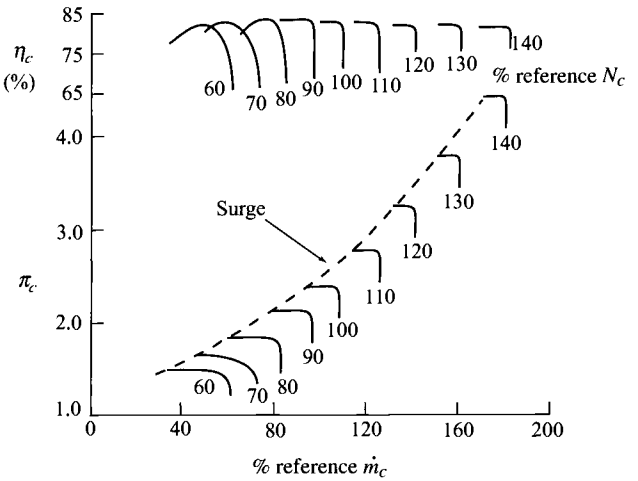

Fig. 9.47 Performance map of typical centrifugal compressor.

Example 9.8

Consider a centrifugal compressor.

Given:

Mass flow rate = 8 kg/s
Pressure ratio $\pi_c = 4.0$
Polytropic efficiency $e_c = 0.85$
Inlet root diameter = 15 cm
Outlet diameter of impeller = 50 cm
$V_3 = 90$ m/s
$P_{t1} = 101.3$ kPa
$T_{t1} = 288.16$ K
Slip factor $\varepsilon = 0.9$
Inlet tip diameter = 30 cm
$w_2 = u_1$

Find:

1) Rotational speed and rpm of the rotor
2) Rotor inlet Mach number, velocity, and relative flow angles at hub and tip
3) Rotor exit velocity, Mach number, total temperature, total pressure, and direction
4) Depth of rotor exit s
5) Diffuser exit Mach number, area, total temperature, and total pressure

Solution:

$$U_t^2 = \frac{g_c c_p T_{t1}}{\varepsilon}(\pi_c^{(\gamma-1)/(\gamma e_c)} - 1)$$

$$= \frac{1004 \times 288.16}{0.9}(4^{1/(3.5\times 0.85)} - 1)$$

$$U_t = 436.8 \text{ m/s}$$

$$N = \frac{60U_t}{\pi d_2} = \frac{60(436.8)}{\pi(0.5)} = 16{,}685 \text{ rpm}$$

$$\text{MFP}(M_1) = \frac{\dot{m}\sqrt{T_n}}{P_{t1}A_1} = \frac{8\sqrt{288.16}}{101{,}300 \times \pi(0.15^2 - 0.075^2)} = 0.025287$$

$$M_1 = 0.3966$$

$$u_1 = V_1 = \sqrt{2g_c c_p T_{t1}\left\{1 - \frac{1}{1 + [(\gamma-1)/2]M_1^2}\right\}}$$

$$= \sqrt{2 \times 1004 \times 288.16\left(1 - \frac{1}{1 + 0.2 \times 0.3966^2}\right)} = 132.8 \text{ m/s}$$

$$v_{1Rh} = \frac{d_{1h}}{d_2}U_t = \frac{15}{50}(436.8) = 131.0 \text{ m/s}$$

$$v_{1R_t} = \frac{d_{1t}}{d_2}U_t = \frac{30}{50}(436.8) = 262.1 \text{ m/s}$$

$$\beta_{1h} = \tan^{-1}\frac{v_{1Rh}}{u_1} = 44.6\,\text{deg}$$

$$\beta_{1t} = \tan^{-1}\frac{v_{1Rt}}{u_1} = 63.1\,\text{deg}$$

$$T_{t3} = T_{t2} = T_{t1} + \frac{\varepsilon U_t^2}{g_c c_p} = 288.16 + \frac{0.9 \times 436.8^2}{1004} = 459.19\,\text{K}$$

$$\eta_c = \frac{(P_{t3}/P_{t1})^{\gamma/(\gamma-1)} - 1}{T_{t3}/T_{t1} - 1} = \frac{4^{1/3.5} - 1}{459.19/288.16 - 1} = 81.9\%$$

$$v_2 = \varepsilon U_t = 0.9 \times 436.8 = 393.1\ \text{m/s}$$

$$w_2 = u_1 = 132.8\ \text{m/s}$$

$$V_2 = \sqrt{w_2^2 + v_2^2} = \sqrt{132.8^2 + 393.1^2} = 414.9\,\text{m/s}$$

$$\alpha_2 = \tan^{-1}\frac{w_2}{v_2} = 18.67\,\text{deg}$$

$$M_2 = \sqrt{\frac{2}{\gamma - 1}\left[\frac{T_{t2}}{T_{t2} - V_2^2/(2g_c c_p)} - 1\right]}$$

$$= \sqrt{5\left(\frac{459.19}{459.19 - 85.73} - 1\right)} = 1.071$$

$$\frac{P_{t3s}}{P_{t1}} = \left(\frac{T_{t3}}{T_{t1}}\right)^{\gamma/(\gamma-1)} = 5.108$$

$$\frac{P_{t2}}{P_{t3s}} = \frac{P_{t3}}{P_{t2}} = \sqrt{\frac{P_{t3}/P_{t1}}{P_{t3s}/P_{t1}}} = 0.8849$$

$$P_{t2} = 0.8849 \times 5.108 \times 101.3 = 457.9\,\text{kPa}$$

$$P_{t3} = 4.0 \times 101.3 = 405.2\,\text{kPa}$$

$$\text{MFP}(M_2) = 0.040326$$

$$A_2 = \frac{\dot{m}\sqrt{T_{t2}}}{P_{t2}\text{MFP}(M_2)(\cos\alpha_2)} = \frac{8\sqrt{459.19}}{457{,}900 \times 0.040326 \times 0.9474} = 0.0098\,\text{m}^2$$

$$b = \frac{A_2}{\pi d_2} = \frac{0.0098}{\pi \times 0.5} = 0.624\,\text{cm}$$

Table 9.11 Results for Example 9.8 centrifugal compressor

Property		Station 1	1*R*	2*R*	2	3
T_t	K	**288.16**	296.70/322.36 (hub/tip)	383.23	459.19	459.19
T	K	279.37	279.37	272.50	373.50	455.16
P_t	kPa	**101.3**	112.2/150.0	243.1	457.9	**405.2**
P	kPa	90.9	90.9	222.2	222.2	392.9
M		0.3966	0.557/0.877	0.361	1.071	0.2105
V	m/s	132.8	186.54/293.82	139.8	414.9	90
u/w	m/s	132.8	132.8	132.8	132.8	
v	m/s	0	131.0/262.1	43.7	393.1	
r	cm		**15/30**	**50.0**	**50.0**	
α	deg	0	——	——	18.67	
β	deg	——	44.6/63.1	69.1	——	

$$M_3 = \sqrt{\frac{2}{\gamma - 1}\left[\frac{T_{t3}}{T_{t3} - V_3^2/(2g_c c_p)} - 1\right]}$$

$$= \sqrt{5\left(\frac{459.19}{459.19 - 4.034} - 1\right)} = 0.2105$$

$$\text{MFP}(M_3) = 0.014343$$

$$A_3 \cos \alpha_3 = \frac{\dot{m}\sqrt{T_{t3}}}{P_{t3}\text{MFP}(M_3)} = \frac{8\sqrt{459.196}}{405{,}200 \times 0.014343} = 0.0295 \text{ m}^2$$

The results of this example are summarized in Table 9.11. Note that different values of flow properties are listed for the hub and tip at station 1*R* and that M_2 is supersonic while M_{2R} is subsonic.

9.5 Axial-Flow Turbine Analysis

The mass flow of a gas turbine engine, which is limited by the maximum permissible Mach number entering the compressor, is generally large enough to require an axial turbine (even for centrifugal compressors). The axial turbine is essentially the reverse of the axial compressor except for one essential difference: the turbine flow operates under a favorable pressure gradient. This permits greater angular changes, greater pressure changes, greater energy changes, and higher efficiency. However, there is more blade stress involved because of the higher work and temperatures. *It is this latter fact that generally dictates the blade shape.*

Conceptually, a turbine is a very simple device because it is fundamentally no different from a pinwheel that spins rapidly when air is blown against it. The pinwheel will turn in one direction or the other, depending on the direction of the impinging air, and a direction can be found for the air that causes no rotation at all. Thus it is important to properly direct the airstream if the desired motion and speed are to be obtained.

A modern turbine is merely an extension of these basic concepts. Considerable care is taken to establish a directed flow of fluid of high velocity by means of stator blades, and then similar care is used in designing the blades on the rotating wheel (the vanes on the pinwheel) so that the fluid applies the required force to these rotor blades most efficiently. Conceptually, the turbine is a cousin to the pinwheel, but such an analogy gives no appreciation for the source of the tremendous power outputs that can be obtained in a modern turbine. The appreciation comes when one witnesses a static test of the stator blades that direct a gas stream to the rotor of a modern aircraft gas turbine. Such a stream exhausting into the quiescent air of a room will literally rip the paint off the wall at a point 6 ft away in line with the jet direction. When blades of the rotating element are pictured in place immediately at the exit of these directing blades, it then becomes difficult to imagine that the rotor could be constrained from turning and producing power.

Terminology can be a problem in the general field of turbomachinery. Compressor development grew out of aerodynamics and aircraft wing technology, while turbines have historically been associated with the mechanical engineers who developed the steam turbine. The symbols as well as the names used in these two fields differ, but for consistency and to minimize problems for the reader, the turbine will be presented using the nomenclature already established in the beginning of this chapter. Where a term or symbol is in such common use that to ignore it would mean an incomplete education, it will be indicated as an alternate. Thus turbine stator blades are usually called *nozzles* and rotor blades are *buckets.*

In the gas turbine, the high-pressure, high-temperature gas from the combustion chamber flows in an annular space to the stationary blades (called *stators, vanes*, or *nozzles*) and is directed tangentially against the rotating blade row (called *rotor blades* or *buckets*). A simple single-stage turbine configuration with nomenclature is shown in Fig. 9.48a. It is convenient to "cut" the blading on a cylindrical surface and look at the section of the stator and rotor blades in two dimensions. This leads to the construction of a vector or velocity diagram for the stage (see Fig. 9.48a) that shows the magnitude and direction of the gas velocities within the stage on the cylindrical surface.

In the stator or nozzle, the fluid is accelerated while the static pressure decreases and the tangential velocity of the fluid is increased in the direction of rotation. The *rotor* decreases the tangential velocity in the direction of rotation, tangential forces are exerted by the fluid on the rotor blades, and a resulting torque is produced on the output shaft. The absolute velocity of the fluid is reduced across the rotor. Relative to the moving blades, typically there is acceleration of the fluid with the associated decrease in static pressure and static temperature. A multistage turbine is made up of consecutive stages, each stage consisting of first a nozzle row followed by a rotor row. Figure 9.48b shows an

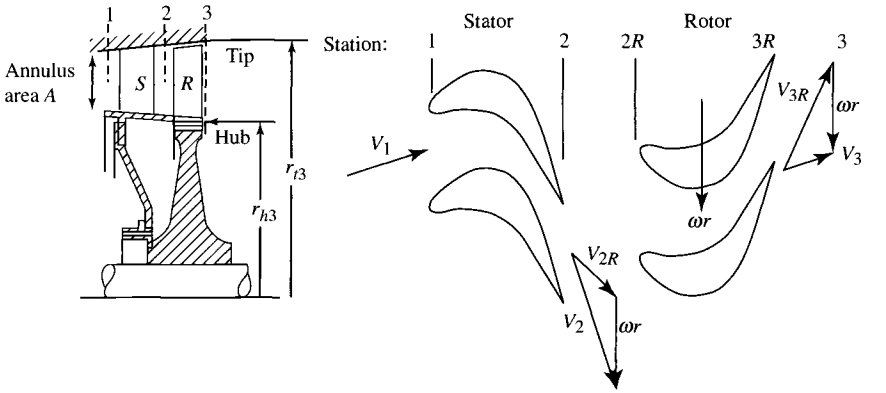

Fig. 9.48a Typical single-stage turbine and velocity diagram.

isometric section of the four-stage turbine for a two-spool, low-bypass-ratio turbofan engine.

The following analysis of the axial-flow turbine stage is performed along the mean radius with radial variations being considered. In many axial-flow turbines, the hub and tip diameters vary little through a stage, and the hub/tip ratio approaches unity. There can be no large radial components of velocity between the annular walls in such stages, there is little variation in static pressure from root to tip, and the flow conditions are little different at each radius.

For these stages of high hub/tip ratio, the two-dimensional analysis is sufficiently accurate. The flow velocity triangles are drawn for the mean-radius

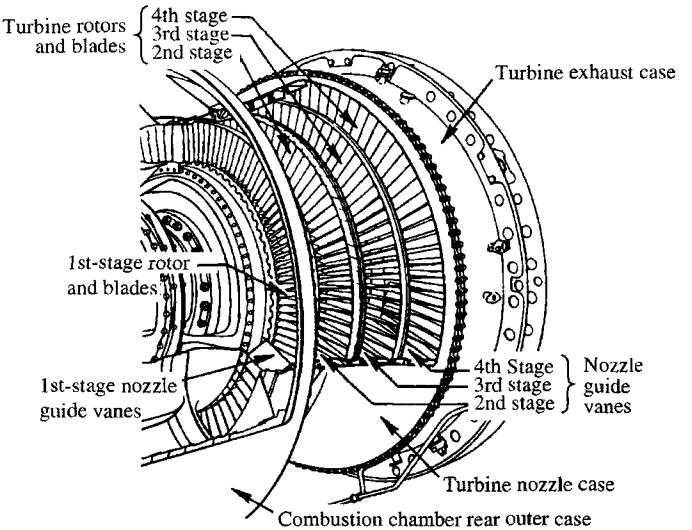

Fig. 9.48b Isometric section of multistage turbine. (Courtesy of Pratt & Whitney.)

condition, but these triangles are assumed to be valid for the other radial sections. The mean-radius analysis presented in this section applies to the total flow for such *two-dimensional* stages: the flow velocity, blade speed, and pressures being assumed constant along the blade length.

From the Euler turbine equation, [Eq. (9.4)], the energy per unit mass flow exchanged between fluid and rotor for $r_2 = r_3$ is

$$h_{t2} - h_{t3} = c_p(T_{t2} - T_{t3}) = \frac{\omega r}{g_c}(v_2 + v_3) \tag{9.74}$$

Inspection of the velocity triangles (Fig. 9.49) shows that because of the large angle α_2 at the stator exit and the large turning possible in the rotor, the value of v_3 is often positive (positive α_3). As a result, the two swirl velocity terms on the right side of Eq. (9.74) add, giving large power output.

The large turning in stator and rotor is possible because, usually, the flow is accelerating through each blade row, that is, $v_2 > v_1$ and $v_{3R} > v_{2R}$. This means that the static pressure drops across both stator and rotor and, under such circumstances, a favorable pressure gradient exists for the boundary layers on the blade and wall surfaces, and separation can be avoided. Accelerating flow is an inherent feature of turbines and means that no general flow breakdown similar to compressor stall will occur.

Note that the vector diagram establishes the characteristics of a stage, and geometrically similar diagrams have the same characteristics. The angles of the vector diagram determine its shape and, therefore, become important design parameters. The velocity magnitudes are not important as performance parameters except in relation to the sonic velocity, i.e., except in terms of the Mach number. The angles may be used directly as design parameters or may be implied through the use of velocity ratios. Thus the magnitude of, say,

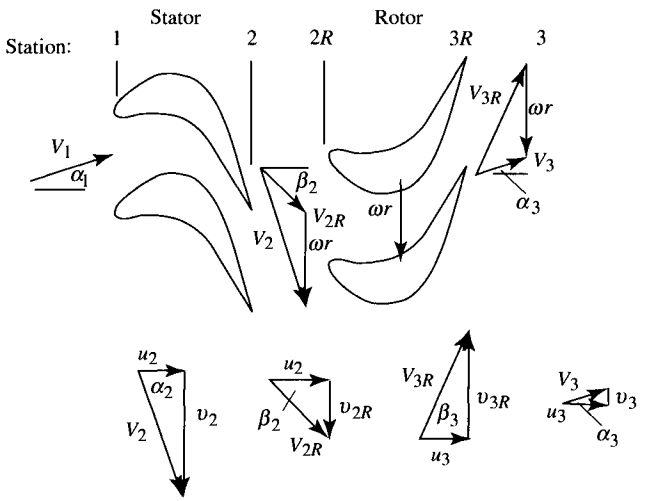

Fig. 9.49 Velocity triangles for a typical turbine stage.

$v_2 + v_3 = \Delta v$, although proportional to the absolute output, is not significant in defining the vector diagram, whereas the ratio $\Delta v/(\omega r)$ helps establish the vector diagram angles and, therefore, the stage characteristics.

The stage analysis in the following sections neglects the influence of cooling air. Thus the flow through the turbine nozzle is assumed to be adiabatic ($T_{t2} = T_{t1}$), as is the flow through the rotor in the relative reference frame ($T_{t3R} = T_{t2R}$). Turbine cooling is discussed at the end of this chapter.

Example 9.9

Consider mean-radius stage calculation—isentropic flow.

Given:

$$T_{t1} = 3200°\text{R}, \quad P_{t1} = 300 \text{ psia}, \quad \alpha_2 = 60 \text{ deg}$$
$$\alpha_3 = 0 \text{ deg}, \quad M_2 = 1.1, \quad \omega r = 1400 \text{ ft/s}$$
$$u_3 = u_2, \quad \gamma = 1.3, \quad R = 53.40 \text{ ft} \cdot \text{lbf/(lbm} \cdot °\text{R)}$$

Find the flow properties for this isentropic turbine stage.

Solution:

$$T_{t2} = T_{t1} = 3200°\text{R}$$

$$T_2 = \frac{T_{t2}}{1 + [(\gamma - 1)/2]M_2^2} = \frac{3200}{1 + 0.15 \times 1.1^2} = 2708.4°\text{R}$$

$$g_c c_p = g_c \left(\frac{\gamma}{\gamma - 1}\right) R = 32.174 \left(\frac{1.3}{0.3}\right) 53.40 = 7445 \text{ ft}^2/(\text{s}^2 \cdot °\text{R})$$

$$V_2 = \sqrt{2 g_c c_p (T_{t2} - T_2)} = \sqrt{2(7445)(3200 - 2708.4)} = 2705.5 \text{ ft/s}$$

$$u_2 = V_2 \cos \alpha_2 = 2705.5 \cos 60 \text{ deg} = 1352.8 \text{ ft/s}$$

$$v_2 = V_2 \sin \alpha_2 = 2705.5 \sin 60 \text{ deg} = 2343.0 \text{ ft/s}$$

$$v_{2R} = v_2 - \omega r = 2343.0 - 1400 = 943.0 \text{ ft/s}$$

$$V_{2R} = \sqrt{u_2^2 + v_{2R}^2} = \sqrt{1352.8^2 + 943.0^2} = 1649.0 \text{ ft/s}$$

$$\beta_2 = \tan^{-1} \frac{v_{2R}}{u_2} = \tan^{-1} \frac{943.0}{1352.8} = 34.88 \text{ deg}$$

$$M_{2R} = M_2 \frac{V_{2R}}{V_2} = 1.1 \left(\frac{1649.0}{2705.5}\right) = 0.670$$

$$T_{t2R} = T_2 + \frac{V_{2R}^2}{2 g_c c_p} = 2708.4 + \frac{1649.0^2}{2(7445)} = 2891.0°\text{R}$$

$$v_3 = 0$$

$$V_3 = u_3 = u_2 = 1352.8 \text{ ft/s}$$

$$v_{3R} = v_3 + \omega r = 0 + 1400 = 1400\,\text{ft/s}$$

$$V_{3R} = \sqrt{u_3^2 + v_{3R}^2} = \sqrt{1352.8^2 + 1400^2} = 1946.8\,\text{ft/s}$$

$$\beta_3 = \tan^{-1}\frac{v_{3R}}{u_3} = \tan^{-1}\frac{1400}{1352.8} = 45.98\,\text{deg}$$

$$T_{t3} = T_{t2} - \frac{\omega r}{g_c c_p}(v_2 + v_3) = 3200 - \frac{1400}{7445}(2343.0 + 0) = 2759.4^\circ\text{R}$$

$$T_3 = T_{t3} - \frac{V_3^2}{2g_c c_p} = 2759.4 - \frac{1352.8^2}{2(7445)} = 2636.5^\circ\text{R}$$

$$M_3 = \sqrt{\frac{2}{\gamma - 1}\left(\frac{T_{t3}}{T_3} - 1\right)} = \sqrt{\frac{2}{0.3}\left(\frac{2759.8}{2636.5} - 1\right)} = 0.558$$

$$M_{3R} = M_3\frac{V_{3R}}{V_3} = 0.558\left(\frac{1946.8}{1352.8}\right) = 0.803$$

$$T_{t3R} = T_{t2R} = 2891.0^\circ\text{R}$$

$$P_{t2} = P_{t1} = 300\,\text{psia}$$

$$P_2 = P_{t2}\left(\frac{T_2}{T_{t2}}\right)^{\gamma/(\gamma-1)} = 300\left(\frac{2708.4}{3200}\right)^{1.3/0.3} = 145.6\,\text{psia}$$

$$P_{t2R} = P_2\left(\frac{T_{t2R}}{T_2}\right)^{\gamma/(\gamma-1)} = 145.6\left(\frac{2891.0}{2708.4}\right)^{1.3/0.3} = 193.2\,\text{psia}$$

$$P_{t3R} = P_{t2R} = 193.2\,\text{psia}$$

$$P_{t3} = P_{t2}\left(\frac{T_{t3}}{T_{t2}}\right)^{\gamma/(\gamma-1)} = 300\left(\frac{2759.4}{3200}\right)^{1.3/0.3} = 157.9\,\text{psia}$$

$$P_3 = P_{t3}\left(\frac{T_3}{T_{t3}}\right)^{\gamma/(\gamma-1)} = 157.9\left(\frac{2636.5}{2759.4}\right)^{1.3/0.3} = 129.6\,\text{psia}$$

Table 9.12 is a summary of the results for this axial-flow turbine stage with isentropic flow. The given data are listed in boldface type. Even though the flow leaving the nozzle (station 2) is supersonic, the relative flow entering the rotor is subsonic. The flow through the rotor is turned 80.8 deg. Figure 9.50 shows the change in temperature and pressure for an isentropic turbine stage.

9.5.1 Stage Parameters

9.5.1.1 Adiabatic efficiency. The adiabatic efficiency (the most common definition of efficiency for turbines) is the ratio of the actual energy output to the

Table 9.12 Results for Example 9.9 axial-flow turbine stage calculation, isentropic flow

Property		Station 1	2	2*R*	3*R*	3
T_t	°R	**3200**	3200.0	2891.0	2891.0	2759.4
	(K)	(1778)	(1777.8)	(1606.1)	(1606.1)	(1533.0)
T	°R		2708.4	2708.4	2636.5	2636.5
	(K)		(1504.7)	(1504.7)	(1464.7)	(1464.7)
P_t	psia	**300**	300	193.2	193.2	157.9
	(kPa)	(2068)	(2068)	(1332)	(1332)	(1089)
P_t	psia		145.6	145.6	129.6	129.6
	(kPa)		(1004)	(1004)	(893.6)	(893.6)
M			**1.10**	0.670	0.803	0.558
V	ft/s		2705.5	1649.0	1946.8	1352.8
	(m/s)		(824.6)	(502.6)	(593.4)	(412.3)
u	ft/s		1352.8	1352.8	1352.8	1352.8
	(m/s)		(412.3)	(412.3)	(412.3)	(412.3)
v	ft/s		2343.0	943.0	1400.0	0
	(m/s)		(714.2)	(287.4)	(426.7)	(0)
α	deg		**60.0**	——	——	**0**
β	deg			34.88	45.98	——

theoretical isentropic output (see Fig. 9.51a) for the same input total state and same exit total pressure:

$$\eta_t = \frac{\text{actual } \Delta h_t}{\text{ideal } \Delta h_t} = \frac{h_{t1} - h_{t3}}{h_{t1} - h_{t3s}} \tag{9.75}$$

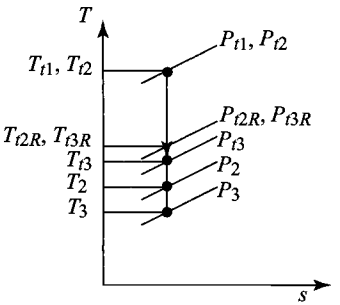

Fig. 9.50 Property changes of an isentropic turbine stage.

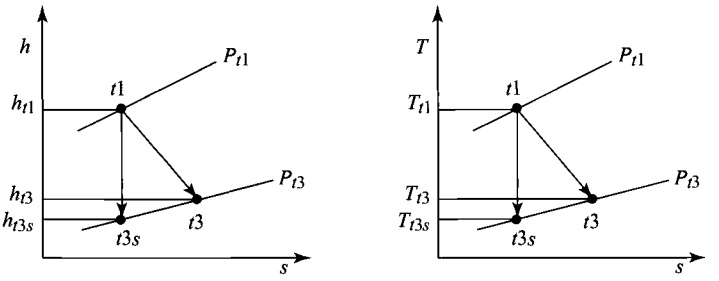

a) *h-s* diagram **b) *T-s* diagram**

Fig. 9.51 Definition of turbine adiabatic efficiency.

For a calorically perfect gas, the efficiency can be written in terms of total temperatures and total pressures (see Fig. 9.51b) as follows:

$$\eta_t = \frac{h_{t1} - h_{t3}}{h_{t1} - h_{t3s}} = \frac{c_p(T_{t1} - T_{t3})}{c_p(T_{t1} - T_{t3s})}$$

$$\eta_t = \frac{1 - T_{t3}/T_{t1}}{1 - (P_{t3}/P_{t1})^{(\gamma-1)/\gamma}} \tag{9.76}$$

The preceding definition is sometimes called the *total-to-total turbine efficiency* η_t, since the theoretical output is based on the leaving total pressure.

9.5.1.2 Exit swirl angle. The absolute angle of the leaving flow α_3 is called the *swirl angle* and, by convention, is positive when opposite to wheel speed direction (*backward*-running). The angle is important for two reasons. It is difficult in any fluid dynamic situation to efficiently convert kinetic energy to pressure or potential energy, and the kinetic energy in the flow leaving a turbine stage can be minimized by having $v_3 = u_3$, that is, by having zero swirl. Conversely, we see that the higher the swirl angle (if backward-running), the higher in magnitude v_3 will be, which generally means higher output from the stage [see Eq. (9.74) and Fig. 9.49].

9.5.1.3 Stage loading and flow coefficients. The *stage loading coefficient*, defined by Eq. (9.19), is the ratio of the stage work per unit mass to the rotor speed squared, or

$$\psi \equiv \frac{g_c \Delta h_t}{(\omega r)^2} = \frac{g_c \Delta h_t}{U^2}$$

For a calorically perfect gas, we write [Eq. (9.20)]

$$\psi = \frac{g_c c_p \Delta T_t}{(\omega r)^2} = \frac{g_c c_p \Delta T_t}{U^2}$$

The ratio of the axial velocity entering the rotor to the rotor speed is called the flow *coefficient* and is defined as

$$\Phi \equiv \frac{u_2}{\omega r} = \frac{u_2}{U} \tag{9.77}$$

The stage loading coefficient and flow coefficient for a turbine stage have a range of values. Figure 9.52 shows the range of these coefficients for several types of turbines. For Example 9.9 data, the stage loading coefficient is 1.67, and the flow coefficient is 0.962, which is well within the range for high-efficiency axial-flow turbines. Both the stage loading and flow coefficients affect the turbine stage efficiency, as shown in Fig. 9.53. Modern high-pressure turbines used for aircraft gas turbine engines have stage loading coefficients in the range of 1.3–2.2 and flow coefficients in the range of 0.5–1.1.

From Fig. 9.49 and Eqs. (9.74), (9.20), and (9.77), we obtain the stage loading coefficient in terms of the flow coefficient, the axial velocity ratio u_3/u_2, and flow angles as

$$\psi = \frac{g_c c_p \Delta T}{(\omega r)^2} = \frac{v_2 + v_3}{\omega r} = \Phi\left(\tan\alpha_2 + \frac{u_3}{u_2}\tan\alpha_3\right) \tag{9.78a}$$

or

$$\psi = \frac{g_c c_p \Delta T}{(\omega r)^2} = \frac{v_2 + v_3}{\omega r} = \Phi\left(\tan\beta_2 + \frac{u_3}{u_2}\tan\beta_3\right) \tag{9.78b}$$

By using Fig. 9.49, the flow coefficient can be expressed in terms of the flow angles as

$$\Phi = (\tan\alpha_2 - \tan\beta_2)^{-1} \tag{9.79}$$

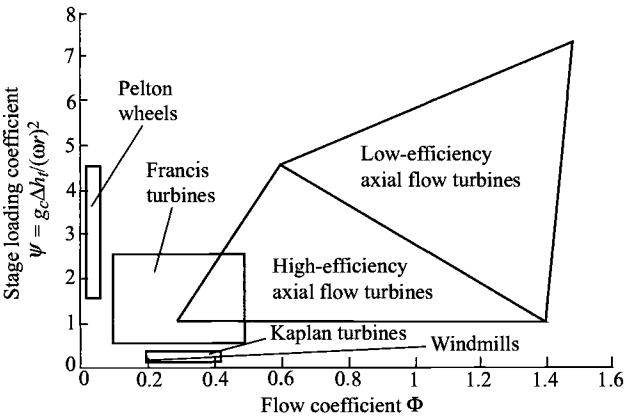

Fig. 9.52 Stage loading vs flow coefficient for different turbine types (Ref. 40).

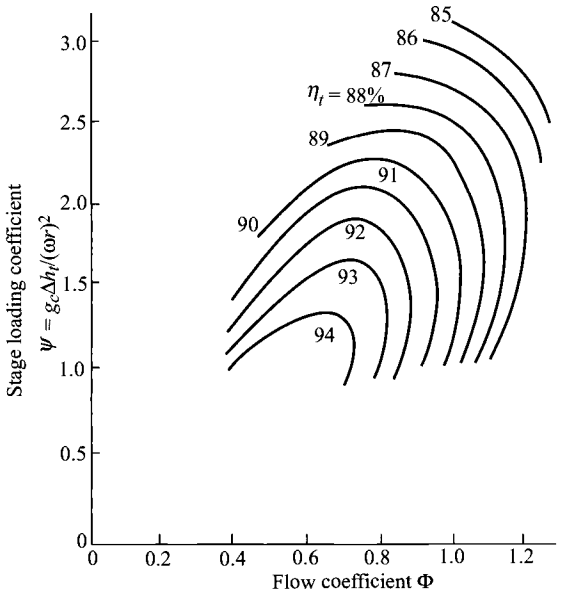

Fig. 9.53 Stage efficiency vs stage loading and flow coefficients, corrected for zero tip leakage (Ref. 40).

We obtain the following expression for the stage loading coefficient in terms of flow angles and u_3/u_2 by combining Eqs. (9.78a) and (9.79):

$$\psi = \frac{\tan \alpha_2 + (u_3/u_2)(\tan \alpha_3)}{\tan \alpha_2 - \tan \beta_2} \tag{9.80}$$

Equations (9.79) and (9.80) are plotted in Fig. 9.54 for constant axial velocity over a range of α_2 and β_2 and specific values of Φ, ψ, and α_3. This figure shows the effect of changing flow angles on Φ and ψ. Increasing α_3 with α_2 and β_2 held constant increases ψ and decreases Φ. Figure 9.54 also can be used to approximately determine the flow coefficient Φ from flow angles α_2 and β_2 and/or the stage loading coefficient ψ from flow angles α_2, β_2, and α_3. For example, given $\alpha_2 = 65$, $\beta_2 = 40$, and $\alpha_3 = 10$, Fig. 9.49 gives Φ of about 0.77 and ψ of about 1.8. More accurate results can be obtained by using Eqs. (9.79) and (9.80).

Figure 9.55 shows the rotor turning ($\varepsilon = \beta_2 + \beta_3$) for constant axial velocity as a function of the flow angle β_2 for different values of the ratio ψ/Φ. This figure can be used in conjunction with Fig. 9.54 to determine the rotor turning ε and the flow angle β_3.

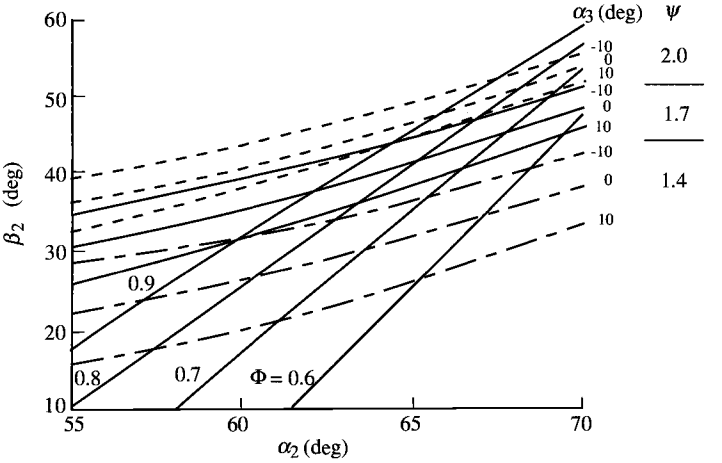

Fig. 9.54 Stage loading and flow coefficients vs flow angles (constant axial velocity).

9.5.1.4 Degree of reaction. The *degree of reaction* is defined as

$$^{\circ}R_t = \frac{h_2 - h_3}{h_{t1} - h_{t3}} \tag{9.81a}$$

For a calorically perfect gas, we can write

$$^{\circ}R_t = \frac{T_2 - T_3}{T_{t1} - T_{t3}} \tag{9.81b}$$

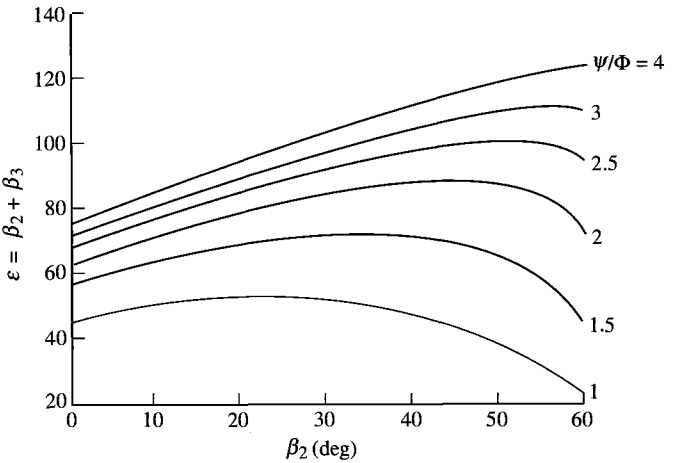

Fig. 9.55 Rotor turning ε vs Ψ/Φ and β_2 (constant axial velocity).

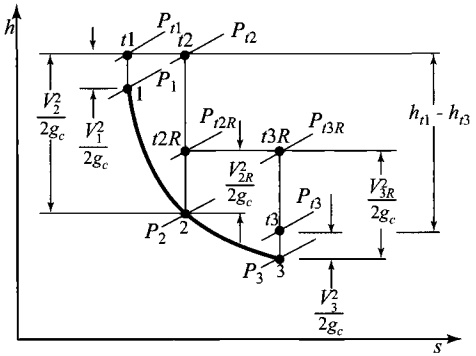

Fig. 9.56 The *h-s* diagram for general turbine stage.

That is, the degree of reaction is the ratio of the static enthalpy drop in the rotor to the drop in total enthalpy across both the rotor and stator. Figure 9.56 gives a complete picture for a general turbine stage. For Example 9.9, the degree of reaction is 0.166.

It can be shown that the degree of reaction may be related to the flow angles for the case of constant axial velocity ($u_3 = u_2$) by

$$^{\circ}R_t = \frac{u_2}{\omega r}\frac{\tan\beta_3 - \tan\beta_2}{2} = \Phi\frac{\tan\beta_3 - \tan\beta_2}{2} \tag{9.82}$$

By using Eq. (9.82), plots of $^{\circ}R_t/\Phi$ were added to Fig. 9.55, giving Fig. 9.57. One can see from this figure that zero reaction corresponds to maximum rotor turning ε for fixed value of ψ/Φ.

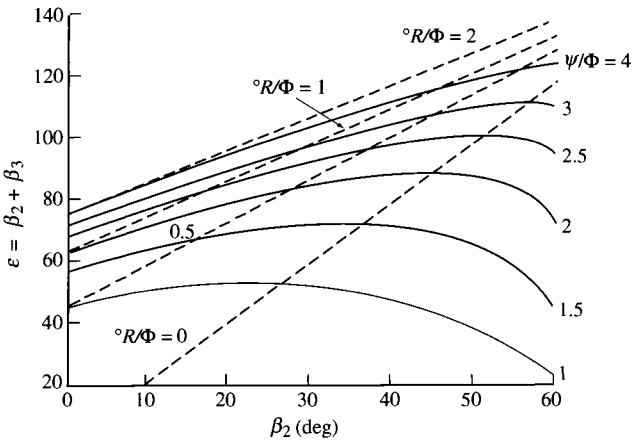

Fig. 9.57 Degree of reaction, stage loading coefficient, and flow coefficient vs rotor flow angles.

Three important basic designs of turbine are related to the choice of reaction—zero reaction, 50% reaction, and axial leaving velocity (variable reaction). It should be emphasized, however, that the designer is not limited to these three types and that in a three-dimensional turbine design, the reaction may vary continuously along the blades.

Zero reaction: From the definition of reaction, if the reaction is selected as zero for the case of constant axial velocity, then

$$h_3 = h_2 \quad \text{and} \quad \tan \beta_3 = \tan \beta_2$$

Therefore,

$$\beta_3 = \beta_2 \quad \text{and} \quad V_{3R} = V_{2R}$$

Velocity triangles for this zero reaction stage are shown in Fig. 9.58a, and the *h-s* diagram is drawn in Fig. 9.58b.

If the flow is isentropic and the fluid is a perfect gas, then the condition of zero enthalpy drop ($h_3 - h_2 = 0$) implies no change in pressure across the rotor. The turbine is then *called* an impulse turbine, with the tangential load arising from impulsive forces only. *It is important to note that reaction is defined here not on the basis of pressure drops, but in terms of static enthalpy changes.* Note, however, that there is a pressure drop from P_2 to P_3 across the rotor, and the

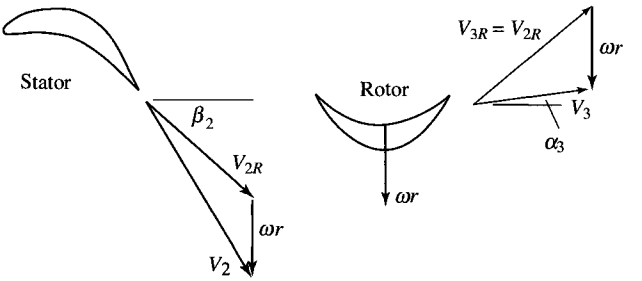

Fig. 9.58a Zero-reaction velocity diagram.

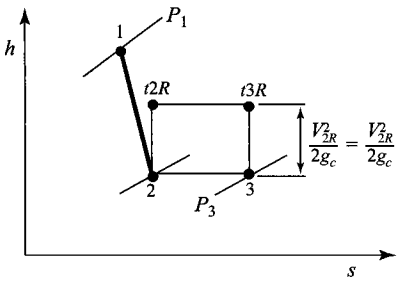

Fig. 9.58b Zero-reaction *h-s* diagram.

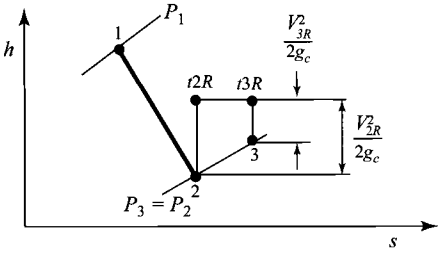

Fig. 9.59 Impulse turbine *h-s* diagram.

stage is not, therefore, truly impulse. The *h-s* diagram for an "impulse" stage of zero pressure drop is shown in Fig. 9.59. There is an enthalpy increase from h_2 to h_3 across the rotor, and the relative velocity decreases. Thus, *the impulse stage is actually one of negative reaction*!

The stage loading coefficient for the impulse stage with constant axial velocity is

$$\psi = \frac{g_c c_p \, \Delta T_t}{(\omega r)^2} = \frac{\omega r \Delta v}{(\omega r)^2} = \frac{\Delta v}{\omega r}$$

with

$$v_2 = u_2 \tan \alpha_2$$
$$v_3 = u_2 \tan \alpha_3 = u_2 \tan \alpha_2 - 2\omega r$$

then

$$\psi = 2(\Phi \tan \alpha_2 - 1) = 2\Phi \tan \beta_2 \tag{9.83}$$

We desire α_2 to be large. However, this leads to large v_2 and large v_{2R}, which lead to large losses. Thus α_2 is generally limited to less than 70 deg.

Also, if (see Fig. 9.58a) $\alpha_3 = 0$ (no exit swirl), then $\tan \alpha_2 = 2\omega r / u_2$ and

$$\psi = 2 \qquad \text{no exit swirl} \tag{9.84}$$

Thus we see that the rotor speed ωr is proportional to $\sqrt{\Delta h_t}$. If the resultant blade speed is too high, we must go to a multistage turbine.

50% reaction: If there is equal enthalpy drop across rotor and stator, then $R_t = 0.5$ and the velocity triangles are symmetrical, as shown in Fig. 9.60. Then, $\alpha_2 = \beta_3$, $\alpha_3 = \beta_2$, and

$$\tan \beta_3 - \tan \beta_2 = \tan \alpha_2 - \tan \alpha_3 = \frac{\omega r}{u_2} = \frac{1}{\Phi}$$

The stage loading coefficient for this turbine with constant axial velocity is

$$\psi = \frac{\Delta v}{\omega r} = 2\Phi \tan \alpha_2 - 1 = 2\Phi \tan \beta_3 - 1 \tag{9.85}$$

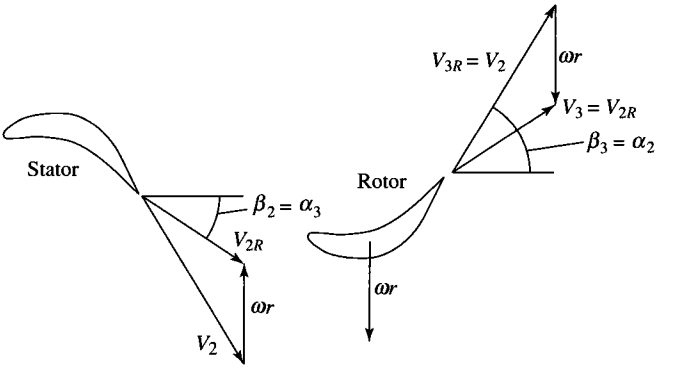

Fig. 9.60 Diagram of 50% reaction turbine velocity.

Again, α_2 should be high but is limited to less than 70 deg. For *zero exit swirl*

$$\tan \beta_3 = \tan \alpha_2 = \frac{\omega r}{u}, \quad \beta_2 = 0, \quad \psi = 1 \tag{9.86}$$

Thus, for the same ωr and $v_3 = 0$, the work per unit mass from a zero-reaction turbine is twice that from the 50% reaction turbine [compare Eqs. (9.84) and (9.86)].

General zero-swirl case (constant axial velocity): If the exit swirl is to be zero (Fig. 9.61), then $\alpha_3 = 0$, $v_3 = 0$, and $\tan \beta_3 = \omega r/u$. From Eq. (9.82), the reaction is then

$$^{\circ}R_t = \frac{u}{2\omega r}\left(\frac{\omega r}{u} - \tan \beta_2\right) = \frac{1}{2} - \frac{u \tan \beta_2}{2\omega r} = 1 - \frac{v_2}{2\omega r}$$

$$^{\circ}R_t = 1 - \frac{v_2}{2\omega r} = 1 - \frac{\psi}{2} \tag{9.87}$$

This equation can be rewritten as

$$\psi = 2(1 - {}^{\circ}R_t) \tag{9.88}$$

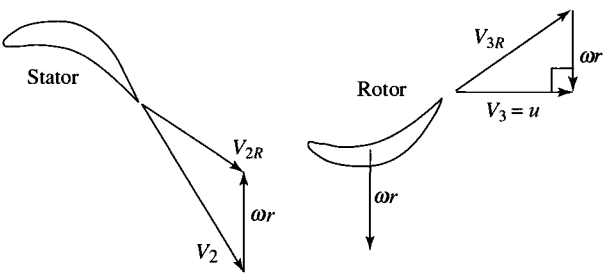

Fig. 9.61 Zero-exit-swirl turbine.

Thus high stage loadings give a low degree of reaction. In aircraft gas turbine engines, engine weight and performance must be balanced. Weight can be reduced by increasing stage loading (reduces the number of turbine stages), but this normally leads to a loss in stage efficiency (see Fig. 9.53).

9.5.1.5 Turbine airfoil nomenclature and design metal angles. The nomenclature for turbine airfoil cascades is presented in Fig. 9.62. The situation in unchoked turbines is similar to that in compressors except that the deviations are markedly smaller because of the thinner boundary layers. Hence

$$\delta_t = \frac{\gamma_i + \gamma_e}{8\sqrt{\sigma}} \tag{9.89}$$

is a good estimate of the turbine exit deviation. More importantly, however, when the turbine airfoil cascade exit Mach number is near unity, the deviation is usually negligible because the cascade passage is similar to a nozzle. In fact, the suction (or convex) surface of the airfoils often has a flat stretch before the trailing edge, which evokes the name *straight-backed.* Finally, the simple concept of deviation loses all meaning at large supersonic exit Mach numbers because expansion or compression waves emanating from the trailing edge can dramatically alter the final flow direction. This is a truly fascinating field of aerodynamics, but one that requires considerable study.

9.5.1.6 Stage temperature ratio τ_s. The stage temperature ratio ($\tau_s = T_{t1}/T_{t3}$) can be expressed as follows, by using the definition of the stage loading coefficient:

$$\tau_s = \frac{T_{t3}}{T_{t1}} = 1 - \psi \frac{(\omega r)^2}{g_c c_p T_{t1}} \tag{9.90}$$

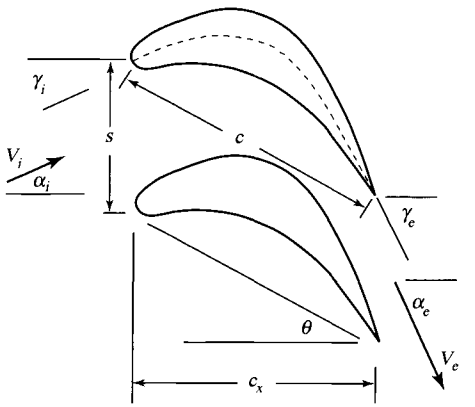

$\alpha_i - \gamma_i$ = incidence angle
$\alpha_i + \alpha_e$ = turning angle
$\gamma_e - \alpha_e = \delta_t$ = exit deviation
$\gamma_i + \gamma_e$ = blade chamber
$\sigma = c/s$ = solidity
θ = stagger angle
c_x = axial chord

Fig. 9.62 Turbine airfoil nomenclature.

Thus, for a given T_{t1} and ωr, the zero-reaction turbine stage will have the lower stage temperature ratio (greater work output per unit mass) than a 50% reaction turbine stage.

9.5.1.7 Stage pressure ratio π_s. Once the stage temperature ratio, flowfield, and airfoil characteristics are established, several avenues are open to predict the stage pressure ratio. The most simple and direct method is to employ the polytropic efficiency e_t. Recall that the polytropic efficiency is

$$e_t = \frac{dh_t}{dh_{t\,\text{ideal}}} = \frac{\gamma}{\gamma - 1}\frac{dT_t/T_t}{dP_t/P_t}$$

Integration with constant γ and e_t yields the following equation for the stage pressure ratio

$$\pi_s = \frac{P_{t3}}{P_{t1}} = \left(\frac{T_{t3}}{T_{t1}}\right)^{\gamma/[(\gamma-1)e_t]} = \tau_s^{\gamma/[(\gamma-1)e_t]} \tag{9.91}$$

where the stage temperature ratio can be obtained from the total temperatures or an equation like Eq. (9.90).

Another approach involves the use of experimental or empirical cascade loss correlations, such as those shown in Figs. 9.63 and 9.64, to the stator and rotor in order to determine the total pressure loss. The *total pressure loss coefficient* for turbine cascade data is defined as

$$\phi_t \equiv \frac{P_{ti} - P_{te}}{P_{te} - P_e} \tag{9.92}$$

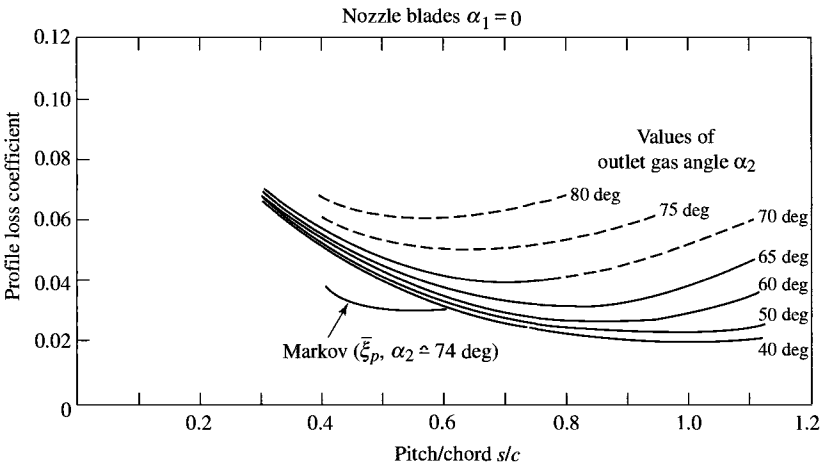

Fig. 9.63 Turbine stator cascade loss coefficient ($\alpha_1 = 0$) (Ref. 40).

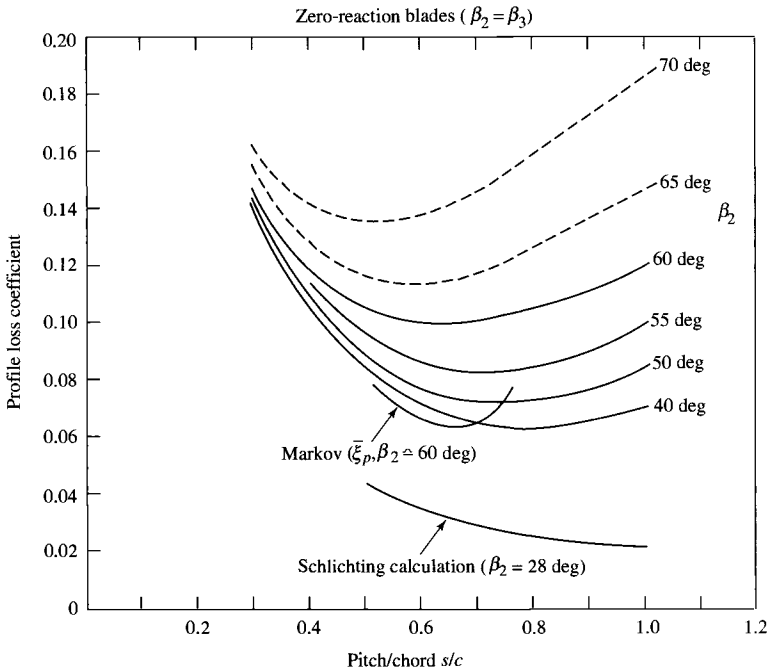

Fig. 9.64 Turbine rotor cascade loss coefficient ($\beta_2 = \beta_3$) (Ref. 40).

where subscripts i and e refer to the inlet and exit states, respectively. This equation can be rewritten for the cascade total pressure ratio as

$$\frac{P_{te}}{P_{ti}} = \frac{1}{1 + \phi_t(1 - P_e/P_{te})} \tag{9.93}$$

where P_e/P_{te} depends only on the usually known airfoil cascade exit Mach number M_e. Note that the total pressure loss coefficient for the rotor is based on the relative total states. The stage total pressure ratio can be written as

$$\frac{P_{t3}}{P_{t1}} = \left(\frac{P_{t2}}{P_{t1}}\right)_{\phi_{t\,\text{stator}},\, M_2} \frac{P_{t2R}}{P_{t2}} \left(\frac{P_{t3R}}{P_{t2R}}\right)_{\phi_{t\,\text{rotor}},\, M_{3R}} \frac{P_{t3}}{P_{t3R}} \tag{9.94}$$

where $\phi_{t\,\text{stator}}$ and $\phi_{t\,\text{rotor}}$ are the loss coefficients for the stator and rotor, respectively, and the subscripted total pressure ratios are obtained from Eq. (9.93) and cascade data. Additional losses are associated with tip leakage, annulus boundary layers, and secondary flows. Then, with all the stator, rotor, and stage properties computed, the stage efficiency can be computed from Eq. (9.76).

9.5.1.8 Blade spacing. The momentum equation relates the tangential force of the blades on the fluid to the change in tangential momentum of the fluid. This force is equal and opposite to that which results from the difference in pressure between the pressure side and the suction side of the airfoil. Figure 9.65 shows the variation in pressure on both the suction and pressure surfaces of a typical turbine airfoil from cascade tests. On the pressure surface, the pressure is nearly equal to the inlet total pressure for 60% of the length before the fluid is accelerated to the exit pressure condition. However, on the suction surface, the fluid is accelerated in the first 60% of the length to a low pressure and then is decelerated to the exit pressure condition. The deceleration on the suction surface is limited and controlled since it can lead to boundary-layer separation.

Enough airfoils must be present in each row that the sum of the tangential force on each is equal to the change in tangential momentum of the fluid. A simple expression for the relationship of the blade spacing to the fluid flow angles is developed in this section based on an incompressible fluid. This same expression correlates to the required blade spacing in a turbine stator or rotor row.

Referring to the cascade nomenclature in Fig. 9.62, we see that the tangential force per unit depth of blades spaced a distance s apart is

$$F_t = \frac{\rho u_i s(v_i + v_e)}{g_c} = \frac{\rho u_i^2 s}{g_c}\left(\tan \alpha_i + \frac{u_e}{u_i}\tan \alpha_e\right) \tag{9.95}$$

Zweifel[53] defines a tangential force coefficient that is the ratio of the force given by Eq. (9.95) to the maximum tangential force $F_{t\ \max}$ that can be achieved efficiently, and $F_{t\ \max}$ is obtained when

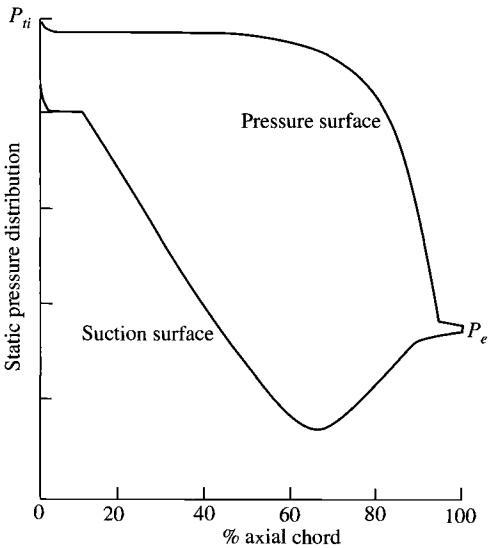

Fig. 9.65 Pressure distribution on a turbine cascade airfoil.

1) The pressure on the pressure surface is maintained at the inlet total pressure and drops to the exit static pressure at the trailing edge.

2) The pressure on the suction surface drops to the exit static pressure at the leading edge and remains at this value.

Thus the maximum tangential force is $F_{t\,\max} = (P_{ti} - P_e)c_x$, where c_x is the axial chord of the blade (see Fig. 9.62). For reversible flow of an incompressible fluid, $F_{t\,\max}$ can be written as

$$F_{t\,\max} = \frac{\rho V_e^2 c_x}{2g_c} = \frac{\rho u_e^2 c_x}{2g_c \cos^2 \alpha_e} \tag{9.96}$$

The *Zweifel tangential force coefficient* Z is defined as

$$Z \equiv \frac{F_t}{F_{t\,\max}} \tag{9.97}$$

From Eqs. (9.95) and (9.96), the equation of Z for a cascade airfoil becomes

$$Z = \frac{2s}{c_x}(\cos^2 \alpha_e)\left(\tan \alpha_t + \frac{u_e}{u_i}\tan \alpha_e\right)\left(\frac{u_i}{u_e}\right)^2$$

For the stator, we write

$$Z_s = \frac{2s}{c_x}(\cos^2 \alpha_2)\left(\tan \alpha_1 + \frac{u_2}{u_1}\tan \alpha_2\right)\left(\frac{u_1}{u_2}\right)^2 \tag{9.98a}$$

Likewise for the rotor, we write

$$Z_r = \frac{2s}{c_x}(\cos^2 \beta_3)\left(\tan \beta_2 + \frac{u_3}{u_2}\tan \beta_3\right)\left(\frac{u_2}{u_3}\right)^2 \tag{9.98b}$$

Because suction surface pressures can be less than the exit static pressure along the blade (see Fig. 9.65), *Z values near unity are attainable*. By using Eq. (9.98b), lines of constant $Z_r c_x/s$ are plotted in Fig. 9.66 vs the relative rotor angles β_2 and β_3. High β_2 and zero reaction (high stage loading ψ, see Fig. 9.57) give high values of $Z_r c_x/s$ (see Fig. 9.66) and require high values of solidity $[\sigma = c/s = (c_x/s)/\cos\theta]$. High solidity at high β_2 and zero reaction can lead to high total pressure losses (see Fig. 9.64). For no exit swirl ($\alpha_3 = 0$), the 50% reaction stage ($\psi = 1$) corresponds to $\beta_2 = 0$, the required solidity is low (Fig. 9.66), and the total pressure losses are low (Fig. 9.64). Thus the turbine design for aircraft engines will be a balance between the number of stages (stage loadings) and the turbine efficiency (total pressure losses).

9.5.1.9 Radial variations. Because the mass flow rate per unit area [that is, $\dot{m}/A = P_t/(\mathrm{MFP}\sqrt{T_t})$] is higher in turbines than in compressors, turbine

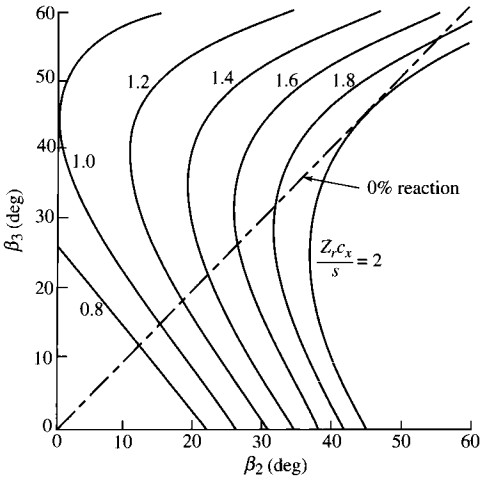

Fig. 9.66 Zc_x/s **of rotor vs** β_2 **and** β_3**.**

airfoils are correspondingly shorter. The result is little radial variation of aerodynamic properties from hub to tip except in the last few stages of the low-pressure turbine. Figure 9.67 is the rotor blade of a low-pressure turbine that shows radial variation from hub to tip. Typically, the degree of reaction varies from near zero at the hub to about 40% at the tip.

If the aerodynamic design of these stages began as free vortex, the swirl distribution with radius is the same as for compressors, given by [Eq. (9.45)]

$$v = v_m \frac{r_m}{r}$$

For constant axial velocity ($u_2 = u_3$), the degree of reaction is

$$^{\circ}R_t = \frac{T_2 - T_3}{T_{t1} - T_{t3}} = \frac{T_2 - T_3}{T_{t2} - T_{t3}} = 1 - \frac{V_2^2 - V_3^2}{2g_c c_p (T_{t1} - T_{t3})} = 1 - \frac{v_2^2 - v_3^2}{2\omega r (v_2 + v_3)}$$

$$= 1 - \frac{v_2 - v_3}{2\omega r}$$

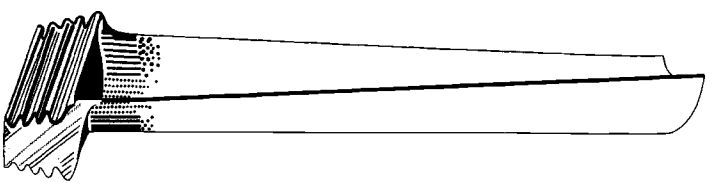

Fig. 9.67 Low-pressure turbine rotor blade. (Courtesy of Pratt & Whitney.)

Substituting Eq. (9.44), we write the degree of reaction at any radius in terms of the degree of reaction at the mean radius as

$$^{\circ}R_t = 1 - \frac{v_{m2} - v_{m3}}{2\omega r}\frac{r_m}{r} = 1 - \frac{v_{m2} - v_{m3}}{2\omega r_m}\left(\frac{r_m}{r}\right)^2$$

$$^{\circ}R_t = 1 - (1 - {}^{\circ}R_{tm})\left(\frac{r_m}{r}\right)^2 \tag{9.99}$$

This is the same result as for compressors [Eqs. (9.51) and (9.52)]. Consequently, the most difficult airfoil contours to design would be at the hub of the rotating airfoils and at the tips of the stationary airfoils where the degree of reaction is low. It is, therefore, possible to find portions of some airfoils near the rear of highly loaded (i.e., high work per stage), low-pressure turbines where the static pressure actually rises across the cascade and boundary-layer separation is hard to avoid. In these cases, turbine designers have used their computers to develop nonfree or controlled vortex machines without these troublesome regions in order to maintain high efficiency at high loading.

Because of radial variations, the degree of reaction is lowest at the hub. Hence the Zweifel tangential force coefficient of the rotor Z_r times c_x/s will be maximum at the hub. Although the blade spacing varies directly with radius, $Z_r c_x/s$ is greatest at the hub and decreases faster than $1/r$ with increasing radius. Thus the value of $Z_r c_x/s$ at the rotor hub determines the spacing and number of rotor blades. For the stator, $Z_s c_x/s$ will be greatest at the tip, and its value determines the spacing and number of stator blades.

9.5.1.10 Velocity ratio. The *velocity ratio* (VR) is defined as the ratio of the rotor speed ($U = \omega r$) to the velocity equivalent of the change in stage total enthalpy, or

$$\text{VR} \equiv \frac{U}{\sqrt{2g_c\,\Delta h_t}} = \frac{\omega r}{\sqrt{2g_c\,\Delta h_t}} \tag{9.100}$$

The velocity ratio is used by some turbine designers rather than the stage loading coefficient ψ, and one can show that

$$\text{VR} = \frac{1}{\sqrt{2\psi}} \tag{9.101}$$

The VR at the mean radius ranges between 0.5 and 0.6 for modern aircraft gas turbine engines. This range corresponds to stage loading coefficients ψ between 1.4 and 2.

9.5.2 Axial-Flow Turbine Stage

Consider the flow through a single-stage turbine as shown in Fig. 9.68. For generality, we will allow the axial velocity to change from station 2 to 3. The

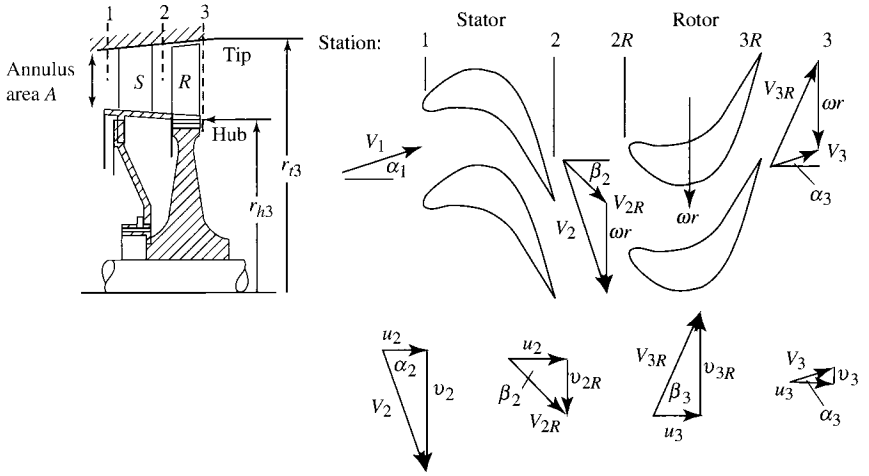

Fig. 9.68 Axial-flow turbine stage (after Ref. 29).

flows through the nozzle (stator) and rotor are assumed to be adiabatic. For solution, we assume that the following data are known: M_2, T_{t1}, T_{t3}, ωr, α_3, c_p, γ, and u_3/u_2. We will develop and write the equations for a general axial-flow turbine based on these known data.

To solve for the flow angle at station $2(\alpha_2)$, we first write the Euler turbine equation

$$c_p(T_{t2} - T_{t3}) = \frac{\omega r}{g_c}(v_2 + v_3) \tag{9.102}$$

Solving for v_2, we have

$$v_2 = \frac{g_c c_p \, \Delta T_t}{\omega r} - v_3$$

Then

$$\sin \alpha_2 = \frac{v_2}{V_2} = \frac{g_c c_p \, \Delta T_t}{\omega r V_2} - \frac{v_3}{V_2} \tag{i}$$

However,

$$\frac{v_3}{V_2} = \frac{u_3}{V_2}\tan \alpha_3 = \frac{u_3}{u_2}\frac{u_2}{V_2}\tan \alpha_3 = \frac{u_3}{u_2}\cos \alpha_2 \tan \alpha_3$$

Thus, Eq. (i) becomes

$$\sin \alpha_2 = \frac{v_2}{V_2} = \frac{g_c c_p \, \Delta T_t}{\omega r V_2} - \frac{u_3}{u_2}\cos \alpha_2 \tan \alpha_3 \tag{ii}$$

By using the stage loading parameter ψ, Eq. (ii) can be written as

$$\sin \alpha_2 = \psi \frac{\omega r}{V_2} - \frac{u_3}{u_2} \cos \alpha_2 \tan \alpha_3 \tag{9.103}$$

The velocity at station 2 can be found from

$$V_2 = M_2 a_2 = \sqrt{\frac{2 g_c c_p T_{t2}}{1 + 2/[(\gamma - 1) M_2^2]}} \tag{9.104}$$

If $\alpha_3 = 0$, then Eq. (9.103) simplifies to

$$\sin \alpha_2 = \psi \frac{\omega r}{V_2} \tag{9.105}$$

If α_3 is not zero, Eq. (9.103) can be solved by substituting $\sqrt{1 - \sin^2 \alpha_2}$ for $\cos \alpha_2$, squaring both sides of the equation, and solving the resulting quadratic equation for $\sin \alpha_2$. The solution is

$$\sin \alpha_2 = \frac{\left(\psi \dfrac{\omega r}{V_2}\right) - \left(\dfrac{u_3}{u_2} \tan \alpha_3\right) \sqrt{1 + \left(\dfrac{u_3}{u_2} \tan \alpha_3\right)^2 - \left(\psi \dfrac{\omega r}{V_2}\right)^2}}{1 + \left(\dfrac{u_3}{u_2} \tan \alpha_3\right)^2} \tag{9.106}$$

The velocity at station 3 can be written in terms of that at station 2 and the two flow angles α_2 and α_3:

$$V_3 = \frac{u_3}{u_2} \frac{\cos \alpha_2}{\cos \alpha_3} V_2 \tag{9.107}$$

The degree of reaction can be written in terms of the given data as follows:

$$\begin{aligned} {}^{\circ}R_t &= \frac{T_2 - T_3}{T_{t2} - T_{t3}} = \frac{T_{t2} - T_{t3} - (T_{t2} - T_2) + T_{t3} - T_3}{T_{t2} - T_{t3}} \\ &= 1 - \frac{V_2^2 - V_3^2}{2 g_c c_p (T_{t2} - T_{t3})} = 1 - \frac{V_2^2 - V_3^2}{2 \psi (\omega r)^2} \\ &= 1 - \frac{1}{2 \psi (\omega r)^2} \left(\frac{u_2^2}{\cos^2 \alpha_2} - \frac{u_3^2}{\cos^2 \alpha_3} \right) \\ {}^{\circ}R_t &= 1 - \frac{1}{2\psi} \left(\frac{V_2}{\omega r} \right)^2 \left[1 - \left(\frac{u_3}{u_2} \frac{\cos \alpha_2}{\cos \alpha_3} \right)^2 \right] \end{aligned} \tag{9.108}$$

The Mach number at station 3 can be found from

$$M_3 = M_2 \frac{V_3}{V_2} \sqrt{\frac{T_2}{T_3}} \tag{9.109}$$

where

$$\frac{T_3}{T_2} = 1 - {}^{\circ}R_t \frac{\Delta T_t}{T_{t2}} \left(1 + \frac{\gamma - 1}{2} M_2^2\right) \tag{9.110}$$

An equation for the Mach number at station $2R$ can be developed as follows:

$$M_{2R} = M_2 \frac{V_{2R}}{V_2}$$

where

$$V_{2R} = \sqrt{u_2^2 + (v_2 - \omega r)^2} = V_2 \sqrt{\cos^2 \alpha_2 + \left(\sin \alpha_2 - \frac{\omega r}{V_2}\right)^2}$$

Thus

$$M_{2R} = M_2 \sqrt{\cos^2 \alpha_2 + \left(\sin \alpha_2 - \frac{\omega r}{V_2}\right)^2} \tag{9.111}$$

Likewise, an equation for the Mach number at station $3R$ is developed as follows:

$$M_{3R} = M_3 \frac{V_{3R}}{V_3}$$

where

$$V_{3R} = \sqrt{u_3^2 + (v_3 + \omega r)^2} = V_3 \sqrt{\cos^2 \alpha_3 + \left(\sin \alpha_3 + \frac{\omega r}{V_3}\right)^2}$$

Thus

$$M_{3R} = M_3 \sqrt{\cos^2 \alpha_3 + \left(\sin \alpha_3 + \frac{\omega r}{V_3}\right)^2} \tag{9.112}$$

An equation for the rotor relative total temperature ($T_{t2R} = T_{t3R}$) can be developed by noting that

$$T_3 = T_{t3} - \frac{V_3^2}{2g_c c_p} = T_{t3R} - \frac{V_{3R}^2}{2g_c c_p}$$

Then

$$T_{t3R} = T_{t3} + \frac{V_{3R}^2 - V_3^2}{2g_c c_p}$$

or

$$T_{t3R} = T_{t3} + \frac{V_3^2}{2g_c c_p}\left[\cos^2\alpha_3 + \left(\sin\alpha_3 + \frac{\omega r}{V_3}\right)^2 - 1\right] \tag{9.113}$$

9.5.3 Summary of Equations—Axial-Flow Turbine Stage

INPUTS:

T_{t1}, T_{t3}, ωr, P_{t1}, M_1, M_2, α_1, α_3, c_p, γ, u_3/u_2, and e_t or $\phi_{t\,\text{stator}}$ and $\phi_{t\,\text{rotor}}$

OUTPUTS:

$\alpha_2, V_2, u_2, v_2, T_2, P_{t2}, P_2, M_{2R}, V_3, u_3, v_3, T_3, P_{t3}, P_3, M_3, M_{3R}, \psi$, VR, ${}^\circ R_t, Z_s c_x/s$, $Z_r c_x/s$, π_s, and η_s

EQUATIONS:

$$T_1 = \frac{T_{t1}}{1 + [(\gamma - 1)/2]M_1^2}$$

$$V_1 = \sqrt{\frac{2g_c c_p T_{t1}}{1 + 2/[(\gamma - 1)M_1^2]}}$$

$$u_1 = V_1 \cos\alpha_1$$

$$T_{t2} = T_{t1}$$

$$T_2 = \frac{T_{t2}}{1 + [(\gamma - 1)/2]M_2^2}$$

$$V_2 = \sqrt{\frac{2g_c c_p T_{t2}}{1 + 2/[(\gamma - 1)M_2^2]}}$$

$$\psi = \frac{g_c c_p (T_{t1} - T_{t3})}{(\omega r)^2}$$

$$\text{VR} = \frac{1}{\sqrt{2\psi}}$$

$$\alpha_2 = \sin^{-1}\frac{\psi\dfrac{\omega r}{V_2} - \dfrac{u_3}{u_2}\tan\alpha_3\sqrt{1 + \left(\dfrac{u_3}{u_2}\tan\alpha_3\right)^2 - \left(\psi\dfrac{\omega r}{V_2}\right)^2}}{1 + \left(\dfrac{u_3}{u_2}\tan\alpha_3\right)^2}$$

$$u_2 = V_2 \cos\alpha_2$$

$$v_2 = V_2 \sin\alpha_2$$

$$V_3 = \frac{u_3}{u_2}\frac{\cos\alpha_2}{\cos\alpha_3}V_2$$

$$u_3 = V_3 \cos \alpha_3$$

$$v_3 = V_3 \sin \alpha_3$$

$$^{\circ}R_t = 1 - \frac{1}{2\psi}\left(\frac{V_2}{\omega r}\right)^2\left[1 - \left(\frac{u_3}{u_2}\frac{\cos \alpha_2}{\cos \alpha_3}\right)^2\right]$$

$$T_3 = T_2 - {}^{\circ}R_t(T_{t1} - T_{t3})$$

$$M_3 = M_2 \frac{V_3}{V_2}\sqrt{\frac{T_2}{T_3}}$$

$$M_{2R} = M_2\sqrt{\cos^2 \alpha_2 + \left(\sin \alpha_2 - \frac{\omega r}{V_2}\right)^2}$$

$$M_{3R} = M_3\sqrt{\cos^2 \alpha_3 + \left(\sin \alpha_3 + \frac{\omega r}{V_3}\right)^2}$$

$$T_{t3R} = T_{t3} + \frac{V_3^2}{2g_c c_p}\left[\cos^2 \alpha_3 + \left(\sin \alpha_3 + \frac{\omega r}{V_3}\right)^2 - 1\right]$$

$$T_{t2R} = T_{t3R}$$

$$P_2 = P_{t1}\left(\frac{T_1}{T_{t1}}\right)^{\gamma/(\gamma-1)}$$

$$\tau_s = \frac{T_{t3}}{T_{t1}}$$

$$\frac{Z_s c_x}{s} = (2\cos^2 \alpha_2)\left(\tan \alpha_1 + \frac{u_2}{u_1}\tan \alpha_2\right)\left(\frac{u_1}{u_2}\right)^2$$

$$\beta_2 = \tan^{-1}\frac{v_2 - \omega r}{u_2}$$

$$\beta_3 = \tan^{-1}\frac{v_3 + \omega r}{u_3}$$

$$\frac{Z_r c_x}{s} = (2\cos^2 \beta_3)\left(\tan \beta_2 + \frac{u_3}{u_2}\tan \beta_3\right)\left(\frac{u_2}{u_3}\right)^2$$

I. $\phi_{r\,\text{stator}}$ and $\phi_{t\,\text{rotor}}$ given:

$$P_{t2} = \frac{P_{t1}}{1 + \phi_{t\,\text{stator}}[1 - (T_2/T_{t2})^{\gamma/(\gamma-1)}]}$$

$$P_2 = P_{t2}\left(\frac{T_2}{T_{t2}}\right)^{\gamma/(\gamma-1)}$$

$$P_{t2R} = P_2\left(\frac{T_{t2R}}{T_2}\right)^{\gamma/(\gamma-1)}$$

$$P_{t3R} = \frac{P_{t2R}}{1 + \phi_{t\,\text{rotor}}[1 - (T_3/T_{t3R})^{\gamma/(\gamma-1)}]}$$

$$P_3 = P_{t3R}\left(\frac{T_3}{T_{t3R}}\right)^{\gamma/(\gamma-1)}$$

$$P_{t3} = P_3\left(\frac{T_{t3}}{T_3}\right)^{\gamma/(\gamma-1)}$$

$$\pi_s = \frac{P_{t3}}{P_{t1}}$$

$$\eta_t = \frac{1 - \tau_s}{1 - \pi_s^{(\gamma-1)/\gamma}}$$

II. e_t given:

$$P_{t3} = P_{t1}\left(\frac{T_{t3}}{T_{t1}}\right)^{\gamma/[(\gamma-1)e_t]}$$

$$\pi_s = \frac{P_{t3}}{P_{t1}}$$

$$\eta_s = \frac{1 - \tau_s}{1 - \pi_s^{(\gamma-1)/\gamma}}$$

$$P_3 = P_{t3}\left(\frac{T_3}{T_{t3}}\right)^{\gamma/(\gamma-1)}$$

$$P_{t3R} = P_3\left(\frac{T_{t3R}}{T_3}\right)^{\gamma/(\gamma-1)}$$

With polytropic efficiency specified, P_2, P_{t2}, and P_{t2R} cannot be calculated without an additional relationship for either P_2 or P_{t2}. For estimation of P_{t2}, the program TURBN has as the user input a value of $\phi_{t\,\text{stator}}$.

Example 9.10

Consider mean-radius stage calculation—flow with losses.

Given:

$$T_{t1} = 1850\ \text{K}, \quad P_{t1} = 1700\ \text{kPa}, \quad M_1 = 0.4, \quad \alpha_1 = 0\ \text{deg}$$

$$T_{t3} = 1560\ \text{K}, \quad M_2 = 1.1, \quad \omega r = 450\ \text{m/s}, \quad \alpha_3 = 10\ \text{deg}$$

$$u_3/u_2 = 0.9, \quad \phi_{t\,\text{stator}} = 0.06, \quad \phi_{t\,\text{rotor}} = 0.15$$

$$\gamma = 1.3, \quad R = 0.2873\ \text{kJ/(kg}\cdot\text{K)}\ [c_p = 1.245\ \text{kJ/(kg}\cdot\text{K)}]$$

Solution:

$$T_1 = \frac{T_{t1}}{1 + [(\gamma - 1)/2]M_1^2} = \frac{1850\,\text{K}}{1 + 0.15 \times 0.4^2} = 1806.6\,\text{K}$$

$$V_1 = \sqrt{\frac{2g_c c_p T_{t1}}{1 + 2/[(\gamma - 1)M_1^2]}} = \sqrt{\frac{2 \times 1 \times 1245 \times 1850}{1 + 2/(0.3 \times 0.4^2)}} = 328.6\,\text{m/s}$$

$$u_1 = V_1 \cos \alpha_1 = 328.6\,\text{m/s}$$

$$v_1 = V_1 \sin \alpha_1 = 0$$

$$T_{t2} = T_{t1} = 1850\,\text{K}$$

$$T_2 = \frac{T_{t2}}{1 + [(\gamma - 1)/2]M_2^2} = \frac{1850\,\text{K}}{1 + 0.15 \times 1.1^2} = 1565.8\,\text{K}$$

$$V_2 = \sqrt{\frac{2g_c c_p T_{t2}}{1 + 2/[(\gamma - 1)M_2^2]}}$$

$$= \sqrt{\frac{2 \times 1 \times 1245 \times 18}{1 + 2/(0.3 \times 1.1^2)}} = 841.2\,\text{m/s}$$

$$\psi = \frac{g_c c_p (T_{t1} - T_{t3})}{(\omega r)^2} = \frac{1245(1850 - 1560)}{450^2} = 1.78296$$

$$\text{VR} = \frac{1}{\sqrt{2\psi}} = \frac{1}{\sqrt{2 \times 1.78296}} = 0.5296$$

$$\alpha_2 = \sin^{-1} \frac{\left(\psi \dfrac{\omega r}{V_2}\right) - \left(\dfrac{u_3}{u_2} \tan \alpha_3\right) \sqrt{1 + \left(\dfrac{u_3}{u_2} \tan \alpha_3\right)^2 - \left(\psi \dfrac{\omega r}{V_2}\right)^2}}{1 + \left(\dfrac{u_3}{u_2} \tan \alpha_3\right)^2}$$

$$\psi \frac{\omega r}{V_2} = 1.78296 \left(\frac{450}{841.2}\right) = 0.95379$$

$$\frac{u_3}{u_2} \tan \alpha_3 = 0.9 \tan 10\,\text{deg} = 0.15869$$

$$\alpha_2 = \sin^{-1} \frac{0.95379 - 0.15869\sqrt{1 + 0.15869^2 - 0.95379^2}}{1.015869^2}$$

$$= \sin^{-1} 0.87776 = 61.37\,\text{deg}$$

$$u_2 = V_2 \cos \alpha_2 = 841.2 \cos 61.37\,\text{deg} = 403.1\,\text{m/s}$$

$$v_2 = V_2 \sin \alpha_2 = 841.2 \sin 61.37 \text{ deg} = 738.3 \text{ m/s}$$

$$\Phi = \frac{u_2}{\omega r} = \frac{403.1}{450} = 0.8958$$

$$V_3 = \frac{u_3}{u_2} \frac{\cos \alpha_2}{\cos \alpha_3} V_2 = 0.9 \left(\frac{\cos 61.37 \text{ deg}}{\cos 10 \text{ deg}} \right) (841.2) = 368.4 \text{ m/s}$$

$$u_3 = V_3 \cos \alpha_3 = 368.4 \cos 10 \text{ deg} = 362.8 \text{ m/s}$$

$$v_3 = V_3 \sin \alpha_3 = 368.4 \sin 10 \text{ deg} = 64.0 \text{ m/s}$$

$$^{\circ}R_t = 1 - \frac{1}{2\psi} \left(\frac{V_2}{\omega r} \right)^2 \left[1 - \left(\frac{u_3 \cos \alpha_2}{u_2 \cos \alpha_3} \right)^2 \right]$$

$$= 1 - \frac{1}{2 \times 1.78296} \left(\frac{841.2}{450} \right)^2 \left[1 - \left(0.9 \frac{\cos 61.37 \text{ deg}}{\cos 10 \text{ deg}} \right)^2 \right] = 0.2080$$

$$T_3 = T_2 - {}^{\circ}R_t (T_{t1} - T_{t3}) = 1565.8 - 0.2080(1850 - 1560) = 1505.5 \text{ K}$$

$$M_3 = M_2 \frac{V_3}{V_2} \sqrt{\frac{T_2}{T_3}} = 1.1 \left(\frac{368.4}{841.2} \right) \sqrt{\frac{1565.8}{1505.5}} = 0.4913$$

$$M_{2R} = M_2 \sqrt{\cos^2 \alpha_2 + \left(\sin \alpha_2 - \frac{\omega r}{V_2} \right)^2}$$

$$= 1.1 \sqrt{\cos^2 61.37 \text{ deg} + \left(\sin 61.37 \text{ deg} - \frac{450}{841.2} \right)^2} = 0.6481$$

$$M_{3R} = M_3 \sqrt{\cos^2 \alpha_3 + \left(\sin \alpha_3 + \frac{\omega r}{V_3} \right)^2}$$

$$= 0.4913 \sqrt{\cos^2 10 \text{ deg} + \left(\sin 10 \text{ deg} + \frac{450}{368.4} \right)^2} = 0.8390$$

$$T_{t3R} = T_{t3} + \frac{V_3^2}{2 g_c c_p} \left[\cos^2 \alpha_3 + \left(\sin \alpha_3 + \frac{\omega r}{V_3} \right)^2 - 1 \right]$$

$$= 1560 + \frac{368.4^2}{2 \times 1 \times 1245} \left[\cos^2 10 \text{ deg} + \left(\sin 10 \text{ deg} + \frac{450}{368.4} \right)^2 - 1 \right]$$

$$= 1664.4 \text{ K}$$

$$T_{t2R} = T_{t3R} = 1664.4 \text{ K}$$

$$\tau_s = \frac{T_{t3}}{T_{t1}} = \frac{1560}{1850} = 0.8432$$

$$\frac{Z_s c_x}{s} = (2\cos^2\alpha_2)\left(\tan\alpha_1 + \frac{u_2}{u_1}\tan\alpha_2\right)\left(\frac{u_1}{u_2}\right)^2$$

$$= (2\cos^2 61.371\,\text{deg})\left(\tan 0\,\text{deg} + \frac{403.1}{328.6}\tan 61.37\,\text{deg}\right)\left(\frac{328.6}{403.1}\right)^2$$

$$= 0.6857$$

$$\beta_2 = \tan^{-1}\frac{v_2 - \omega r}{u_2} = \tan^{-1}\frac{738.3 - 450}{403.1} = 35.57\,\text{deg}$$

$$\beta_3 = \tan^{-1}\frac{v_3 + \omega r}{u_3} = \tan^{-1}\frac{64.0 + 450}{362.8} = 54.78\,\text{deg}$$

$$\frac{Z_r c_x}{s} = (2\cos^2\beta_3)\left(\tan\beta_2 + \frac{u_3}{u_2}\tan\beta_3\right)\left(\frac{u_2}{u_3}\right)^2$$

$$= (2\cos^2 54.78\,\text{deg})(\tan 35.573\,\text{deg} + 0.9\tan 54.78\,\text{deg})\left(\frac{1}{0.9}\right)^2$$

$$= 1.6330$$

$$P_1 = P_{t1}\left(\frac{T_1}{T_{t1}}\right)^{\gamma/(\gamma-1)} = 1700\left(\frac{1806.6}{1850}\right)^{1.3/0.3} = 1533.8\,\text{kPa}$$

$$P_{t2} = \frac{P_{t1}}{1 + \phi_{t\,\text{stator}}[1 - (T_2/T_{t2})^{\gamma/(\gamma-1)}]}$$

$$= \frac{1700}{1 + 0.06[1 - (1565.8/1850)^{1.3/0.3}]} = 1649.1\,\text{kPa}$$

$$P_2 = P_{t2}\left(\frac{T_2}{T_{t2}}\right)^{\gamma/(\gamma-1)} = 1649.1\left(\frac{1565.8}{1850}\right)^{1.3/0.3} = 800.5\,\text{kPa}$$

$$P_{t2R} = P_2\left(\frac{T_{t2R}}{T_2}\right)^{\gamma/(\gamma-1)} = 800.5\left(\frac{1664.4}{1565.8}\right)^{1.3/0.3} = 1043.0\,\text{kPa}$$

$$P_{t3R} = \frac{P_{t2R}}{1 + \phi_{t\,\text{rotor}}[1 - (T_3/T_{t3R})^{\gamma/(\gamma-1)}]}$$

$$= \frac{1043.0}{1 + 0.15[1 - (1505.5/1664.4)^{1.3/0.3}]} = 990.6\,\text{kPa}$$

$$P_3 = P_{t3R}\left(\frac{T_3}{T_{t3R}}\right)^{\gamma/(\gamma-1)} = 990.6\left(\frac{1505.5}{1664.4}\right)^{1.3/0.3} = 641.3\,\text{kPa}$$

$$P_{t3} = P_3\left(\frac{T_{t3}}{T_3}\right)^{\gamma/(\gamma-1)} = 641.3\left(\frac{1560}{1505.5}\right)^{1.3/0.3} = 748.1\,\text{kPa}$$

$$\pi_s = \frac{P_{t3}}{P_{t1}} = \frac{748.1}{1700} = 0.441$$

$$\eta_s = \frac{1 - \tau_s}{1 - \pi_s^{(\gamma-1)/\gamma}} = \frac{1 - 0.8432}{1 - 0.4401^{0.3/1.3}} = 90.87\%$$

9.5.4 Flow Path Dimensions

9.5.4.1 Annulus area. The annulus area (see Fig. 9.26) at any station of a turbine stage is based on the flow properties (T_t, P_t, Mach number, and flow angle) at the mean radius and the total mass flow rate. Equation (9.8) is the easiest equation to use to calculate the flow area at any station i:

$$A_i = \frac{\dot{m}\sqrt{T_{ti}}}{P_{ti}(\cos \alpha_i)\text{MFP}(M_i)}$$

By using the relationships of Fig. 9.26, the radii at any station i can be determined, given the flow annulus area [Eq. (9.8)] and either the mean radius r_m or the hub/tip ratio r_h/r_t.

9.5.4.2 Axial dimensions and number of blades. Figure 9.69 shows the cross section of a typical turbine stage that can be used to estimate its axial length. The chord/height ratio c/h of turbine blades varies from about 0.3 to 1.0. Assuming constant chord length and circular arc chamber line, the program TURBN calculates the axial blade widths W_s and W_r of a stage, the blade spacings $W_s/4$ and $W_r/4$, and the number of blades based on user inputs of the tangential force coefficient Z and chord/height ratio c/h for both the stator and rotor blades. A minimum width of $\frac{1}{4}$ in. (0.6 cm) and spacing of $\frac{1}{8}$ in. (0.3 cm) are used in the plot of a turbine cross section and calculation of axial length.

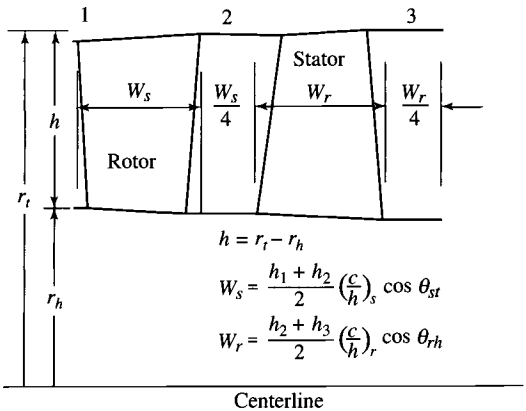

Fig. 9.69 Typical axial dimensions of a turbine stage.

The stagger angle θ of a blade depends on the shape of the chamber line and blade angles γ_i and γ_e (see Fig. 9.62). For a circular arc chamber line, the stagger angle θ is simply given by $\theta = (\gamma_e - \gamma_i)/2$. For constant-chord blades, the axial chord (and axial blade width) is greatest where the stagger angle is closest to zero. This normally occurs at the tip of the stator and hub of the rotor blades. For estimation purposes, a turbine blade's incidence angle is normally small and can be considered to be zero. Thus $\gamma_i = \alpha_i$. The blade's exit angle γ_e can be obtained using Eq. (9.89) for the exit deviation. However, Eq. (9.89) requires that the solidity ($\sigma = c/s$) be known. For known flow conditions (α_1, α_2, u_2/u_1, α_2, α_3, and u_3/u_2) and given tangential force coefficients (Z_s and Z_r), Eqs. (9.98a) and (9.98b) will give the required axial chord/spacing ratio c_x/s for the stator and rotor, respectively. An initial guess for the blade's solidity σ is needed to obtain the stagger angle θ from c_x/s.

After the solidities are determined at the hub, mean, and tip that give the desired tangential force coefficient Z, the number of required blades follows directly from the chord/height ratio c/h, the circumference, and the blade spacing at each radius. The following example shows the calculations needed to find the axial blade width and number of blades.

Example 9.11

Here we consider the turbine stator of Example 9.10 with a mass flow rate of 60 kg/s, a mean radius of 0.3 m, a tangential force coefficient Z_s of 0.9, and a chord/height ratio c/h of 1.0. The flow annulus areas and radii at stations 1 and 2 are as follows.

Station 1:

$$\text{MFP}(M_1) = 0.024569$$

$$A_1 = \frac{\dot{m}\sqrt{T_{t1}}}{P_{t1}\text{MFP}(M_1)(\cos\alpha_1)} = \frac{60\sqrt{1850}}{1{,}700{,}00 \times 0.024569 \times 1}$$

$$= 0.0617788\ \text{m}^2$$

$$h_1 = \frac{A_1}{2\pi r_m} = \frac{0.061788}{0.6\pi} = 0.03278\ \text{m}$$

$$r_{t1} = 0.3164\ \text{m} \qquad r_{h1} = 0.2836\ \text{m}$$

$$v_{1h} = v_{1m} = v_{1t} = 0$$

Station 2:

$$\text{MFP}(M_2) = 0.039042$$

$$A_2 = \frac{\dot{m}\sqrt{T_{t2}}}{P_{t2}\text{MFP}(M_2)(\cos\alpha_2)}$$

$$= \frac{60\sqrt{1850}}{1{,}649{,}100 \times 0.039042 \times \cos 61.37\ \text{deg}} = 0.083654\ \text{m}^2$$

$$h_2 = \frac{A_2}{2\pi r_m} = \frac{0.083654}{0.6\pi} = 0.04438\,\text{m}$$

$$r_{t2} = 0.3222\,\text{m} \qquad r_{h2} = 0.2778\,\text{m}$$

$$v_{2h} = v_{2m}\frac{r_m}{r_{2h}} = 738.3\left(\frac{0.3}{0.2778}\right) = 797.3\,\text{m/s}$$

$$\alpha_{2h} = \tan^{-1}\frac{v_{2h}}{u_2} = \tan^{-1}\frac{797.3}{403.1} = 63.18\,\text{deg}$$

$$v_{2t} = v_{2m}\frac{r_m}{r_{2t}} = 738.3\left(\frac{0.3}{0.3222}\right) = 687.4\,\text{m/s}$$

$$\alpha_{2t} = \tan^{-1}\frac{v_{2t}}{u_2} = \tan^{-1}\frac{687.4}{403.1} = 59.61\,\text{deg}$$

The chord of the stator is

$$c = \frac{c}{h}\frac{h_1 + h_2}{2} = 1.0\frac{0.03278 + 0.04438}{2} = 0.03858\,\text{m}$$

For the specified tangential force coefficient Z_s, we calculate the stagger angle, solidity, and spacing of the stator at the mean line, hub, and tip.

Mean line:

$$Z_s\left(\frac{c_x}{s}\right)_m = (2\cos^2\alpha_{2m})\left(\tan\alpha_{1m} + \frac{u_2}{u_1}\tan\alpha_{2m}\right)\left(\frac{u_1}{u_2}\right)^2$$

$$= (2\cos^2 61.37\,\text{deg})\left(\tan 0\,\text{deg} + \frac{403.1}{328.6}\tan 61.37\,\text{deg}\right)$$

$$\times\left(\frac{328.6}{403.1}\right)^2 = 0.6857$$

$$\left(\frac{c_x}{s}\right)_m = \frac{0.6857}{0.9} = 0.7619$$

$$\gamma_{1m} = \alpha_{1m} = 0$$

Initially, we assume a solidity σ of 1.0. Then,

$$\gamma_{2m} = \frac{\gamma_{1m} + 8\sqrt{\sigma_m}\alpha_{2m}}{8\sqrt{\sigma_m} - 1} = \frac{0 + 8\sqrt{1}61.37}{8\sqrt{1} - 1} = 70.14\,\text{deg}$$

$$\theta_m = \frac{\gamma_{2m} - \gamma_{1m}}{2} = \frac{70.14}{2} = 35.07\,\text{deg}$$

$$\sigma_m = \frac{(c_x/s)_m}{\cos\theta_m} = \frac{0.7619}{\cos 35.07\,\text{deg}} = 0.9309$$

After several iterations, the results are $\gamma_{2m} = 70.49$ deg, $\theta_m = 35.25$ deg, and $\sigma_m = 0.9329$. The blade spacing s is 0.04135 m, and the axial chord is 0.03150 m.

Hub:

$$Z_s\left(\frac{c_x}{s}\right)_h = (2\cos^2\alpha_{2h})\left(\tan\alpha_{1h} + \frac{u_2}{u_1}\tan\alpha_{2h}\right)\left(\frac{u_1}{u_2}\right)^2$$

$$= (2\cos^2 63.18\,\text{deg})\left(\tan 0\,\text{deg} + \frac{403.1}{328.6}\tan 63.18\,\text{deg}\right)$$

$$\times \left(\frac{328.6}{403.1}\right)^2 = 0.6565$$

$$\left(\frac{c_x}{s}\right)_h = \frac{0.6565}{0.9} = 0.7294$$

$$\gamma_{1h} = \alpha_{1h} = 0$$

Initially, we assume a solidity σ of 1.0. Then,

$$\gamma_{2h} = \frac{\gamma_{1h} + 8\sqrt{\sigma_h}\alpha_{2h}}{8\sqrt{\sigma_h} - 1} = \frac{0 + 8\sqrt{1}63.18}{8\sqrt{1} - 1} = 72.21\,\text{deg}$$

$$\theta_h = \frac{\gamma_{2h} - \gamma_{1h}}{2} = \frac{72.21}{2} = 36.10\,\text{deg}$$

$$\sigma_h = \frac{(c_x/s)_h}{\cos\theta_h} = \frac{0.7294}{\cos 361.0\,\text{deg}} = 0.9027$$

After several iterations, the results are $\gamma_{2h} = 72.73$ deg, $\theta_h = 36.37$ deg, and $\sigma_h = 0.9058$. The blade spacing s is 0.04259 m, and the axial chord is 0.03107 m.

Tip:

$$Z_x\left(\frac{c_x}{s}\right)_t = (2\cos^2\alpha_{2t})\left(\tan\alpha_{1t} + \frac{u_2}{u_1}\tan\alpha_{2t}\right)\left(\frac{u_1}{u_2}\right)^2$$

$$= (2\cos^2 59.61\,\text{deg})\left(\tan 0\,\text{deg} + \frac{403.1}{328.6}\tan 59.61\,\text{deg}\right)$$

$$\times \left(\frac{328.6}{403.1}\right)^2 = 0.7115$$

$$\left(\frac{c_x}{s}\right)_t = \frac{0.7115}{0.9} = 0.7905$$

$$\gamma_{1t} = \alpha_{1t} = 0$$

Table 9.13 Summary of Example 9.11 results

Location	Average radius, m	Solidity	Spacing, m	Number of blades	Axial chord, m
Tip	0.3193	0.9555	0.04038	49.7	0.03192
Mean	0.3000	0.9329	0.04135	45.6	0.03150
Hub	0.2807	0.9058	0.04259	41.4	0.03107

Initially, we assume a solidity σ of 1.0:

$$\gamma_{2t} = \frac{\gamma_{1t} + 8\sqrt{\sigma_t}\alpha_{2t}}{8\sqrt{\sigma_t} - 1} = \frac{0 + 8\sqrt{1}59.61}{8\sqrt{1} - 1} = 68.13 \text{ deg}$$

$$\theta_t = \frac{\gamma_{2t} - \gamma_{1t}}{2} = \frac{68.13}{2} = 34.06 \text{ deg}$$

$$\sigma_t = \frac{(c_x/s)_t}{\cos\theta_t} = \frac{0.7905}{\cos 34.06 \text{ deg}} = 0.9542$$

After several iterations, the results are $\gamma_{2t} = 68.35$ deg, $\theta_t = 34.18$ deg, and $\sigma_t = 0.9555$. The blade spacing s is 0.04038 m, and the axial chord is 0.03192 m.

For this stator blade with a chord of 0.03858 m, we require the information in Table 9.13. Thus the number of required stator blades is 50, which will have a mean-radius spacing s of 0.03770 m and solidity σ of 1.023 (= 0.03858/0.03770) on the mean radius. The blade has an axial width W_s of 0.03192 m (see Fig. 9.69).

9.5.4.3 Blade profile. The shapes of turbine stator and rotor blades are based on airfoil shapes developed specifically for turbine applications. Two airfoil shapes are included in the program TURBN to sketch the blade shapes for a stage: the C4 and T6 British profiles. The base profile of the C4 airfoil is listed in Table 9.14 and shown in Fig. 9.70 for a 10% thickness. Table 9.15 and Fig. 9.71 give the base profile of the T6 airfoil for a 10% thickness. The program TURBN assumes a circular arc mean line for sketching the blade shapes.

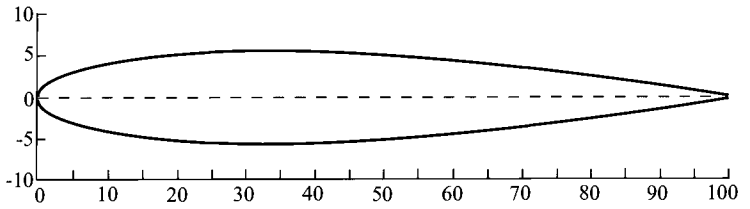

Fig. 9.70 The C4 turbine airfoil base profile.

Table 9.14 C4 airfoil profile ($t/c = 0.10$)[a,b]

x/c, %	y/c, %	x/c, %	y/c, %
0.0	0.0	40	4.89
1.25	1.65	50	4.57
2.5	2.27	60	4.05
5	3.08	70	3.37
7.5	3.62	80	2.54
10	4.02	90	1.60
15	4.55	95	1.06
20	4.83	100	0.0
30	5.00		

[a]Leading-edge radius = $0.12t$.
[b]Trailing-edge radius = $0.06t$.

Table 9.15 T6 airfoil profile ($t/c = 0.10$)[a,b]

x/c, %	y/c, %	x/c, %	y/c, %
0.0	0.0	40	5.00
1.25	1.17	50	4.67
2.5	1.54	60	3.70
5	1.99	70	2.51
7.5	2.37	80	1.42
10	2.74	90	0.85
15	3.4	95	0.72
20	3.95	100	0.0
30	4.72		

[a]Leading-edge radius = $0.12t$.
[b]Trailing-edge radius = $0.06t$.

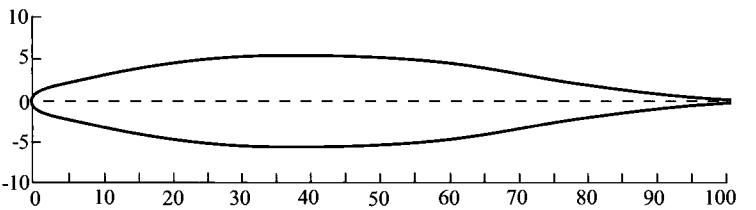

Fig. 9.71 The T6 turbine airfoil base profile.

Example 9.12

Consider a single-stage turbine using the computer program TURBN.

Given:

$$\dot{m} = 200\ \text{lbm/s}, \quad M_1 = 0.4, \quad T_{t1} = 3400°\text{R}$$

$$T_{t3} = 2860°\text{R}, \quad M_2 = 1.1, \quad \omega r = 1500\ \text{ft/s}, \quad r_m = 12\ \text{in.}$$

$$P_{t1} = 250\ \text{psia}, \quad \alpha_1 = 0\ \text{deg}, \quad \alpha_3 = 0\ \text{deg}, \quad \gamma = 1.3$$

$$R = 53.40\ \text{ft} \cdot \text{lbf/(lbm} \cdot °\text{R)}, \quad u_3/u_2 = 0.90, \quad \psi_{t\,\text{stator}} = 0.06, \quad \phi_{t\,\text{rotor}} = 0.15$$

Solution: The program TURBN is run with α_2 as the unknown. The results are given in Table 9.16 with the hub and tip tangential velocities based on free-vortex swirl distribution. The cross section of the stage sketched by the computer program is shown in Fig. 9.72 for stator $c/h = 0.8$ and rotor $c/h = 0.6$. The very high AN^2 of 4.18×10^{10} in.$^2 \cdot$ rpm^2 at a relative total temperature of 3052°R is not possible with current materials unless the blades are cooled. Also, the high rim speed of about 1206 ft/s would require existing materials to be cooled.

9.5.5 Axial-Flow Turbine Stage—α_2 Known

The preceding method of calculation assumed that α_2 was unknown. The program TURBN will handle the case when any one of the following four variables is unknown:

$$\alpha_2,\ T_{t3},\ \alpha_3,\ \text{or}\ M_2$$

When T_{t3} is unknown, Eqs. (9.20) and (9.103) are solved for T_{t3}, giving

$$T_{t3} = T_{t1} - \frac{\omega r V_2}{g_c c_p}\left(\sin\alpha_2 + \frac{u_3}{u_2}\cos\alpha_2 \tan\alpha_3\right) \tag{9.114}$$

When α_3 is unknown, Eqs. (9.20) and (9.103) are solved for α_3, giving

$$\tan\alpha_3 = \frac{1}{u_3/u_2}\left(\frac{\psi}{\cos\alpha_2}\frac{\omega\gamma}{V_2} - \tan\alpha_2\right) \tag{9.115}$$

When M_2 is unknown, the velocity at station 2 (v_2) is obtained from Eq. (9.103), giving

$$V_2 = \frac{\psi\,\omega r}{\sin\alpha_2 + (u_3/u_2)\cos\alpha_2 \tan\alpha_3} \tag{9.116}$$

Then M_2 is obtained from Eq. (9.104) rewritten as

$$M_2 = \frac{V_2}{\sqrt{(\gamma-1)g_c c_p T_{t2} - [(\gamma-1)/2]V_2^2}} \tag{9.117}$$

9.5.6 Axial-Flow Turbine Stage Analysis—No Exit Swirl

Consider the flow through a single-stage turbine as shown in Fig. 9.73 with zero exit swirl. We will consider the case where there is no exit swirl ($v_3 = 0$,

Table 9.16 Results for Example 9.12 axial-flow turbine stage calculation using TURBN

Property		Station										
		1*h*	1*m*	1*t*	2*h*	2*m*	2*t*	2*Rm*	3*Rm*	3*h*	3*m*	3*t*
T_t	°R	3400	3400	3400	3400	3400	3400	3052	3052	2860	2860	2860
T	°R	3320	3320	3320	2767	2878	2957	2878	2768	2767	2768	2769
P_t	psia	250.0	250.0	250.0	242.5	242.5	242.5	151.9	144.4	109.0	109.0	109.0
P	psia	225.6	225.6	225.6	99.2	117.7	132.4	117.7	94.6	94.4	94.6	94.7
M		0.400	0.400	0.400	1.236	1.100	1.100	0.636	0.827	0.474	0.471	0.469
V	ft/s	1089	1089	1089	3071	2789	2569	1611	2057	1178	1171	1167
u	ft/s	1089	1089	1089	1282	1282	1282	1282	1153	1153	1153	1153
v	ft/s	0	0	0	2791	2477	2226	977	1703	239	203	177
α	deg	0	0	0	65.34	62.64	60.07	——	——	11.68	10.00	8.74
β	deg	——	——	——	——	——	——	37.32	55.90	——	——	——
Radii	in.	11.04	12.00	12.96	10.65	12.00	13.35	12.00	12.00	10.20	12.00	13.80

Hub: $^\circ R_t = -0.0005$ $A_1 = 144.31$ in.^{2}

Mean: $^\circ R_t = 0.2034$ $A_2 = 203.72$ in.^{2}

Tip: $^\circ R, = 0.3487$ $A_3 = 271.04$ in.^{2}

$\tau_s = 0.8412$ $\pi_s = 0.4359$ RPM = 14,324 $\psi = 1.7868$ $\phi = 0.8544$

$\eta_s = 91.08\%$ and AN^2 at $2 = 4.18 \times 10^{10}$ in.$^2 \cdot$ rpm^2

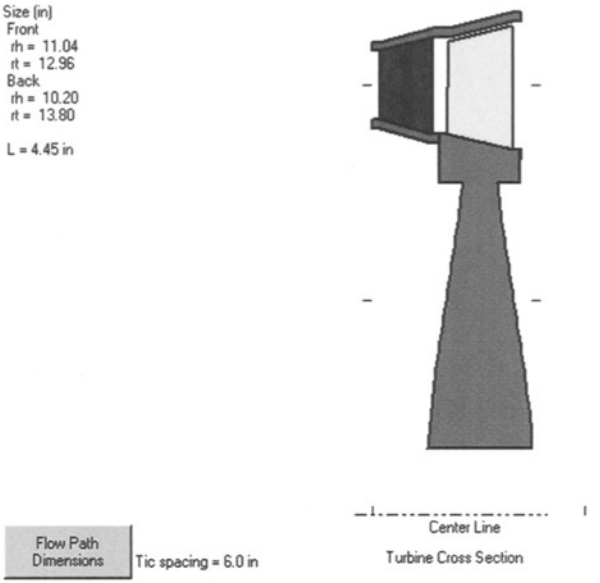

Fig. 9.72 Sketch of cross section for turbine stage of Example 9.12 from TURBN.

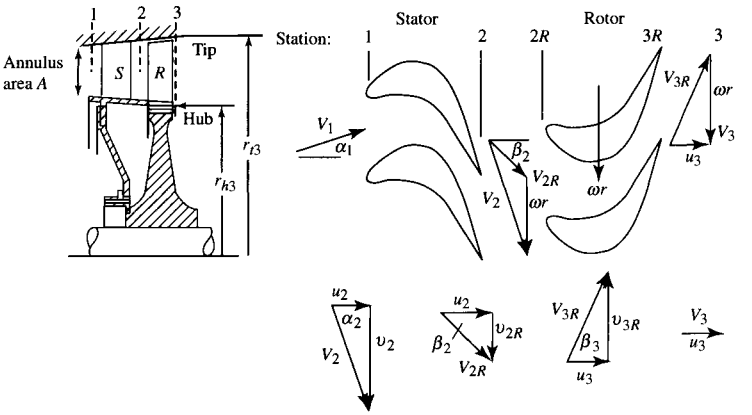

Fig. 9.73 Generalized turbine stage, zero exit swirl.

$\alpha_3 = 0$) and the axial velocities at stations 2 to 3 are the same ($u_2 = u_3$). The flows through the nozzle (stator) and rotor are assumed to be adiabatic. For solution, we assume the following data are known:

$$M_2,\ T_{t1},\ T_{t3},\ \omega r,\ c_p, \text{ and } \gamma$$

The equations for solution of a zero exit swirl, axial-flow turbine based on these known data are developed in this section.

At station 2, v_2 is given by

$$V_2 = \sqrt{\frac{2g_c c_p T_{t2}}{1 + 2/[(\gamma - 1)M_2^2]}}$$

$$= \omega r \sqrt{\frac{2\psi/(1 - \tau_s)}{1 + 2/[(\gamma - 1)M_2^2]}} \tag{9.118}$$

and α_2 by

$$\sin \alpha_2 = \psi \frac{\omega \gamma}{V_2} = \sqrt{(1 - \tau_s)\frac{\psi}{2}\left[1 + \frac{2}{(\gamma - 1)M_2^2}\right]} \tag{9.119}$$

Because the axial velocities at stations 2 and 3 are equal, the velocity at station 3 is given by

$$V_3 = V_2 \cos \alpha_2 \tag{9.120}$$

The degree of reaction is given by Eq. (9.87):

$$^{\circ}R_t = 1 - \frac{\psi}{2}$$

The stage exit Mach number M_3 is derived as follows. Given that

$$\frac{M_3}{M_2} = \frac{u_3/a_3}{V_2/a_2} = \frac{u_2}{V_2}\frac{a_2}{a_3} = \cos \alpha_2 \sqrt{\frac{T_2}{T_3}}$$

Then from Eq. (9.81b), we write

$$^{\circ}R_t = \frac{T_2 - T_3}{T_{t1} - T_{t3}} = 1 - \frac{\psi}{2}$$

which allows the temperature ratio T_2/T_3 to be written as

$$\frac{T_2}{T_3} = \frac{1}{1 - (T_{t2}/T_2)(1 - \tau_s)(1 - \psi/2)} \tag{9.121}$$

Thus the Mach number M_3 can be written as

$$M_3 = \frac{M_2 \cos \alpha_2}{\sqrt{1 - (1 - \tau_s)(1 - \psi/2)\{1 + (\gamma - 1)/2]M_2^2\}}} \tag{9.122}$$

A compact equation for the rotor exit relative Mach number M_{3R} is developed as follows. Since

$$\frac{M_{3R}}{M_2} = \frac{V_{3R}}{a_3}\frac{a_2}{V_2} = \frac{V_{3R}}{V_2}\sqrt{\frac{T_2}{T_3}}$$

the velocity ratio is obtained by first writing

$$V_{3R}^2 = u^2 + (\omega r)^2 = V_2^2 - v_2^2 + (\omega r)^2$$

Thus

$$\frac{V_{3R}^2}{V_2^2} = 1 - \frac{v_2^2}{V_2^2} + \frac{(\omega r)^2}{V_2^2} = 1 - \left(\frac{\omega r}{V_2}\right)^2\left[\left(\frac{v_2}{\omega r}\right)^2 - 1\right]$$

$$= 1 - \left(\frac{\omega r}{V_2}\right)^2(\psi^2 - 1)$$

Since

$$\frac{M_{3R}}{M_2} = \frac{V_{3R}}{V_2}\sqrt{\frac{T_2}{T_3}}$$

then by using Eq. (9.121), the Mach number ratio is found by

$$\frac{M_{3R}}{M_2} = \sqrt{\frac{1 - (\omega r/V_2)^2(\psi^2 - 1)}{1 - (T_{t2}/T_2)(1 - \tau_s)(1 - \psi/2)}} \tag{9.123}$$

which with Eq. (9.119) becomes (and is actually used as)

$$\frac{M_{3R}}{M_2} = \sqrt{\frac{1 - (1 - \tau_s)\dfrac{\psi^2 - 1}{2\psi}\left[1 + \dfrac{2}{(\gamma - 1)M_2^2}\right]}{1 - (1 - \tau_s)\left(1 - \dfrac{\psi}{2}\right)\left(1 + \dfrac{\gamma - 1}{2}M_2^2\right)}} \tag{9.124}$$

This equation contains an interesting and unexpected piece of guidance for the design of turbine stages. To ensure that stator cascade choking controls the turbine mass flow rate, M_2 should be greater than unity and M_{3R} should be less than unity. Equation (9.124) reveals, however, that when the stage loading coefficient is unity (degree of reaction is 0.5), the opposite must be true. Therefore, even though it would appear preferable to aim for a degree of reaction near 0.5 to balance the difficulty of designing the stator and rotor airfoils, the requirement to reduce M_{3R} translates to lower allowable values of the degree of reaction and correspondingly higher stage loadings. In actual practice, the degree of reaction is usually found in the range of 0.2 to 0.4, so that a substantial, but minority, fraction of the overall static enthalpy (and static presssure) drop still takes place across the rotor and is available to prevent the separation of the suction surface boundary layer. It is important to bear in mind that even turbine airfoil boundary layers can separate, and when they do, the effect on efficiency (and heat transfer) is usually disastrous.

The rotor relative total temperature ($T_{t2R} = T_{t3R}$), which is useful for heat transfer and structural analyses, is given by Eq. (9.113). For our case of zero exit swirl and constant axial velocity ($u_3 = u_2$), this equation reduces to

$$\frac{T_{t3R}}{T_{t2}} = \tau_s + \frac{1 - \tau_s}{2\psi} \tag{9.125}$$

Example 9.13

To illustrate the application of this method, a single-stage turbine with zero exit swirl will be designed for the following conditions:

$M_1 = 0.4$	$M_2 = 1.10$
$\omega r = U = 300$ m/s	$T_{t2} = T_{t1} = 1400$ K
$R = 0.2872$ kJ/(kg · K)	$g_c c_p = 1.158$ KJ/(kg · K)
$T_{t3} = 1260$ K	$\gamma = 1.33$
$\tau_s = \dfrac{T_{t3}}{T_{t1}} = 0.900$	$\psi = 1.8006$ Eq. (9.20)

If one chooses to assume $e_t = 0.90$, the results are

$^{\circ}R_t = 0.0997$	Eq. (9.87)	$M_{3R} = 0.8756$	Eq. (9.124)
$\alpha_2 = 47.35$ deg	Eq. (9.119)	$T_{t3R} = 1299$ K	Eq. (9.125)
$M_3 = 0.7498$	Eq. (9.122)	$\Phi = 1.6586$	Eq. (9.78a)
$\pi_s = 0.6239$	Eq. (9.91)	$\eta_t = 0.9053$	Eq. (9.76)

These results provide the basis for step-by-step calculations leading to the summary of flow properties given in Table 9.17.

Table 9.17 Results for Example 9.13 axial-flow turbine state calculation with zero exit swirl

	Station				
Property	1	2	2R	3R	3
T_t	1400.0	1400.0	1298.9	1298.9	1260.0
T	1364.0	1167.0	1167.0	2012.7	2012.7
$\dfrac{P_t}{P_{t1}}$	1.0000	?	?	0.7053	0.6239
$\dfrac{P}{P_{t1}}$	0.9003	?	?	0.4364	0.4364
M	0.400	1.100	0.8586	0.8756	0.7498
V m/s	288.7	734.4	552.5	581.0	497.6
u m/s	288.7	497.6	497.6	497.6	497.6
v m/s	0	540.2	240.2	300.0	0
α deg	0	47.35	——	——	0
β deg	——	——	25.76	31.09	——

9.5.6.1 General solution. When γ and e_t are fixed, closer examination of the turbine stage design equation set reveals that the results depend only on the dimensionless quantities M_2, τ_s, and ψ. Under these conditions, it is therefore possible to generate graphical representations that reveal the general tendencies of such turbine stages and serve the important purpose of defining the limits of reasonable stage designs.

This has been done for typical ranges of the prevailing dimensionless parameters and γ values of 1.33 and 1.3; the results are presented in Figs. 9.74 and 9.75, respectively. These charts may be used to obtain initial ballpark-stage design estimates and also reveal some important trends. If values of M_{3R} less than 1 and stage loading coefficients ψ less than or equal to 2.0 are taken as reasonable limits, it is clear that better (i.e., lower) values of ψ are available for the same ΔT_t as τ_s decreases (lower inlet temperatures) and/or ωr increases (higher wheel speeds). By noting that ψ does not depend on M_2 [Eq. (9.87)], it is also clear that M_2 determines only M_{3R}. Larger values of M_2 are desirable because they reduce the annulus flow area A and the rotating airfoil centrifugal stresses, and ensure choking of the stator airfoil passages over a wider turbine operating range; but Figs. 9.74 and 9.75 show that increasing M_2 reduces the number of acceptable solutions. Finally, all other things being equal, stages having lower τ_s (i.e., more energy extraction) suffer the dual disadvantages of increased stage loading coefficient ψ and increased annulus flow area A.

Figures 9.74 and 9.75 exhibit an extremely interesting mathematical behavior in the region where all the curves for a value of M_2 appear to, and indeed do, pass through a single point. This fact may be verified by equating the numerator and denominator on the right side of the equals sign in Eq. (9.124), and this reveals that $M_{3R} = M_2$ is independent of either M_2 or τ_s provided only that

$$\psi^2 - 1 = \frac{\gamma - 1}{2}(2\psi - \psi^2)M_2^2$$

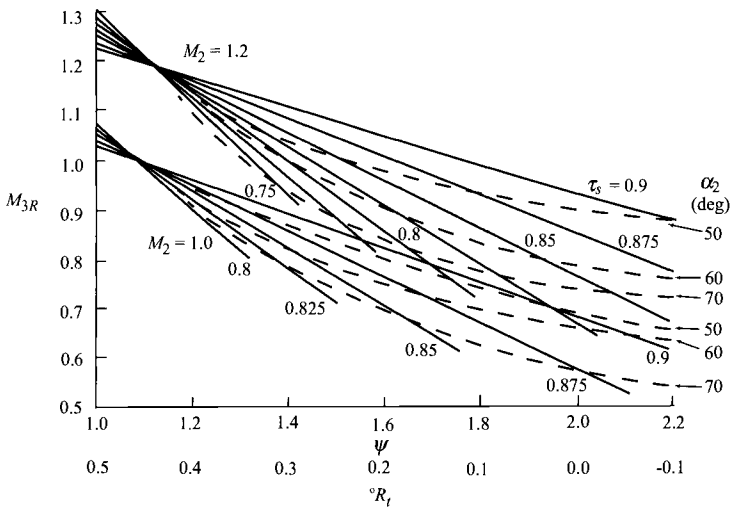

Fig. 9.74 Generalized turbine stage behavior, zero exit swirl ($\gamma = 1.33$).

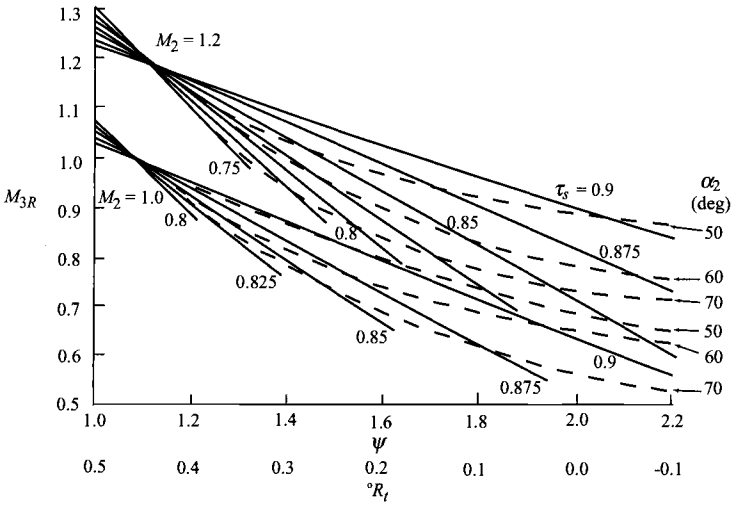

Fig. 9.75 Generalized turbine stage behavior, zero exit swirl ($\gamma = 1.3$).

Hence, for each γ, there are two values of ψ that satisfy this condition. When $M_{3R} = M_2 = 1.0$ and $\gamma = 1.3$, they are 1.072 and -0.82, the former obviously being the one that appears in Fig. 9.75 and the latter having no practical use. For $M_{3R} = M_2 = 1.2$ and $\gamma = 1.3$, they are 1.102 and -0.746. The physical meaning of this convenient convergence is clear enough, namely, that near $M_{3R} = M_2$, where the stator and rotor airfoil exit conditions are similar, the stage loading parameter ψ must be near unity regardless of the other stage parameters.

9.5.6.2 Multistage turbine design. When the required stage loading coefficient ψ for a design is greater than 2.0, a single-stage design would require a hopeless negative reaction [Eq. (9.87)] and would be impossible to design with high aerodynamic efficiency. A desirable multistage design would have the total temperature difference distributed evenly among the stages:

$$(\Delta T_t)_{\text{turbine}} = (\text{number of stages}) \times (\Delta T_t)_{\text{stage}}$$

This would result in stages with the same stage loading coefficients [Eq. (9.20)] and same degree of reaction [Eq. (9.87)] for the same rotor speed U. For a three-stage design, we get

$$\psi_{s1} = \psi_{s2} = \psi_{s3} \quad \text{and} \quad (^\circ R_t)_{s1} = (^\circ R_t)_{s2} = (^\circ R_t)_{s3}$$

To obtain the choked flow in the first-stage stator (nozzle), the Mach number entering the rotor M_2 is slightly supersonic. The Mach numbers in the remaining stages are kept subsonic. The net result is that the stage loading of the first stage is larger than the loading of any of the other stages. For a three-stage design, the

stage loading coefficient and degree of reaction of the second and third stages are nearly equal.

9.5.7 Shaft Speed

The design rotational speed of a spool (shaft) having stages of compression driven by a turbine is initially determined by that component that limits the speed because of high stresses. For a low-pressure spool, the first stage of compression, since it has the greatest AN^2, normally dictates the rotational speed. The first stage of turbine on the high-pressure spool normally determines that spool's rotational speed because of its high AN^2 or high disk rim speed at elevated temperature.

9.5.8 Design Process

The design process requires both engineering judgment and knowledge of typical design values. Table 9.18a gives the range of design parameters for axial-flow turbines that can be used for guidance. The comparison of turbines for Pratt & Whitney engines in Table 9.18b shows typical turbine design values and the leading trends in turbine technology. Note the increases over the years in inlet temperature, mass flow rate, and output power.

From Table 9.18b, comparison of the JT3D and JT9D high-pressure turbines shows that the stage loading coefficient did not appreciably change between the designs. However, the turbine inlet temperature increased to a value above the working temperature of available materials, requiring extensive use of cooling air. The stage loading coefficient for the low-pressure turbine increased dramatically, reducing the number of stages to four. If the stage loading coefficient of the low-pressure turbine of the JT3D were not increased significantly in the design of the JT9D, about six or seven stages of low-pressure turbine would have been required—increasing both cost and weight.

Table 9.18a Range of axial-flow turbine design parameters

Parameter	Design range
High-pressure turbine	
Maximum AN^2	$4-5 \times 10^{10}$ in.$^2 \cdot$ rpm^2
Stage loading coefficient	1.4–2.0
Exit Mach number	0.40–0.50
Exit swirl angle, deg	0–20
Low-pressure turbine	
Inlet corrected mass flow rate	40–44 lbm/(s $\cdot$ ft^2)
Hub/tip ratio at inlet	0.35–0.50
Maximum stage loading at hub	2.4
Exit Mach number	0.40–0.50
Exit swirl angle, deg	0–20

Table 9.18b Comparison of Pratt & Whitney engines

Parameter	JT3D	JT9D
Year of introduction	1961	1970
Engine bypass ratio	1.45	4.86
Engine overall pressure ratio	13.6	24.5
Core engine flow, lb/s	187.7	272.0
High-pressure turbine		
Inlet temperature, °F	1745	2500
Power output, hp	24,100	71,700
Number of stages	1	2
Average stage loading coefficient	1.72	1.76
Coolant plus leakage flow, %	2.5	16.1
Low-pressure turbine		
inlet temperature, °F	1410	1600
Power output, hp	31,800	61,050
Number of stages	3	4
Average stage loading coefficient	1.44	2.47
Coolant plus leakage flow, %	0.7	1.4

9.5.8.1 Steps of design. The material presented in previous sections can now be applied to the design of an axial-flow turbine. The complete design process for a turbine will include the following items:

1) Selection of rotational speed and annulus dimensions
2) Selection of the number of stages
3) Calculation of airflow angles for each stage at the mean radius
4) Calculation of airflow angle variations from the hub to tip for each stage
5) Selection of blade material
6) Selection of blading using experimental cascade data
7) Selection of turbine cooling, if needed
8) Verification of turbine efficiency based on cascade loss data
9) Prediction of off-design performance
10) Rig testing of design

Items 1–5 will be covered in this section. The other steps are covered in Refs. 42, 43, 22, and 29. The design process is inherently iterative, often requiring the return to an earlier step when prior assumptions are found to be invalid. Many technical specialities are interwoven in a design, e.g., an axial-flow turbine involves at least thermodynamics, aerodynamics, structures, materials, heat transfer, and manufacturing processes. Design requires the active participation and disciplined communication by many technical specialists.

Example 9.14

We will consider the design of a turbine suitable to power the eight-stage, axial-flow compressor designed earlier in this chapter for a simple turbojet gas turbine

engine (see Example 9.7). From engine cycle and compressor design calculations, a suitable design point for the turbine of such an engine at sea-level, standard-day conditions ($P = 14.696$ psia and $T = 518.7°R$) may emerge as follows:

Compressor pressure ratio: 10.41	Rotor speed ω: 800 rad/s
Compressor flow rate: 150 lbm/s	Turbine flow rate: 156 lbm/s
Compressor efficiency: 86.3%	T_t entering turbine: 3200°R
Compressor exit T_t: 1086°R	P_t entering turbine: 143.1 psia
Compressor γ: 1.4	Turbine γ: 1.3
Compressor R: 53.34 ft · lbf/(lbm · °R)	Turbine R: 53.40 ft · lbf/(lbm · °R)

From these specified data, we now investigate the aerodynamic design of an axial-flow turbine.

The compressor input power is

$$\dot{W}_c = \dot{m}c_p(T_{te} - T_{ti}) = (150 \times 0.240)(1086 - 518.7) = 20{,}423 \text{ Btu/s}$$
$$= 21.55 \text{ MW}$$

Assuming that the compressor input power is 0.98 of the turbine output power (the other 2% of turbine power goes to shaft takeoff power and bearing losses), the required output power of the turbine is 22.0 MW (21.55 MW/0.98). The total temperature leaving the turbine is

$$T_{tc} = T_{ti} - \frac{\dot{W}_t}{\dot{m}c_p} = 3200 - \frac{22{,}000/1.055}{156 \times 0.297} = 3200 - 450.1 = 2749.9°R$$

The turbine temperature ratio ($\tau_t = T_{te}/T_{ti}$) is 0.8593. If the flow entering the rotor has a Mach number of 1.2 at 60 deg to the centerline of the turbine and a 1 % total pressure loss through the turbine stator (nozzle), the annulus area entering the rotor is

$$A_2 = \frac{\dot{m}\sqrt{T_{t2}}}{(\cos \alpha_2)(P_{t2})\text{MFP}(M_2)}$$
$$= \frac{156\sqrt{3200}}{\cos 60 \text{ deg} \times 143.1 \times 0.99 \times 0.502075\sqrt{53.34/53.40}} = 248.3 \text{ in.}^2$$

For a rotor angular speed ω of 800 rad/s, AN^2 for the rotor is 1.45×10^{10} in.$^2 \cdot$ rpm^2—this blade stress is within the capability of modern cooled turbine materials (about 2 to 3×10^{10} in.$^2 \cdot$ rpm^2).

Calculation of the stage loading coefficient for the turbine helps in determining the number of turbine stages. For the turbine mean radius equal to that of the compressor, the stage loading coefficient on the mean line is

$$\psi = \frac{g_c c_p \Delta T_t}{(\omega r_m)^2} = \frac{7455 \times 450.1}{(800 \times 17.04/12)^2} = 2.600$$

Using Fig. 9.73, we see that this value of stage loading coefficient is larger than that possible for a single-stage turbine. Either the mean rotor speed ωr_m must be

Table 9.19 Variation of stage loading, radii, and rim speed with mean radius for Example 9.14 single-stage design

r_m, in.	ψ	r_t, in.	r_h, in.	r_h/r_t	U_r, ft/s
16.00	2.949	17.23	14.77	0.857	918
17.04	2.600	18.20	15.88	0.873	992
18.00	2.330	19.10	16.90	0.885	1060
19.00	2.091	20.04	17.96	0.896	1131
20.00	1.887	20.99	19.01	0.906	1201
21.00	1.712	21.94	20.06	0.914	1271

increased to reduce the stage loading coefficient for a single-stage turbine, or a two-stage turbine will be required. Because increasing the rotor angular speed ω will increase the blade stress AN^2 and because only a little margin exists, we will investigate the effect of increasing the mean radius on stage loading coefficient, annulus radii (r_t and r_h), and rim speed (U_r—assuming the rim radius is 1 in. smaller than that of the hub). From the results given in Table 9.19, we can see that a single-stage turbine would require a mean radius of 19 to 20 in. to reduce the stage loading coefficient and keep the rim speed below about 1200 ft/s. This would result in a tip radius equal to or larger than the compressor's inlet radius. In addition, the tip radius of 20 to 21 in. is much larger than current turbines for gas turbine engines that range between 10 and 17 in. Although a single-stage turbine is desirable because of the reduced weight, the low rotor angular speed of 800 rad/s makes this size undesirable.

For a smaller turbine, the designer might consider increasing the rotor angular speed and redesigning the compressor. A rotor angular speed of 1000 rad/s for a turbine with a 16-in. mean radius has a stage loading coefficient for the mean radius of 1.885 and a rim speed of 1148 ft/s, which is possible for a single stage.

The designs of both a single-stage turbine and a two-stage turbine are performed in the following sections. The computer program TURBN is used to ease the calculational burden in both designs.

9.5.8.2 Single-stage design. We consider a single-stage turbine with the following characteristics:

Rotor angular speed ω: 800 rad/s
T_t entering turbine: 3200°R
T_t leaving turbine: 2749.1°R
Turbine R: 53.40 ft · lbf/(lbm · °R)
Turbine mass flow rate: 156 lbm/s
P_t entering turbine: 143.1 psia
Ratio of specific heats: 1.3

To keep the degree of reaction at the hub from being too negative at a reasonable value of the stage loading coefficient ψ, we consider a nonzero exit swirl angle α_3 for a stage with a hub speed of about 1200 ft/s (this corresponds to a rim speed of about 1130 ft/s, which will limit the disk stress). This hub speed corresponds to a hub radius of 18 in. and a tip radius of about 20.1 in. The

computer program TURBN was run with the exit swirl angle α_3 unknown, the data just listed, and the following additional input data:

Mean rotor speed ωr: 1270 ft/s	ω: 800 rad/s
M_2: 1.1	α_2: 60 deg
M_1: 0.4	α_1: 0 deg
u_3/u_2: 1.0	$\phi_{t\,\text{stator}} = 0.06$ and $\phi_{t\,\text{rotor}} = 0.15$
Z_s: 0.9	$(c/h)_s$: 1.0
Z_r: 0.9	$(c/h)_r$: 1.0

Computer calculations yield the single-stage turbine summarized in Table 9.20 with hub and tip tangential velocities based on free-vortex swirl distribution. This is a viable single-stage design with moderate exit swirl α_3, positive reaction, and subsonic M_{3R} at the tip.

This design gives a blade AN^2 of 1.44×10^{10} in.$^2 \cdot$rpm ^{2} and hub speed of 1201 ft/s. This AN^2 value is well within the limits of cooled turbine materials, and the low hub speed is below the limiting speed of turbine disk materials.

A cross-sectional sketch of the single-stage turbine just designed and plotted by the computer program TURBN is shown in Fig. 9.76. Note that this sketch does not show the required exit guide vanes that will turn the flow back to axial. The estimated axial length L shown in Fig. 9.76 is based on the input values of Z and c/h for the stator and rotor blades and the scaling relationships of Fig. 9.69. For the input values of Z and c/h, the resulting solidity at the mean radius, number of blades, and chord length for the stator and rotor are as shown in Table 9.21.

The selected axial chord and number of blades for the stator or rotor depend on many factors (e.g., flow through the blades, vibration, blade attachment). Figure 9.77 shows the computer sketch of the blades at the mean radius, using C4 base profiles.

9.5.8.3 Two-stage design. In a two-stage design, the stage loading coefficients ψ are lower and the temperature ratios τ_s are higher than those for a single-stage design. This results in higher reactions, less turning of the flow, and lower loss coefficients. For good flow control of the turbine, the first-stage stator (nozzle) should be choked, which requires that M_2 for this stage be supersonic. Inspection of Fig. 9.75 shows that at low ψ and high τ_s, the value of M_{3R} is a little less than M_2—thus, we will want to select a low supersonic value of M_2 (about 1.05) for the first stage. A balanced design would have about the same α_2 values for both stages with the first-stage M_{3Rt} below 0.9.

The two-stage turbine will be designed with a 17.04-in. mean radius (same as multistage compressor) at an rpm of 7640 ($\omega = 800$ rad/s), giving a mean rotor speed $U_m = \omega r_m$ of 1136 ft/s. An initial starting point for the design of this two-stage turbine is constant axial velocity through the rotor ($u_3 = u_2$), zero exit swirl ($\alpha_3 = 0$), and a second-stage M_2 of 0.7. The stage loading coefficients and other flow properties depend on the split in temperature drop between the stages. Calculations were performed by using the computer program TURBN

Table 9.20 Results for Example 9.14 single-stage axial-flow turbine design

Property		Station										
		1*h*	1*m*	1*t*	2*h*	2*m*	2*t*	2*Rm*	3*Rm*	3*h*	3*m*	3*t*
T_1	°R	3200	3200	3200	3200	3200	3200	2909	2909	2750	2750	2750
T	°R	3125	3125	3125	2665	2708	2745	2708	2621	2620	2621	2622
Pt	psia	143.1	143.1	143.1	138.8	138.8	138.8	91.8	87.0	68.3	68.3	68.3
P	psia	129.1	129.1	129.1	62.8	67.4	71.5	67.4	55.4	55.4	55.4	55.5
M		0.400	0.400	0.400	1.157	1.100	1.051	0.702	0.855	0.574	0.572	0.571
V	ft/s	1057	1057	1057	2823	2705	2602	1727	2069	1389	1385	1381
u	ft/s	1057	1057	1057	1353	1353	1353	1353	1353	1353	1353	1353
v	ft/s	0	0	0	2477	2343	2222	1073	1566	316	296	278
α	deg	0	0	0	61.36	60.00	58.67	——	——	13.14	12.33	11.61
β	deg	——	——	——	——	——	——	38.42	49.17	——	——	——
Radii	in.	18.25	19.05	19.85	18.02	19.05	20.08	19.05	19.05	17.83	19.05	20.27

Hub: $^{\circ}R_t = 0.0990$ $A_1 = 190.78$ in.^{2}
Mean: $^{\circ}R_t = 0.1939$ $A_2 = 247.52$ in.^{2}
Tip: $^{\circ}R_t = 0.2746$ $A_3 = 291.11$ in.^{2}

$M_{3Rt} = 0.875$ $\tau_s = 0.8593$ $\pi_s = 0.4770$ $\psi = 2.0776$ $\Phi = 1.0652$

$\eta_s = 89.57\%$ AN^2 at $2 = 1.44 \times 10^{10}$ in.$^2 \cdot$rpm^2

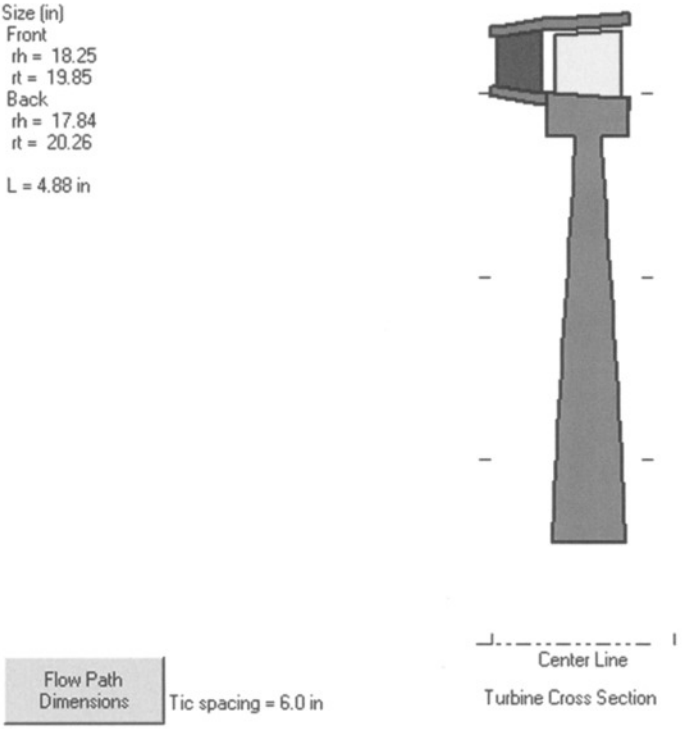

Fig. 9.76 Sketch of cross section for single-stage turbine design.

with α_2 unknown at different values of the temperature leaving the first-stage turbine. The resulting α_2 and M_{3Rt} values are listed in Table 9.22. An interstage temperature of 2925°R gives a balance design for α_2 values with the first stage M_{3Rt}, above 0.9. The value of M_{3Rt} can be reduced by selecting a value for the axial velocity ratio u_3/u_2 less than unity.

A design with an interstage temperature of 2925°R and first-stage u_3/u_2 of 0.9 is selected to reduce M_{3Rt}. The losses for the first stage and second stage are estimated by using polytropic efficiencies of 0.9 and 0.92, respectively, and stator loss coefficients of 0.06 and 0.02, respectively. For all blades, a value of 0.9 is used for the tangential force coefficient Z, and a value of 1.0 is used for the chord/height ratio c/h. Results for both stages are presented in Tables 9.23

Table 9.21 Blade results for single-stage turbine

	Solidity	Number of blades	Chord, in.
Stator	0.979	64	1.831
Rotor	1.936	103	2.250

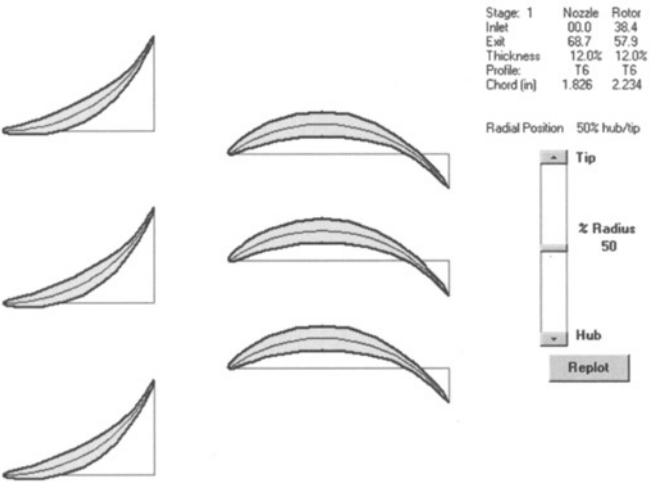

Fig. 9.77 Sketch of blades for single-stage turbine design.

and 9.24 with hub and tip tangential velocities based on free-vortex swirl distribution.

A cross-sectional sketch of the two-stage turbine just designed and plotted by TURBN is shown in Fig. 9.78. The sketch shows the stator and rotor for both stages. Note that the turbine exit stator is not shown in the sketch. For the input values of Z and c/h, the resulting solidity at the mean radius, number of blades, and chord length for the stator and rotor blades of the two stages are as shown in Table 9.25.

The selected axial chord and number of blades for the stator and rotor depend on many factors (e.g., flow through the blades, vibration, blade attachment). Figures 9.79 and 9.80 show the computer sketch of the blades at the mean radius, using C4 base profiles for the first and second stages, respectively.

Table 9.22 Variation of stage parameters with interstage temperature for Example 9.14 two-stage design

	Stage 1				Stage 2		
T_{t3}, °R	ψ	τ_s	α_2, deg	M_{3Rt}	ψ	τ_s	α_2, deg
2875	1.8750	0.8984	55.0	0.7774	1.0034	0.9565	28.61
2900	1.7307	0.9063	49.12	0.8467	0.8659	0.9482	34.90
2925	1.5865	0.9141	43.88	0.9068	1.0102	0.9401	41.65
2950	1.4423	0.9219	39.06	0.9587	1.1544	0.9322	49.13
2975	1.2981	0.9297	34.55	1.0034	1.2986	0.9243	57.90

Table 9.23 Results for Example 9.14, first stage of two-stage axial-flow turbine design

Property		Station										
		1*h*	1*m*	1*t*	2*h*	2*m*	2*t*	2*Rm*	3*Rm*	3*h*	3*m*	3*t*
T_t	°R	3200	3200	3200	3200	3200	3200	3012	3012	2925	2925	2925
T	°R	3125	3135	3125	2724	2746	2765	2746	2734	2734	2734	2734
P_t	psia	143.1	143.1	143.1	139.1	139.1	139.1	106.9	105.4	92.8	92.8	92.8
P	psia	129.1	129.1	129.1	69.2	71.6	73.8	71.6	69.3	69.3	69.3	69.3
M		0.400	0.400	0.400	1.079	1.050	1.024	0.803	0.823	0.683	0.683	0.683
V	ft/s	1057	1057	1057	2662	2600	2545	1989	2034	1687	1687	1687
u	ft/s	1057	1057	1057	1874	1874	1874	1874	1687	1687	1687	1687
v	ft/s	0	0	0	1891	1802	1722	666	1136	0	0	0
α	deg	0	0	0	45.25	43.88	42.57	——	——	0	0	0
β	deg	——	——	——	——	——	——	19.57	33.96	——	——	——
Radii	in.	16.15	17.04	17.93	16.24	17.04	17.84	17.04	17.04	16.13	17.04	17.95

Hub: $^\circ R_t = 0.0359$ $A_1 = 190.78$ in.^{2}
Mean: $^\circ R_t = 0.0437$ $A_2 = 170.34$ in.^{2}
Tip: $^\circ R_t = 0.1129$ $A_3 = 194.88$ in.^{2}

$M_{3Rt} = 0.8370$ $\tau_s = 0.9141$ $\pi_s = 0.6488$ $\psi = 1.5865$ $\Phi = 1.650$

$\eta_s = 90.44\%$ AN^2 at 2 $= 9.94 \times 10^{10}$ in.$^2 \cdot$ rpm^2

Table 9.24 Results for Example 9.14 second stage of two-stage axial-flow turbine design

Property		Station										
		1*h*	1*m*	1*t*	2*h*	2*m*	2*t*	2*Rm*	3*Rm*	3*h*	3*m*	3*t*
T_t	°R	2925	2925	2925	2925	2925	2925	2837	2837	2750	2750	2750
T	°R	2734	2734	2734	2711	2725	2736	2725	2638	2638	2638	2638
P_t	psia	92.84	92.84	92.84	92.35	92.35	92.35	80.85	79.41	69.42	69.42	69.42
P	psia	69.27	69.27	69.27	66.41	67.92	69.15	67.92	57.99	57.99	57.99	57.99
M		0.683	0.683	0.683	0.726	0.700	0.678	0.523	0.708	0.532	0.532	0.532
V	ft/s	1687	1687	1687	1786	1727	1677	1290	1719	1290	1290	1290
u	ft/s	1687	1687	1687	1290	1290	1290	1290	1290	1290	1290	1290
v	ft/s	0	0	0	1235	1148	1072	12	1136	0	0	0
α	deg	0	0	0	43.75	41.65	39.71	—	—	0	0	0
β	deg	—	—	—	—	—	—	0.51	41.36	—	—	—
Radii	in.	16.13	17.04	17.95	15.83	17.04	18.25	17.04	17.04	15.67	17.04	18.41

Hub: $^\circ R_t = 0.4148$ $A_1 = 194.88$ in.^{2}
Mean: $^\circ R_t = 0.4949$ $A_2 = 258.99$ in.^{2}
Tip: $^\circ R_t = 0.5596$ $A_3 = 293.69$ in.^{2}

$M_{3Rt} = 0.7337$ $\tau_s = 0.9401$ $\pi_s = 0.7477$ $\psi = 1.0102$ $\Phi = 1.136$

$\eta_s = 92.24\%$ AN^2 at 2 $= 1.51 \times 10^{10}$ in.$^2 \cdot$ rpm^2

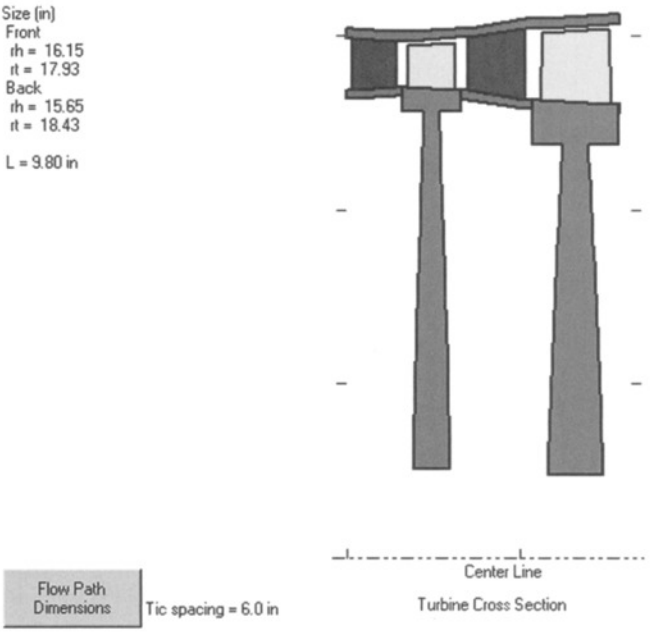

Fig. 9.78 Sketch of cross section for two-stage turbine design.

For the first stage, this design gives a blade AN^2 of 9.94×10^9 in.$^2 \cdot$ rpm^2 and disk speed of about 1020 ft/s. This AN^2 is well within the limits of cooled turbine materials, and the low rim speed is below the limiting speed of turbine disk materials.

9.5.9 Turbine Cooling

The turbine components are subjected to much higher temperatures in the modern gas turbine engines being designed and built today than was possible 60 years ago. This is due mainly to improvements in metallurgy and cooling of turbine components. The cooling air to cool the turbine is bleed air from the compressor. A schematic of a typical turbine cooling system is shown in

Table 9.25 Blade results for two-stage turbine

	Stage 1		Stage 2	
	Stator	Rotor	Stator	Rotor
Solidity	0.725	1.880	1.643	1.254
Blades	46	118	83	52
Chord, in.	1.686	1.706	2.120	2.581

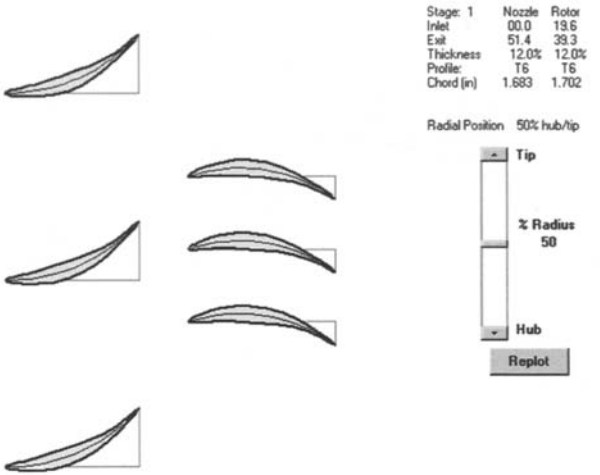

Fig. 9.79 Sketch of blades for first stage of two-stage turbine design.

Fig. 9.81. The stator blades and the outer wall of the turbine flow passage use cooling air that travels from the compressor between the combustor and outer engine case. The turbine rotor blades, disks, and inner wall of the turbine flow passage use cooling air that is routed through inner passageways.

The first-stage stator blades (nozzles) are exposed to the highest turbine temperatures (including the hot spots from the combustor). The first-stage rotor blades are exposed to a somewhat lower temperature because of circumferential averaging, dilution of turbine gases with first-stage stator cooling air, and relative

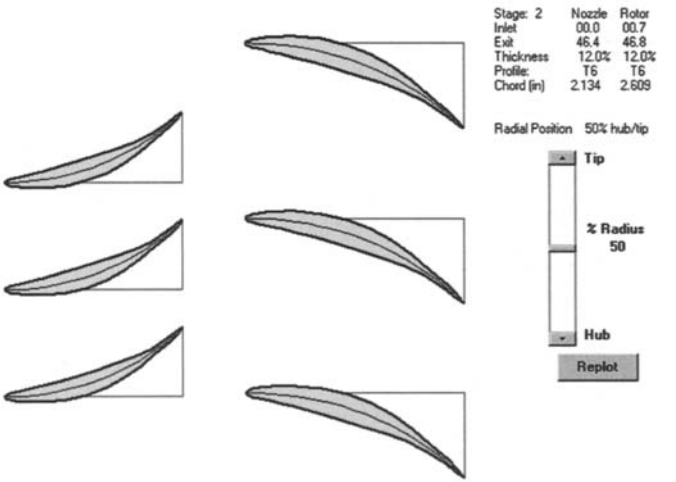

Fig. 9.80 Sketch of blades for second stage of two-stage turbine design.

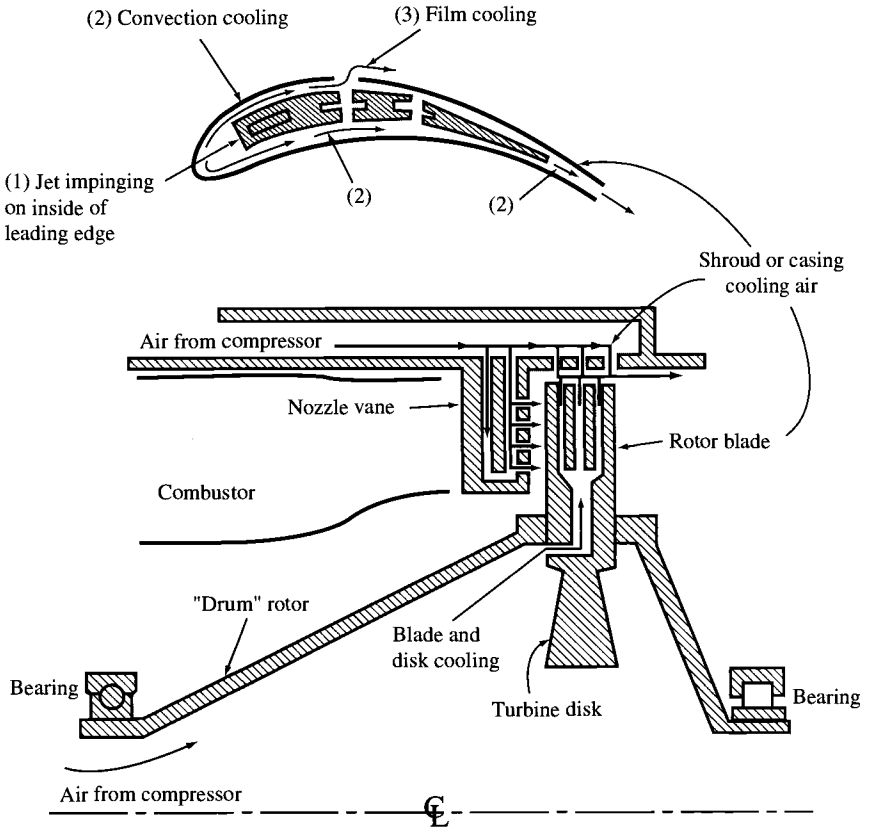

Fig. 9.81 Schematic of air-cooled turbine (from Ref. 28).

velocity effects. The second-stage stator blades are exposed to an even lower temperature because of additional cooling air dilution and power extraction from the turbine gases. The turbine temperature decreases in a like manner through each blade row.

The cooling methods used in the turbine are illustrated in Fig. 9.82 and can be divided into the following categories:

1) Convection cooling
2) Impingement cooling
3) Film cooling
4) Full-coverage film cooling
5) Transpiration cooling

Applications of these five methods of cooling to turbine blades are shown in Fig. 9.83.

Figure 9.84 shows a typical first-stage stator (nozzle) blade with cooling. This stator has cooling holes along its nose (leading edge) and pressure surface (gill

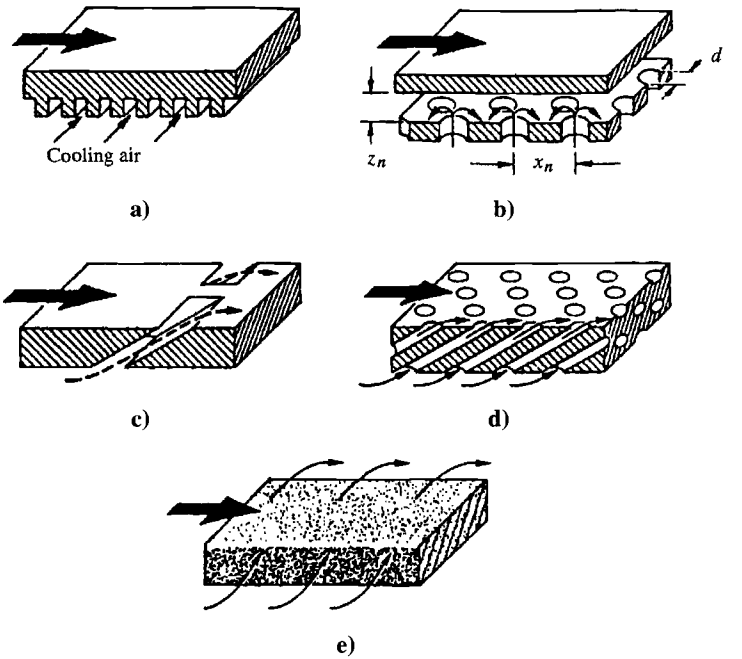

Fig. 9.82 Methods of turbine cooling (Ref. 42): a) convection cooling, b) impingement cooling, c) film cooling, d) full-coverage film cooling, e) transpiration cooling.

holes) in addition to cooling flow exiting at its trailing edge. The cooling holes on the inside wall are also shown.

A rotor blade of the General Electric CF6-50 engine is shown in Fig. 9.85. The cross section of the blade shows the elaborate internal cooling and flow exiting the blade tip (through its cap) and along the trailing edge. The blade isometric shows flow through the gill holes on the pressure surface in addition to the tip and trailing-edge cooling flows.

9.5.10 Turbine Performance

The flow enters a turbine through stationary airfoils (often called *stator blades* or *nozzles*) that turn and accelerate the fluid, increasing its tangential momentum. Then the flow passes through rotating airfoils (called *rotor blades*) that remove energy from the fluid as they change its tangential momentum. Successive pairs of stationary airfoils followed by rotating airfoils remove additional energy from the fluid. To obtain high output power to weight from a turbine, the flow entering the first-stage turbine rotor is normally supersonic, which requires the flow to pass through sonic conditions at the minimum passage area in the first-stage stators (nozzles). From Eq. (8.3), the corrected inlet mass flow rate based on this minimum passage area (throat) will be constant for fixed-inlet-area turbines. This flow characteristic is shown in the typical turbine flow map (Fig. 9.86) when the expansion ratio across the turbine (ratio

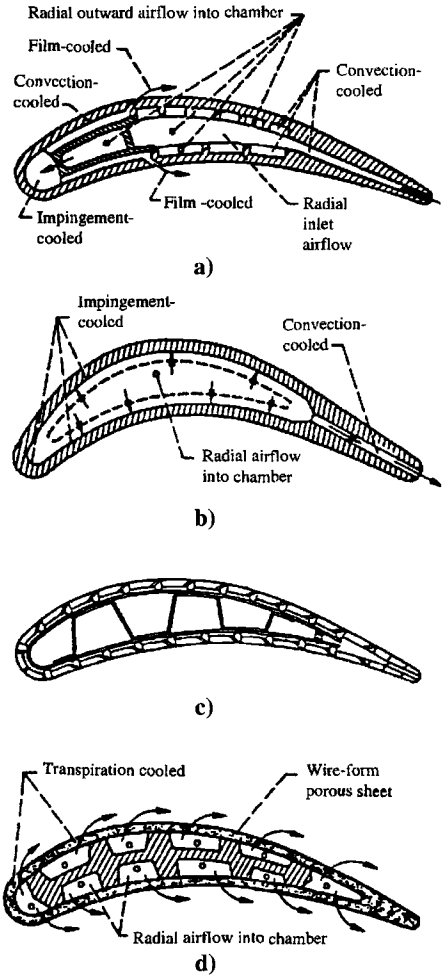

Fig. 9.83 Turbine blade cooling (Ref. 42): a) convection-, impingement-, and film-cooled blade configuration, b) convection- and impingement-cooled blade configuration, c) full-coverage film-cooled blade configuration, d) transpiration-cooled blade configuration.

of total pressure at exit to total pressure at entrance $P_{t4}/P_{t5} = 1/\pi_t$ is greater than about 2 and the flow at the throat is choked.

The performance of a turbine is normally shown by using the total pressure ratio, corrected mass flow rate, corrected turbine speed, and component efficiency. This performance is presented in either two maps or one consolidated map. One map shows the interrelationship of the total pressure ratio, corrected mass flow rate, and corrected turbine speed, like that depicted in Fig. 9.86 for a single-stage turbine. Because the corrected-speed lines collapse into one line when the turbine is choked, the turbine efficiency must be shown in a

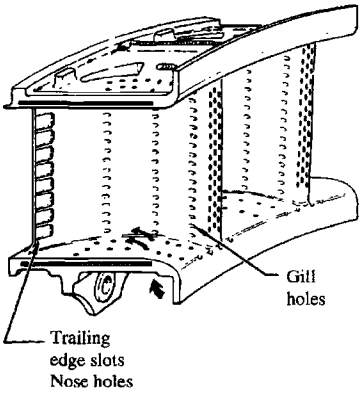

Fig. 9.84 Typical cooled turbine nozzle. (Courtesy of General Electric.)

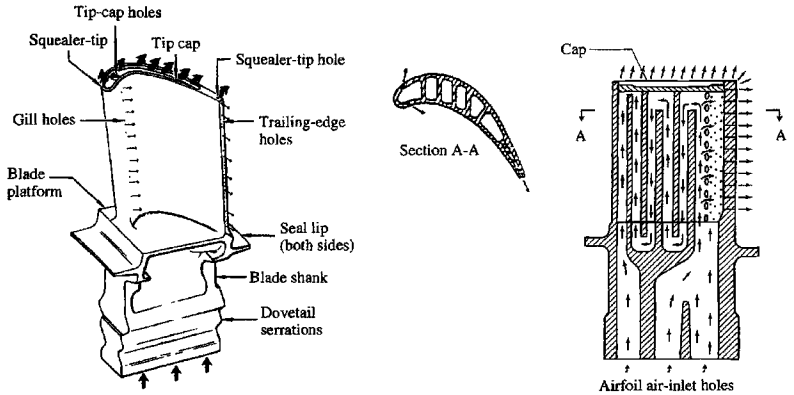

Fig. 9.85 Construction features of air-cooled turbine blade. (Courtesy of General Electric.)

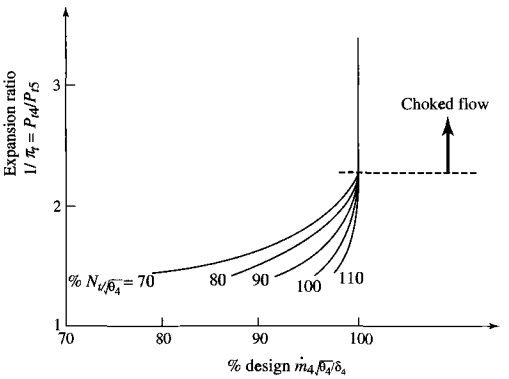

Fig. 9.86 Typical turbine flow map.

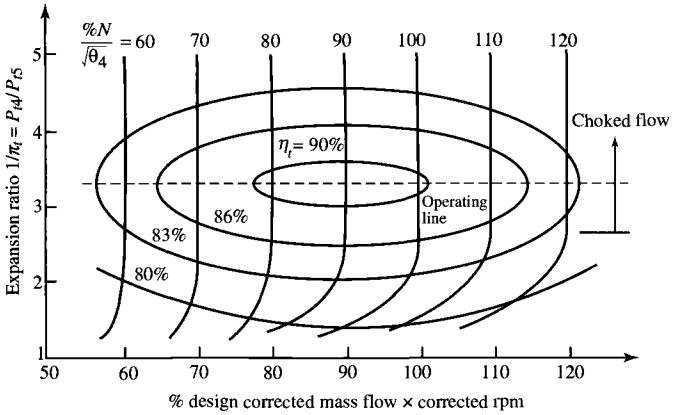

Fig. 9.87 Typical turbine consolidated performance map.

separate map (see Fig. 8.5b). The constant corrected speed lines of Fig. 9.86 can be spread out horizontally by multiplying the corrected mass flow rate by the percentage of corrected speed. Now the turbine efficiency lines can be superimposed without cluttering the resulting performance map. Figure 9.87 shows the consolidated turbine performance map of a multistage turbine with all four performance parameters: total pressure ratio, corrected mass flow rate, corrected turbine speed, and efficiency.

For the majority of aircraft gas turbine engine operation, the turbine expansion ratio is constant and the turbine operating line can be drawn as a horizontal line in Fig. 9.87 (it would collapse to an operating point on the flow map of Fig. 9.86). At off-design conditions, the corrected speed and efficiency of a turbine change very little from their design values. In the analysis of gas turbine engine performance of Chapter 8, we considered that the turbine efficiency was constant.

9.6 Centrifugal-Flow Turbine Analysis

The flow through the stators (nozzles) and rotor of a centrifugal flow turbine is shown in Fig. 9.88. The stators accelerate the flow and increase its tangential velocity. The rotor decreases the tangential velocity of the flow as it removes energy from the flow. Flow exiting the rotor is normally axial, but some tangential (swirl) velocity may still be present. This type of turbine was used in the turbojet engine of von Ohain and is used extensively in turbochargers and very small gas turbine engines.

Figure 9.89 shows the station numbering used in the analysis of the centrifugal-flow turbine. The flow enters the stators at station 1 and leaves at station 2. It then passes through the rotor and leaves at station 3. Normally the flow leaving the rotor is axial ($V_3 = u_3$). Application of the Euler turbine equation to the flow through the stator and rotor, assuming adiabatic stator, gives

$$h_{t1} - h_{t3} = \frac{U_t v_2}{g_c} \tag{9.126}$$

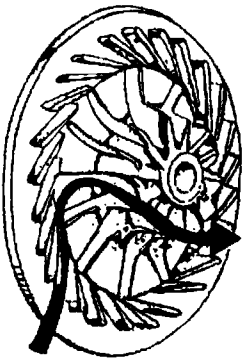

Fig. 9.88 Flow through a centrifugal-flow turbine.

The relative velocity V_{2R} at the entrance to the rotor is designed to be radial ($v_{2R} = 0$, $V_{2R} = w_2$); thus, the tangential velocity at station 2 (v_2) equals the rotor speed at its tip U_t. For this case, Eq. (9.126) becomes

$$h_{t1} - h_{t3} = \frac{U_t^2}{g_c} \tag{9.127}$$

For a calorically perfect gas, Eq. (9.127) can be written in terms of the total temperature change, or

$$T_{t1} - T_{t3} = \frac{U_t^2}{g_c c_p} \tag{9.128}$$

Note that the temperature drop through a centrifugal turbine is directly proportional to the rotor speed squared. Using the polytropic turbine efficiency e_t

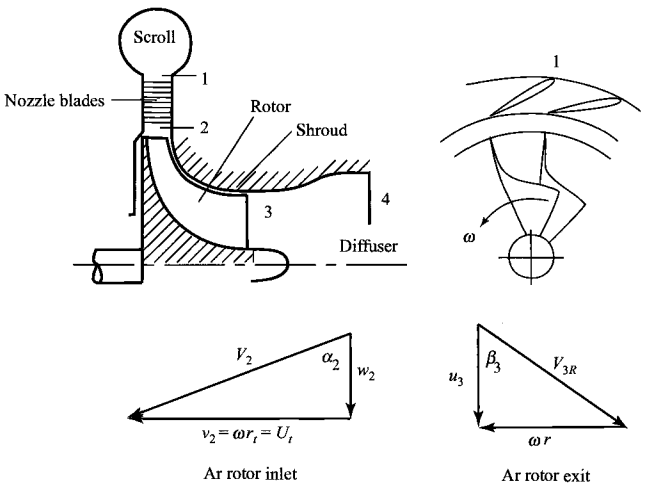

Fig. 9.89 Station numbering for centrifugal-flow turbine (after Dixon, Ref. 37).

and Eq. (9.128), we can express the turbine pressure ratio π_t as

$$\pi_t = \frac{P_{t3}}{P_{t1}} = \left(\frac{T_{t3}}{T_{t1}}\right)^{\gamma/[(\gamma-1)e_t]} = \left(1 - \frac{U_t^2}{g_c c_p T_{t1}}\right)^{\gamma/[(\gamma-1)e_t]} \tag{9.129}$$

The tip speed U_t can be written in terms of T_{t2}, M_2, and α_2. From the velocity triangle at station 2, we can write

$$U_t = v_2 = V_2 \sin \alpha_2 \tag{9.130}$$

V_2 can be expressed in terms of T_{t1} and M_2 as

$$V_2 = \sqrt{\frac{2g_c c_p T_{t2}}{1 + 2/[(\gamma - 1)M_2^2]}}$$

$$= \sqrt{\frac{2g_c c_p T_{t1}}{1 + 2/[(\gamma - 1)M_2^2]}}$$

Thus

$$U_t = \sin \alpha_2 \sqrt{\frac{2g_c c_p T_{t1}}{1 + 2/[(\gamma - 1)M_2^2]}} \tag{9.131}$$

The rotor speed U_t is plotted vs T_{t1}, α_2, and M_2 in Fig. 9.90 by using Eq. (9.131). The maximum swirl angle at station 2 (α_2) is normally 70 deg. The maximum rotor tip speed is limited to between 350 and 500 m/s by the

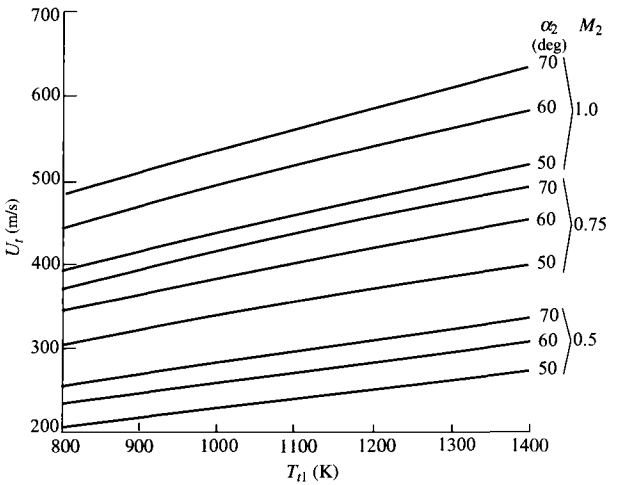

Fig. 9.90 Rotor speed U_t vs T_{t1}, M_2, and α_2 [$\gamma = 1.33$, $c_p = 1.158$ kJ/(kg · K)].

maximum centrifugal stresses of the rotor. These stresses are a function of the relative total temperature T_{t2R} of the rotor; T_{t2R} can be written as

$$T_{t2R} = T_{t2} - \frac{U_t^2}{2g_c c_p} \tag{9.132}$$

Example 9.15

Consider a radial-flow turbine.

Given:

Mass flow rate = 2.5 kg/s
$T_{t1} = 1100$ K
Polytropic efficiency $e_t = 0.85$
$\alpha_2 = 70$ deg
$\gamma = 1.33$
Hub/tip ratio at 3 = 0.4
$P_{t2} = 0.99\ P_{t1}$
$P_{t1} = 400$ kPa
$T_{t3} = 935$ K
Rotor diameter = 0.40 m
$u_3 = w_2$
$R = 0.2872$ kJ/(kg · K)
$g_c c_p = 1.158$ kJ/(kg · K)

Find:

1) Tip speed, rotational speed, and rpm of rotor
2) Mach number, velocities, rotor depth, and T_{tR} at station 2
3) Total pressure, Mach number, and hub and tip radius at station 3
4) Values of V_{3R}, T_{t3R}, β_3, and M_{3R} at mean radius
5) Variation of M_{3R} and β_3 with radius

Solution:

$$U_t = \sqrt{g_c c_p (T_{t1} - T_{t3})} = \sqrt{1158(1100 - 935)} = 437.1 \text{ m/s}$$

$$\omega = \frac{U_t}{r_t} = \frac{437.1}{0.20} = 2185.5 \text{ rad/s}$$

$$\text{RPM} = \frac{30}{\pi}\omega = \frac{30}{\pi}(2185.5) = 20{,}870 \text{ rpm}$$

$$M_2 = \sqrt{\frac{2/(\gamma - 1)}{2g_c c_p T_{t1} \sin^2 \alpha_2 / U_t^2 - 1}}$$

$$= \sqrt{\frac{2/0.33}{2 \times 1158 \times 1100 \sin^2 70 \text{ deg}/437.1^2 - 1}}$$

$$= 0.750$$

$$V_2 = \frac{U_t}{\sin \alpha_2} = \frac{437.1}{\sin 70 \text{ deg}} = 465.2 \text{ m/s}$$

$$w_2 = V_2 \cos \alpha_2 = 465.2 \cos 70 \text{ deg} = 159.1 \text{ m/s}$$

$$\text{MFP}(M_2) = 0.03731$$

$$A_2 = \frac{\dot{m}\sqrt{T_{t2}}}{(P_{t2})(\cos\alpha_2)\text{MFP}(M_2)}$$

$$= \frac{2.5\sqrt{1100}}{(0.99 \times 400{,}000)(\cos 70\,\text{deg})(0.03731)} = 0.01641\,\text{m}^2$$

$$b = \frac{A_2}{2\pi r_t} = \frac{0.01641}{2\pi \times 0.2} = 0.01306\,\text{m}$$

$$T_{t2R} = T_{t2} - \frac{U_t^2}{2g_c c_p} = 1100 - \frac{437.1^2}{2 \times 1158} = 1017.5\,\text{K}$$

$$\pi_t = \frac{P_{t3}}{P_{t1}} = \left(\frac{T_{t3}}{T_{t1}}\right)^{\gamma/[(\gamma-1)e_t]}$$

$$= \left(\frac{935}{1100}\right)^{1.33/(0.33\times 0.85)} = 0.4627$$

$$P_{t3} = 0.4627 P_{t1} = 0.4627 \times 400 = 185.1\,\text{kPa}$$

$$V_3 = u_3 = w_2 = 159.1\,\text{m/s}$$

$$M_3 = \sqrt{\frac{2/(\gamma-1)}{2g_c c_p T_{t3}/V_3^2 - 1}}$$

$$= \sqrt{\frac{2/0.33}{2 \times 1158 \times 935/159.1^2 - 1}} = 0.2677$$

$$\text{MFP}(M_3) = 0.01748$$

$$A_3 = \frac{\dot{m}\sqrt{T_{t3}}}{P_{t3}\text{MFP}(M_3)}$$

$$= \frac{2.5\sqrt{935}}{185{,}100 \times 0.01748} = 0.02363\,\text{m}^2$$

$$r_{3t} = \sqrt{\frac{A_3}{\pi[1-(r_h/r_t)^2]}} = \sqrt{\frac{0.02363}{\pi(1-0.4^2)}} = 0.09463\,\text{m}$$

$$r_{3h} = 0.4 r_{3t} = 0.4 \times 0.09463 = 0.03785\,\text{m}$$

$$r_{3m} = \frac{r_{3t} + r_{3h}}{2} = 0.06624\,\text{m}$$

$$v_{3Rm} = \omega r_{3m} = 2185.5 \times 0.06624 = 144.8\,\text{m/s}$$

Table 9.26 Results for Example 9.15 radial-flow turbine

Property		Station				
		1	2	$2R$	$3Rm$	$3m$
T_t	K	**1100.0**	1100.0	1017.5	944.1	**935.0**
T	K		1006.6	1006.6	924.1	924.1
P_t	kPa	**400.0**	**396.0**	289.2	192.4	185.1
P	kPa		276.9	276.9	176.5	176.5
M			0.7500	0.2565	0.3619	0.2677
V	m/s		465.2	159.1	215.1	159.1
u/w	m/s		159.1	159.1	159.1	159.1
v	m/s	0	437.1	0	144.8	0
r	m		0.2000	0.2000	0.06624	
α	deg	0	**70.0**	——	——	0
β	deg		——	0	42.31	——

$$V_{3Rm} = \sqrt{u_3^2 + v_{3Rm}^2} = \sqrt{159.1^2 + 144.8^2} = 215.1 \text{ m/s}$$

$$T_{t3Rm} = T_3 + \frac{V_{3Rm}^2}{2g_c c_p} = T_{t3} + \frac{v_{3Rm}^2}{2g_c c_p}$$

$$= 935 + \frac{144.8^2}{2 \times 1158} = 944.1 \text{ K}$$

$$M_{3Rm} = M_3 \frac{V_{3Rm}}{V_3} = 0.2677\left(\frac{215.1}{159.1}\right) = 0.3619$$

$$\beta_{3m} = \tan^{-1}\frac{v_{3Rm}}{u_3} = \tan^{-1}\frac{144.8}{159.1} = 42.31 \text{ deg}$$

The results of this example are summarized in Table 9.26. The radial variation of β_3 and M_{3R} are given in Fig. 9.91, using the following relationships:

$$\beta_3 = \tan^{-1}\frac{v_{3R}}{u_3} = \tan^{-1}\frac{\omega r_3}{u_3}$$

$$M_{3R} = M_3\sqrt{1 + \tan^2\beta_3}$$

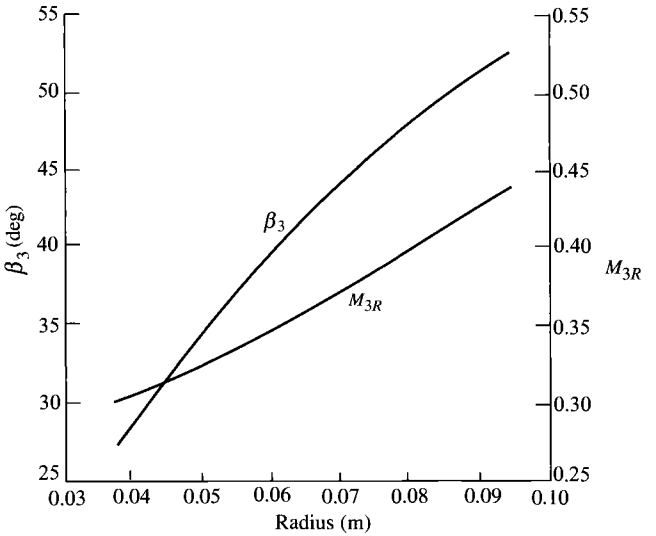

Fig. 9.91 β_3 and M_{3R} vs radius for Example 9.15.

Problems

9.1 Relative velocities are an important concept in the analysis of turbomachines. To help understand relative velocity, consider that a baseball is thrown at a moving train as shown in Fig. P9.1. If the baseball has a velocity of 60 mph and the train is traveling at 80 mph, find the magnitude and direction of the baseball velocity relative to the train.

9.2 A small fan used to circulate air in a room is shown in Fig. P9.2. The fan blades are twisted and change their angle relative to the centerline of the fan as the radius increases. If the relative velocity of the air makes the same angle to the centerline of the fan as the blades and if the blade at a radius of 0.2 m has an angle of 60 deg, determine the speed of the air for fan speeds of 1725 and 3450 rpm.

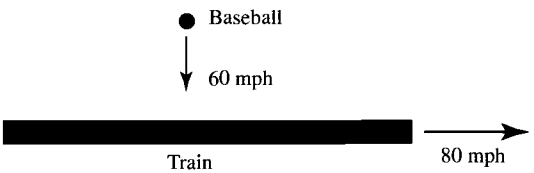

Fig. P9.1

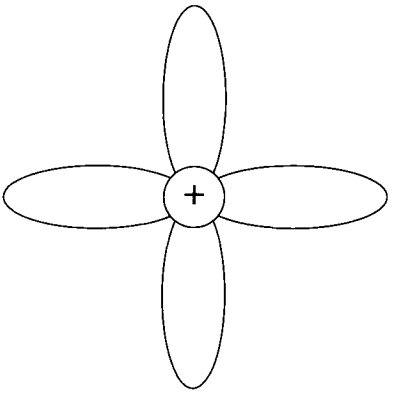

Fig. P9.2

9.3 Air flows through an axial compressor stage with the following properties:

$$T_{t1} = 300 \text{ K}, \quad u_2/u_t = 1.0, \quad v_1 = 120 \text{ m/s}, \quad \alpha = 0 \text{ deg}$$
$$\beta_2 = 45 \text{ deg}, \quad U = \omega r_m = 240 \text{ m/s}$$

Note: For air, use $\gamma = 1.4$ and $R = 0.286 \text{ kJ/(kg} \cdot \text{ K)}$. Determine the change in tangential velocity and the total pressure ratio of the stage for a stage efficiency of 0.88.

9.4 Air flows through an axial compressor stage with the following properties:

$$T_{t1} = 540 \text{ deg R}, \quad u_2/u_1 = 1.0, \quad v_1 = 400 \text{ ft/s}$$
$$\alpha_1 = 0 \text{ deg}, \quad \beta_2 = 45 \text{ deg}, \quad U = \omega r_m = 800 \text{ ft/s}$$

Note: For air, use $\gamma = 1.4$ and $R = 53.34 \text{ ft} \cdot \text{lbf/(lbm} \cdot {}^\circ\text{R)}$. Determine the change in tangential velocity and the total pressure ratio of the stage for a stage efficiency of 0.9.

9.5 Air flows through an axial compressor stage with the following properties:

$$T_{t1} = 290 \text{ K}, \quad P_{t1} = 101.3 \text{ kPa}, \quad u_2/u_1 = 1.0$$
$$M_1 = 0.6, \quad \alpha_1 = 40 \text{ deg}, \quad \alpha_2 = 57.67 \text{ deg}, \quad U = \omega r_m = 360 \text{ m/s}.$$

Note: For air, use $\gamma = 1.4$ and $R = 0.286 \text{ kJ/(kg} \cdot \text{K)}$. Determine the following:

(a) V_1, u_1, and v_1
(b) u_2, V_2, and V_2
(c) ΔT_t and τ_s for the stage
(d) π_s and P_{t3} for a polytropic efficiency of 0.88

9.6 Air flows through an axial compressor stage with the following properties:

$$T_{t1} = 518.7°R, \quad P_{t1} = 14.696 \text{ psia}, \quad u_2/u_1 = 1.0, \quad M_1 = 0.6$$

$$\alpha_1 = 40 \text{ deg}, \quad \alpha_2 = 57.67 \text{ deg}, \quad U = \omega r_m = 1200 \text{ ft/s}$$

Note: For air, use $\gamma = 1.4$ and $R = 53.34 \text{ ft} \cdot \text{lbf}/(\text{lbm} \cdot °R)$. Determine the following:

(a) V_1, u_1, and v_1
(b) u_2, v_2, and V_2
(c) ΔT_t and τ_s for the stage
(d) π_s and P_{t3} for a polytropic efficiency of 0.9

9.7 Air enters a compressor stage that has the following properties:

$$\dot{m} = 50 \text{ kg/s}, \quad \omega = 800 \text{ rad/s}, \quad r = 0.5 \text{ m}$$

$$M_1 = M_3 = 0.5, \quad \alpha_1 = \alpha_3 = 45 \text{ deg}, \quad T_{t1} = 290 \text{ K}$$

$$P_{t1} = 101.3 \text{ kPa}, \quad u_2/u_1 = 1.0, \quad T_{t3} - T_{t1} = 45 \text{ K}$$

$$\phi_{cr} = 0.10, \quad \phi_{cs} = 0.03, \quad \sigma = 1$$

Note: For air, use $\gamma = 1.4$ and $R = 0.286 \text{ kJ}/(\text{kg} \cdot \text{K})$. Make and fill out a table of flow properties like Table 9.3, and determine the diffusion factors, degree of reaction, stage efficiency, polytropic efficiency, and flow areas and associated hub and tip radii at stations 1, 2, and 3.

9.8 Air enters a compressor stage that has the following properties:

$$\dot{m} = 100 \text{ lbm/s}, \quad \omega = 1000 \text{ rad/s}, \quad r = 12 \text{ in.}, \quad M_1 = M_3 = 0.6$$

$$\alpha_1 = \alpha_3 = 42 \text{ deg}, \quad T_{t1} = 518.7°R, \quad P_{t1} = 14.7 \text{ psia}, \quad u_2/u_1 = 1.0$$

$$T_{t3} - T_{t1} = 50°R, \quad \phi_{cr} = 0.12, \quad \phi_{cs} = 0.03, \quad \sigma = 1$$

Note: For air, use $\gamma = 1.4$ and $R = 53.34 \text{ ft} \cdot \text{lbf}/(\text{lbm} \cdot °R)$. Make and fill out a table of flow properties like Table 9.3, and determine the diffusion factors, degree of reaction, stage efficiency, polytropic efficiency, and flow areas and associated hub and tip radii at stations 1, 2, and 3.

9.9 Some axial-flow compressors have inlet guide vanes to add tangential velocity to the axial flow and thus set up the airflow for the first-stage rotor.

(a) Assuming reversible, adiabatic flow through the inlet guide vanes, use the continuity equation and the mass flow parameter to show that

$$(\cos \alpha_1)(A_1)\text{MFP}(M_1) = A_0\text{MFP}(M_0)$$

where the subscripts 0 and 1 refer to the inlet and exit of the inlet guide vanes and the areas are those normal to the centerline of the axial-flow compressor.

(b) For $A_0/A_1 = 1$ and 1.1, plot a curve of α_1 vs M_1 for $M_0 = 0.3$, 0.4, and 0.5 (see Fig. 9.35).

9.10 In the analysis of turbomachinery, many authors use the dimensionless stage loading coefficient ψ, defined as

$$\psi = \frac{g_c c_p \Delta T_t}{(\omega r)^2}$$

For a repeating-stage, repeating-row compressor stage, show that the stage loading coefficient can be written as

$$\psi = \frac{g_c c_p \Delta T_t}{(\omega r)^2} = \frac{\tan \alpha_2 - \tan \alpha_1}{\tan \alpha_2 + \tan \alpha_1} = 1 - \frac{2 \tan \alpha_1}{\tan \alpha_2 + \tan \alpha_1}$$

9.11 Air enters a repeating-row, repeating-stage compressor that has the following properties:

$$\dot{m} = 40\,\text{kg/s}, \quad T_{t1} = 290\,\text{K}, \quad P_{t1} = 101.3\,\text{kPa}, \quad M_1 = 0.5$$
$$\alpha_1 = 38\ \text{deg}, \quad D = 0.5, \quad e_c = 0.9$$
$$\omega = 1000\ \text{rad/s}, \quad \phi_{cs} = 0.03, \quad \sigma = 1$$

Note: For air, use $\gamma = 1.4$ and $R = 0.286\,\text{kJ/(kg} \cdot \text{K)}$. Make and fill out a table of flow properties like Table 9.3, and determine the temperature rise, pressure ratio, mean radius, and flow areas and associated hub and tip radii at stations 1, 2, and 3.

9.12 Air enters a repeating-row, repeating-stage compressor that has the following properties:

$$\dot{m} = 50\,\text{lbm/s}, \quad T_{t1} = 518.7^\circ\text{R}, \quad P_{t1} = 14.7\,\text{psia}, \quad M_1 = 0.5$$
$$\alpha_1 = 35\ \text{deg}, \quad D = 0.5, \quad e_c = 0.9$$
$$\omega = 1200\ \text{rad/s}, \quad \phi_{cs} = 0.03, \quad \sigma = 1$$

Note: For air, use $\gamma = 1.4$ and $R = 53.34\,\text{ft} \cdot \text{lbf/(lbm} \cdot {}^\circ\text{R)}$. Make and fill out a table of flow properties like Table 9.3, and determine the temperature rise, pressure ratio, mean radius, and flow areas and associated hub and tip radii at stations 1, 2, and 3.

9.13 For an exponential swirl distribution and the data of Problem 9.11, calculate and plot the variation of u_1, v_1, u_2, and v_2 vs radius from hub to tip (see Fig. 9.34).

9.14 For an exponential swirl distribution and the data of Problem 9.12, calculate and plot the variation of u_1, v_1, u_2, and v_2 vs radius from hub to tip (see Fig. 9.34).

9.15 For the data of Problem 9.11, determine the shape of both the rotor and the stator blades on the mean radius, using NACA 65-series airfoils with circular camber line. Assume $c/h = 0.3$ and 10% thickness.

9.16 For the data of Problem 9.12, determine the shape of both the rotor and the stator blades on the mean radius, using NACA 65-series airfoils with circular camber line. Assume $c/h = 0.3$ and 10% thickness.

9.17 For the data of Problem 9.11, determine AN^2 at station 1.

9.18 For the data of Problem 9.12, determine AN^2 at station 1.

9.19 A 0.4-m-diam rotor of a centrifugal compressor for air is needed to produce a pressure ratio of 3.8. Assuming a polytropic efficiency of 0.85, determine the angular speed ω, total temperature rise, and adiabatic efficiency. Determine the input power for a mass flow rate of 2 kg/s at 1 atm and 288.2 K. Assume a slip factor of 0.9.

9.20 A 12-in. diam rotor of a centrifugal compressor for air is needed to produce a pressure ratio of 4. Assuming a polytropic efficiency of 0.86, determine the angular speed ω, total temperature rise, and adiabatic efficiency. Determine the input power for a mass flow rate of 10 lbm/s at 1 atm and 518.7°R. Assume a slip factor of 0.9.

9.21 Products of combustion flow through an axial turbine stage with the following properties:

$$T_{t1} = 1800 \text{ K}, \quad P_{t1} = 1000 \text{ kPa}, \quad u_3/u_2 = 1, \quad M_2 = 1.1$$

$$U = \omega r_m = 360 \text{ m/s}, \quad \alpha_2 = 45 \text{ deg}, \quad \alpha_3 = 5 \text{ deg}$$

Note: For the gas, use $\gamma = 1.3$ and $R = 0.287$ kJ/(kg · K). Determine the following:

(a) V_2, u_2, and v_2
(b) u_3, v_3, and V_3
(c) ΔT_t and τ_s for the stage
(d) π_s and P_{t3} for a polytropic efficiency of 0.89

9.22 Products of combustion flow through an axial turbine stage with the following properties:

$$T_{t1} = 3200°\text{R}, \quad \text{P}_{t1} = 200 \text{ psia}, \quad u_3/u_2 = 1$$

$$M_2 = 1.05, \quad U = \omega r_m = 1200 \text{ ft/s}, \quad \alpha_2 = 40 \text{ deg}, \quad \alpha_3 = 25 \text{ deg}$$

Note: For the gas, use $\gamma = 1.3$ and $R = 53.4$ ft · lbf/(lbm · °R). Determine the following:

(a) V_2, u_2, and v_2
(b) u_3, v_3, and V_3
(c) ΔT_t and τ_s for the stage
(d) π_s and P_{t3} for a polytropic efficiency of 0.9

9.23 In the preliminary design of turbines, many designers use the dimensionless work coefficient ψ, defined as

$$\psi \equiv \frac{g_c c_p \Delta T_t}{(\omega r)^2}$$

(a) For a turbine stage with $\alpha_3 = 0$, show that the degree of reaction can be written as

$$^{\circ}R_t = 1 - \frac{\psi}{2}$$

(b) For a turbine stage with $\alpha_3 = 0$, $\gamma = 1.3$, $R = 0.287$ kJ/(kg · K), and $\psi = 1$ and 2, plot ΔT_t vs ωr for $250 < \omega r < 450$ m/s.

9.24 Products of combustion enter a turbine stage with the following properties:

$$\dot{m} = 40\,\text{kg/s}, \quad T_{t1} = 1780\,\text{K}, \quad P_{t1} = 1.40\,\text{MPa}, \quad M_1 = 0.3$$
$$M_2 = 1.15, \quad \omega r = 400\,\text{m/s}, \quad T_{t3} = 1550\,\text{K}, \quad \alpha_1 = \alpha_3 = 0$$
$$r_m = 0.4\,\text{m}, \quad u_3/u_2 = 1.0, \quad \phi_{t\,\text{stator}} = 0.04, \quad \phi_{t\,\text{rotor}} = 0.08$$

Note: For the gas, use $\gamma = 1.3$ and $R = 0.287$ kJ/(kg · K). Make and fill out a table of flow properties like Table 9.12 for the mean line, and determine the degree of reaction, total temperature change, stage efficiency, polytropic efficiency, and flow areas and associated hub and tip radii at stations 1, 2, and 3.

9.25 Products of combustion enter a turbine stage with the following properties:

$$\dot{m} = 105\,\text{lbm/s}, \quad T_{t1} = 3200^{\circ}\text{R}, \quad P_{t1} = 280\,\text{psia}, \quad M_1 = 0.3$$
$$M_2 = 1.2, \quad \omega r = 1400\,\text{ft/s}, \quad T_{t3} = 2700^{\circ}\text{R}, \quad \alpha_1 = \alpha_3 = 0$$
$$r_m = 14\,\text{in.}, \quad u_3/u_2 = 1.0, \quad \phi_{t\,\text{stator}} = 0.04, \quad \phi_{t\,\text{rotor}} = 0.08$$

Note: For the gas, use $\gamma = 1.3$ and $R = 53.34$ ft · lbf/(lbm · °R). Make and fill out a table of flow properties like Table 9.12 for the mean line, and determine the degree of reaction, total temperature change, stage efficiency, polytropic efficiency, and flow areas and associated hub and tip radii at stations 1, 2, and 3.

9.26 For the data of Problem 9.24, determine the shape of both the nozzle and the rotor blades on the mean radius, using a C4 profile with circular camber line for the nozzle blades and T6 profile with circular camber line for the rotor blades. Assume $c/h = 1$, $Z = 0.9$, and 10% thickness for both nozzle and rotor blades.

9.27 For the data of Problem 9.25, determine the shape of both the nozzle and the rotor blades on the mean radius, using a C4 profile with circular camber line for the nozzle blades and a T6 profile with circular camber line for the rotor blades. Assume $c/h = 1$, $Z = 0.9$, and 10% thickness for both nozzle and rotor blades.

9.28 For the data of Problem 9.24, determine AN^2 at station 2.

9.29 For the data of Problem 9.25, determine AN^2 at station 2.

9.30 Products of combustion [$\gamma = 1.3$, $R = 0.287$ kJ/(kg · K)] exit from a set of axial-flow turbine nozzles at a swirl angle of 60 deg, $M = 1.1$, $P_t = 2.0$ MPa, and $T_t = 1670$ K. This gas then enters, the turbine rotor.

(a) For a mass flow rate of 150 kg/s, determine the area of the flow annulus upstream of the turbine rotor.

(b) If the maximum centrifugal load on the turbine blade is 70 MPa, determine the maximum shaft speed (rpm, N). Assume a blade taper factor of 0.9 and material density of 8700 kg/m^3.

(c) For the shaft speed determined in part b, the turbine disk designer has determined that the maximum radius of the hub is 0.6 m. Determine the tip radius, mean radius, and the total temperature drop through the turbine rotor based on the mean rotor velocity and zero exit swirl.

9.31 Products of combustion [$\gamma = 1.3$, $R = 53.34$ ft · lbf/(lbm · °R)] exit from a set of axial-flow turbine nozzles at a swirl angle of 65 deg, $M = 1.2$, $P_t = 300$ psia, and $T_t = 3000$°R. This gas then enters the turbine rotor.

(a) For a mass flow rate of 325 lbm/s, determine the area of the flow annulus upstream of the turbine rotor.

(b) If the maximum centrifugal load on the turbine blade is 10,000 psia, determine the maximum shaft speed (rpm, N). Assume a blade taper factor of 0.9 and material density of 0.25 lb/in.^{3}

(c) For the shaft speed determined in part b, the turbine disk designer has determined that the maximum radius of the hub is 15 in. Determine the tip radius, mean radius, and the total temperature drop through the turbine rotor based on the mean rotor velocity and zero exit swirl.

9.32 A centrifugal turbine has products of combustion [$\gamma = 1.33$, $R = 0.287$ kJ/(kg · K)] entering at 1200 K and 1.5 MPa and leaving at 1000 K. For a rotor diameter of 0.3 m, flow angle α_2 of 60 deg, and polytropic efficiency of 0.9, determine the following:

(a) Rotor tip speed and angular speed ω

(b) Mach number at station 2

(c) Total pressure at the exit

(d) Adiabatic efficiency

9.33 A centrifugal turbine has products of combustion [$\gamma = 1.33$, $R = 53.34$ ft · lbf/(lbm · °R)] entering at 2100°R and 200 psia and leaving at 1800°R. For

an 8-in. rotor diameter, flow angle α_2 of 55 deg, and polytropic efficiency of 0.85, determine the following:
(a) Rotor tip speed and angular speed ω
(b) Mach number at station 2
(c) Total pressure at the exit
(d) Adiabatic efficiency

9.34 At a total pressure of 1 atm and total temperature of 288.2 K, 2.0 kg/s of air enters the centrifugal compressor of a turbocharger and leaves the compressor at a total pressure of 1.225 atm. This compressor is directly driven by a radial-flow turbine. Products of combustion with a mass flow rate of 2.06 kg/s enter the turbine at a total temperature of 900 K and leave the turbine at a total pressure of 1.02 atm. Assume adiabatic flow through both compressor and turbine, no loss of power to bearings from the drive shaft that connects the compressor and turbine, $e_c = 0.80$, $e_t = 0.82$, a slip factor of 0.9 for the compressor, and the following gas properties:

For air	$\gamma = 1.40$ and $c_p = 1.004$ kJ/ (kg · K)
For products of combustion	$\gamma = 1.33$ and $c_p = 1.157$ kJ/ (kg · K)

Determine the following:
(a) Compressor rotor tip speed U_t m/s and exit total temperature in Kelvins
(b) Turbine rotor tip speed U_t m/s and inlet total pressure in atmospheres
(c) Turbine exit total temperatures in Kelvins
(d) Tip radius of compressor rotor and tip radius of turbine rotor for $N = 20{,}000$ rpm

9.35 At a total pressure of 14.696 psia and total temperature of 518.7°R, 2.0 lbm/s of air enters the centrifugal compressor of a turbocharger and leaves the compressor at a total pressure of 18 psia. This compressor is directly driven by a radial-flow turbine. Products of combustion with a mass flow rate of 2.06 lbm/s enter the turbine at a total temperature of 1600°R and leave the turbine at a total pressure of 15.0 psia. Assume adiabatic flow through both compressor and turbine, no loss of power to bearings from the drive shaft that connects the compressor and turbine, $e_c = 0.80$, $e_t = 0.82$, a slip factor of 0.9 for the compressor, and the following gas properties:

For air	$\gamma = 1.40$ and $g_c c_p = 6000$ ft^2/(s^2 · °R)
For products of combustion	$\gamma = 1.33$ and $g_c c_p = 6860$ ft^2/(s^2 · °R)

Determine the following:
(a) Compressor rotor tip speed U_t ft/s and exit total temperature in degrees Rankine
(b) Turbine rotor tip speed U_t ft/s and inlet total pressure in pounds per square inch absolute
(c) Turbine exit total temperatures in degrees Rankine
(d) Tip radius of compressor rotor and tip radius of turbine rotor for $N = 20{,}000$ rpm

Table P9.D1 Compressor and turbine design data for a 25,000-lb turbojet[a]

π_c	T_{t3}, °R	P_{t3}, psia	T_{t5}, °R	P_{t4}, psia	P_{t5}, psia	$\dot{m}_{\text{compr}}$, lbm/s	$\dot{m}_{\text{turb}}$, lbm/s	$\dot{W}_c$, kW	$\dot{W}_t$, kW
7.0	962.06	102.87	2853.21	98.76	56.85	200.28	208.66	22,298	22,523
7.5	983.36	110.22	2836.44	105.81	59.20	197.79	206.01	23,079	23,312
8.0	1003.72	117.57	2820.41	112.87	61.45	195.61	203.68	23,824	24,065
8.5	1023.22	124.92	2805.04	119.92	63.60	193.69	201.63	24,539	24,786
9.0	1041.96	132.26	2790.27	126.97	65.65	191.97	199.79	25,225	25,480
9.5	1060.00	139.61	2776.04	134.03	67.61	190.44	198.15	25,886	26,147
10.0	1077.40	146.96	2762.31	141.08	69.49	189.05	196.66	26,523	26,791
10.5	1094.22	154.31	2749.03	148.14	71.29	187.80	195.31	27,140	27,415
11.0	1110.50	161.66	2736.18	155.19	73.02	186.65	194.08	27,738	28,018
11.5	1126.28	169.00	2723.71	162.24	74.68	185.61	192.95	28,318	28,605
12.0	1141.60	176.35	2711.60	169.30	76.27	184.65	191.91	28,882	29,174
12.5	1156.49	183.70	2699.82	176.35	77.80	183.77	190.96	29,431	29,729
13.0	1170.98	191.05	2688.36	183.41	79.27	182.95	190.07	29,966	30,269

[a]Air entering compressor has $T_t = 518.7$°R and $P_t = 14.696$ psia. Gas enters turbine at 3200°R and P_{t4}. Polytropic efficiencies: $e_c = 0.90$ and $e_t = 0.90$. Also, $\dot{W}_t = \dfrac{\dot{W}_c}{0.99}$ $P_{t4} = 0.96\,P_{t3}$.

Axial Flow Turbomachinery Design Problems

9.D1 Perform the preliminary design of the turbomachinery for a turbojet engine having a thrust of 25,000 lbf at sea-level static conditions. Based on polytropic efficiencies of 0.9 for both compressor and turbine, the engineers in the engine cycle analysis group have determined the compressor and turbine inlet and exit conditions for a range of compressor pressure ratios that will give the required engine thrust. The results of their analysis are presented in Table P9.D1. Note that the mass flow rate through the compressor and turbine decreases with increasing compressor pressure ratio. To minimize on engine weight, it is desirable to have the maximum compressor pressure that can be driven by a single-stage turbine with exit guide vanes. The number of compressor stages depends on both the compressor design and the turbine design. As you can see, there are many sets of compressor/turbine designs that meet the thrust need; however, some of the designs cannot be done with one turbine stage or may be too large (high mass flow rate). Data for other compressor pressure ratios between 7 and 13 not listed in the table can be obtained by interpolation.

Assume that a turbine disk material exists that permits a rim speed of 1200 ft/s and that the turbine rotor airfoils can withstand an AN^2 of 5×10^{10} in.$^2 \cdot$ rpm^2. Use Fig. E.8 from Appendix E and computed AN^2 stresses to select material for each compressor stage.

For the compressor, use

$$\gamma = 1.4 \quad \text{and} \quad R = 53.34\,\text{ft} \cdot \text{lbf}/(\text{lbm} \cdot {}^\circ\text{R})$$

For the turbine, use

$$\gamma = 1.3 \quad \text{and} \quad R = 53.39\,\text{ft} \cdot \text{lbf}/(\text{lbm} \cdot {}^\circ\text{R})$$

Suggested Design Process.

1) Select a set of compressor and turbine design data from Table P9.D1.
2) For the design turbine rim speed, estimate the mean turbine rotor speed ωr_m and determine the variation of turbine radii (hub, mean, and tip) and AN^2 vs rpm. Select a shaft speed (rpm).
3) Determine the turbine mean-line design, using TURBN. Make sure the turbine meets the design criteria listed below.
4) For the selected shaft speed (rpm) and compressor pressure ratio, determine the number of compressor stages and the compressor mean-line design, using the repeating-row, repeating-stage design choice in COMPR. Make sure the compressor meets the design criteria listed below.
5) Check that 99% of power from turbine equals the power required by the compressor.
6) Check alignment of compressor and turbine. If the mean radii are not more than 2 in. apart, go back to item 2 and select a new rpm.
7) Determine the inlet and exit flow conditions for the turbine exit guide vanes (include estimate of losses).

8) Determine the inlet and exit flow conditions for the inlet guide vanes (include estimate of losses).
9) Specify compressor material for each stage based on the rotor's relative total temperature and blade AN^2.
10) Make a combined scale drawing of the compressor and turbine flow path. Allow 12 in. between the compressor exit and turbine inlet for the combustor. Show the shaft centerline.

Compressor Design Criteria.
1) Axial flow entering inlet guide vanes and leaving compressor
2) Reactions at all radii >0
3) Diffusion at all radii <0.6
4) M_{1R} at tip of first stage <1.05
5) M_2 at hub of first stage <1
6) Flow coefficient at mean radius between 0.45 and 0.55
7) Stage loading coefficient at mean radius between 0.3 and 0.35
8) Number of blades for rotor or stator of any stage <85
9) Number of blades for inlet guide vanes <85
10) AN^2 at entrance of rotor within material limits

Turbine Design Criteria.
1) Axial flow entering turbine nozzle at $M = 0.3$
2) Axial flow leaving exit guide vanes of turbine
3) Reaction at all radii >-0.15
4) Number of blades for nozzle, rotor, or exit guide vanes <85
5) $M_2 < 1.2$ at hub and >1 at tip
6) M_{3R} at tip of rotor <0.9
7) Velocity ratio at mean radius between 0.5 and 0.6
8) AN^2 at entrance of rotor within material limits
9) Tangential force coefficient Z for stator or rotor <1.0

9.D2 Perform the preliminary design of the turbomachinery for a turbojet engine of Problem 9.D1 but with no inlet guide vanes for the compressor or exit guide vanes from the turbine. Thus the turbine must have zero exit swirl.

9.D3 Perform the preliminary design of the turbomachinery for a turbojet engine of Problem 9.D1 scaled for a thrust of 16,000 lbf at sea-level, static conditions. Thus the mass flow rates and powers will be 64% of the values listed in Table P9.D1.

9.D4 You are to perform the preliminary design of the turbomachinery for a turbojet engine of Problem 9.D3 but with no inlet guide vanes for the compressor or exit guide vanes from the turbine. Thus the turbine must have zero exit swirl.